COMPARATIVE STUDY OF SLOPE STABILITY BY GEOTECHNICAL SOFTWARE PROGRAMS

A THESIS SUBMITTED TO THE GRADUATE SCHOOL OF APPLIED SCIENCES OF NEAR EAST UNIVERSITY

By
ABDALLA SHLASH

In Partial Fulfillment of the Requirements for the Degree of Master of Science In Civil Engineering

NICOSIA, 2020

ABDALLA SHLASH COMPARATIVE STUDY OF SLOPE STABILITY BY GEOTECHNICAL SOFTWARE PROGRAMS NEU 2020

COMPARATIVE STUDY OF SLOPE STABILITY BY GEOTECHNICAL SOFTWARE PROGRAMS

A THESIS SUBMITTED TO THE GRADUATE SCHOOL OF APPLIED SCIENCES OF NEAR EAST UNIVERSITY

By

ABDALLA SHLASH

In Partial Fulfillment of the Requirements for the Degree of Master of Science
in
Civil Engineering

NICOSIA, 2020

Abdalla SHLASH: COMPARATIVE STUDY OF SLOPE STABILITY BY GEOTECHNICAL SOFTWARE PROGRAMS

Approval of Director of Graduate School of Applied Sciences

Prof. Dr. Nadire ÇAVUŞ

We certify this thesis is satisfactory for the award of the degree of Master of Science in Civil Engineering

Examining Committee in Charge:

Assoc. Prof. Dr. Rifat Reşatoğlu	Committee Chairman, Department of Civil Engineering, Near East University
Assist. Prof. Dr. Youssef Kassem	Department of Mechanical Engineering, Near East University
Assist. Prof. Dr. Anoosheh Iravanian	Supervisor, Department of Civil Engineering, Near East University

I hereby declare that all information in this document has been obtained and presented in accordance with academic rules and ethical conduct. I also declare that, as required by these rules and conduct, I have fully cited and referenced all material and results that are not original to this work.

Name, Last name: Abdalla SHLASH
Signature:
Date

ACKNOWLEDGEMENTS

Foremost, I’d like to express my sincere gratitude my supervisor Assist. Prof. Dr. Anoosheh Iravanian of the Civil Engineering Department at Near East University for her patience, motivation and valuable guidance. The door to Assist. Prof. Dr. Iravanian office was always open whenever had a question about my research or when I ran into a trouble. This thesis would not have been possible without her.

Fınally, I want to express my very profound gratitude to my pacemaker my prestigious father Dr. Mohammed Saleh Shlash for his unlimited support and my sparking mother and sisters for their love and pray, and my beloved brother Dr. Mohammed Noor.

To my family…

ABSTRACT

Soil slopes analysis and design has always been a major field in geotechnical engineering. Different methods have been developed and created to examine two and three dimensional slopes based on various methods of assumption and assessment. The factor of safety can only be acquired accurately if the slope's critical failure surface is appropriately detected. Different software programs for analyzing and examining slope stability were used and compared by knowing the parameters of soil strength.

Throughout this study, software programs such as PLAXIS, SLOPE/W and FLAC/Slope were used to examine the difficulties of slope stability and determine the critical surface of failure. Different values of shear strength parameters were chosen to investigate the authenticity and efficiency of these programs: cohesion (c), soil's unit weight (ɤ) and internal friction angle (Ø), and their effect on the value of the factor of safety were examined. Eventually, to obtain from various software programs the results have been contrasted and shared. The research findings showed that the slope's factor of safety changes with changing cohesion, soil's unit weight and internal friction angle. In addition, the slip surface is affected by (λ) the dimensionless function associated with the cohesion, the internal friction angle and the unit weight.

The conclusions showed that, compared to SLOPE/W, PLAXIS is easier to use as slope stability assessment software. It gives about 5% lower factor of safety value than SLOPE/W. On the other hand, FLAC/Slope is the most complicated software and usually gives lower value for the factor of safety than SLOPE/W and PLAXIS.

***Keywords*:** slope stability; PLAXIS; SLOPE/W; FLAC/SLOPE; factor of safety; length of failure arc

ÖZET

Zemin şev stabilitesive tasarımı, jeoteknik mühendisliğinde her zaman önemli bir alan olmuştur. Çeşitli varsayım ve değerlendirme yöntemlerine dayanarak iki ve üç boyutlu eğimleri incelemek için farklı yöntemler geliştirildi ve yaratıldı. Güvenlik faktörü ancak eğimin kritik kayma yüzeyi uygun şekilde tespit edildiğinde doğru bir şekilde elde edilebilir. Şev stabilitesini analiz etmek ve incelemek için farklı yazılım programları kullanılmış ve zemin dayanımı parametreleri karşılaştırılmıştır.

Bu çalışma boyunca, şev stabilitesinin zorluklarını incelemek ve kritik kayma yüzeyini belirlemek için PLAXIS, SLOPE/W ve FLAC/Slope gibi yazılım programları kullanılmıştır. Bu programların gerçekliğini ve verimliliğini araştırmak için farklı kayma dayanımı parametrelerinin değerleri seçilmiştir: kohezyon , zeminin birim hacim ağırlığı ve iç sürtünme açısı ve bunların güvenlik faktörünün değeri üzerindeki etkileri incelenmiştir. Sonunda, çeşitli yazılım programlarından elde edilen sonuçlar karşılaştırıldı ve paylaşıldı. Araştırma bulguları, eğimin güvenlik faktörünün değişen kohezyon , zeminin birim hacim ağırlığı ve iç sürtünme açısı ile değiştiğini göstermiştir. Ek olarak, kayma yüzeyi, kohezyon, iç sürtünme açısı ve birim hacim ağırlık ile ilişkili boyutsuz bir fonksiyondan (λ) etkilenir.

Elde edilen sonuçlar, SLOPE/W ile karşılaştırıldığında PLAXIS'in şev stabilitesi değerlendirme yazılımının daha kolay olduğunu göstermiştir. SLOPE/W'den yaklaşık 5% daha düşük güvenlik faktörü verir. Öte yandan, FLAC/SLOPE, güvenlik faktörü için SLOPE/W ve PLAXIS'ten daha düşük bir değer verir.

Anahtar Kelimeler: şev stabilitesi; PLAXIS; SLOPE/W; FLAC/SLOPE; emniyet faktörü; arıza uzunluğu

TABLE OF CONTENTS

CHAPTER 2: LITERATURE REVIEW

CHAPTER 3: METHODOLOGY

CHAPTER 5: CONCLUSION AND RECOMMENDATIONS

APPENDICES

LIST OF TABLES

LIST OF FIGURES

LIST OF SYMBOLS AND ABBREVIATIONS

FOS: Factor of Safety

FEM: Finite Elements Method

LEM: Limit Equilibrium Method

C: Cohesion

γ: Unit Weight

Ø: Internal Friction Angle

α: Horizontal Angle of Slope (Figure 4.4)

β: Vertical Angle of Slope (Figure 4.4)

AutoCAD: Automatic Computer Aided Design

FLAC: Fast Lagrangian Analysis of Continua

H: Height of Slope

La: Length of Failure Arc

Le: Slope Surface Entry Distance

CHAPTER 1
INTRODUCTION

1.1 Overview

There are many problems encountered by the engineer, student or executor when it comes to slope stability subject. The groundwork should be set up for predicting such problems and devising appropriate solutions in case of failure occurrence. One of the common cases that is needed to be studied is the balance and stability of the earthworks in some installation cases such as buildings and archaeological walls on slopes. Practically every phenomenon in nature, geological or mechanical could be described with the help of geotechnical laws, so the use of mathematical models for studying the behavior of geotechnical structures is an important part of geometrical analysis, hence the importance of understanding is how to handle modeling the software programs.

The goal of any natural or manmade slope's stability analysis is to determine the failure surface with the minimum value of factor of safety. It is important to identify the critical failure surface for the specified slope to find the minimum factor of safety. Therefore, different methods of searching and optimizing have been used in the past. They all, however, have the same limitation which is the problem of using hand calculations. Throughout this study, the impact of parameters of soil on the slope’s failure surface and factor of safety was studied. It is possible to determine the critical failure surface for a given slope by comparing the factor of safety from several experiment slip surfaces. The surface of the slip with the smallest factor of safety is viewed to be the surface of critical failure.

Basically there’re two types of slopes, natural and manmade (artificial). Each of these types may be composed of rock or soil. Natural slopes are also divided into two types, infinite slopes e.g. the highway between two cities with different sea level rise or mountains. The other type of natural slopes is finite slopes (e.g. hills). This study is about finite slopes but will discuss about infinite slops too and how it is analyzed.

Instances for natural slopes could be named as: slope of the mountains, slopes on both sides of the rivers, slope of the bottoms of the rivers from the source up to the downstream. Examples on manmade slopes could be counted as slopes of the bridges and slopes of sides of roads, railways and dams.

These slopes have internal forces make them balanced against the forces that cause the collapse of the slope. The failure triggering forces could be named as gravity, the forces of water flow through the soil and the low value of cohesion of soil granules. On the other hand the force that resists the collapse of slope is mainly shear force (AbdelRahman, 2019). If λ (the correlation between shear strength parameters and potential slip surface Eq 2.45) is constant, the surface of the slip does not adjust with the switch in the parameters of the shear strength.

With the development in technology software packages using the finite difference and finite element methods have increased in popularity as they head to possess a wide range of characteristics (Hammouri et al. 2008).

The outputs of this study showed that the slopes formed of smaller grains of soil the more stable will be, silty and well-graded soils are more stable than soils with coarse grains such as gravel and sandy soils, also slopes with the heavier soil in terms of unit weight has less stability. Slopes made from boulders or the ones with high content of larger grains have less stability than slopes formed by gravelly soil.

In this study, it found that all slopes failed when soil unit weight value more than 15 kN/m^3 and the other two parameters are constant, which represent clayey and silty sands, also when both parameters ɤ and Ø changed together and the third parameter cohesion is constant (which represent silty clay) the slopes have failed as well.

1.2 Importance of Research

During the 1960s the science of soil mechanic was adopted on theory and limited empirical information (Oghli, 2011). Modeling of soils with heterogeneous and variable characteristics varying with ambient conditions was very difficult, especially experimental techniques were doing simple tests when computers were not available at the time, but given the rapid scientific development of the world and the computer revolution, using programming that relies on numerical methods has become easier and contributes to the solution of many geotechnical issues. The design of the complex installations of our time relies on the use of modern computer and software to complete the design in its optimal form.

This research focuses on theory and practice, in which we hope to help narrow the gap between theory and practice by contributing to the use and selection of the best modeling software packages that are being used by geotechnical engineers globally, thus enable colleague engineers to use these programs and to realize how to deal with the results obtained from this software.

Combining the analysis of slope stability within the design will help to prevent any geotechnical collapse during the life of the design and throughout construction (Bromhead, 1992).

1.3 Aim of the Study

The widespread use of computers in engineering is the result of progress in production of easy to use software and the proliferation of personal computers in the world. So it can be said that the design of structures or complexed slopes without the use of computers have become very rare. The design of complex installations of our time relies on the use of modern computer and software to complete the design in its optimal form.

At present, the problem of slope stability is one of the main issues facing workers and engineers in soil field; there is still a big distinction between the scientists about the best way to calculate the stability of the slopes (Oghli, 2011).

The main objectives of this study are as follows:

1- Extensive literature review to study the theoretical background of the most widely and commonly used methods of analyzing slope stability as well as analyses of critical surface techniques.

2- Using various slope stability analysis software programs to evaluate the impacts of soil strength parameters (cohesion, unit weight, internal friction angle) and slope geometry parameters (Height of the slope, vertical angle of the studied slope Alpha and the horizontal angle of the slope, Beta) as shown in Figure 4.4 on factor of safety and critical slip surface.

3- Compare the results of the different analysis software programs of slope stability in this thesis.

4- Correlate the relationship between parameters of soil strength and slope geometry and critical slip surface and obtain a numerical equations about the relation between failure arc's length and soil strength parameters.

1.4 The Shear Strength Parameters as Input Data

Cohesion, unit weight and internal friction angle are the shear strength parameters were chosen as input for software, the reason can be mainly explained as

a- Main soil properties and altering each of them is possible in real life not only by software packages but by many methods (e.g. injections) which it happened in two areas in Hong Kong, Fung Fae Terrance and Thorpe Manor (Fredlund, 1987).

b- Cohesion (c), internal friction angle (Ø), and soil unit weight (ɤ) are the interpolation of the software used in this study.

c- Cohesion, internal friction angle and unit weight are the only factors affecting the length of failure arc (Naderi, 2013).

d- The increase of C, Ø positively affect FOS, on the other hand increasing of unit weight decrease Factor of Safety, FOS, so it will be a combination of decreasing and increasing FOS and soil parameters. Realizing the range can change each of these parameters which it will help in predicting the situation in real life.

1.5 Common Causes of Slope Failure

To determine where to start the prevention of slope failure in the property, first of all, we need to take the time to understand the factors that lead to slope failure. All things considered, slope restoration is definitely not a one size fits all arrangement. Each slope is diverse with regards to geography, soil creation, vegetation and several other variables. Therefore, for any slope stability strategy to viably prevent the risk of avalanches and mudslides, it ought to be tailor-fit to the slope on which it is to be implemented on and the factors of the instability of such a slope. Here are some of the common reasons of slope failure.

1.5.1 Steepness of the slope

It's known that the steeper a slope is the more volatile it becomes. It's valid for making sand castles and it's valid for making hillside homes. The natural response of steep slopes is to move a portion of its materials downwards until it achieves a natural angle of repose. Any type of slope adjustment, regardless of whether it is through natural methods, for example, a stream undercutting the banks of a river, or by laborers expelling an area of the slope's base to construct streets, will affect the slope's stability (Sinai, 2012). Figure 1.1 shows a steep slope in Northern Cyprus.

Figure 1.1: Steepness of the Slope (Güzelyurt-Cyprus)

1.5.2 Water and drainage

Water is denser than air multiple times. Amid overwhelming downpours when the water replaces air between the grains of soil, the earth in slopes turns significantly heavier.

This turns into an issue when the earth is being kept down by a retaining wall at its base. In particular, if the heaviness of the earth behind the retaining wall surpasses the retaining wall's capacity limit, the retaining wall will collapse in a disastrous deluge.

And likewise water decreases grain-to-grain contact which lessens the cohesiveness. Beside changes in the groundwater fluid weight in slope rocks amid the rainy season, water saturation increases downslope mass movement's probability.

1.5.3 Soil composition

The structure of the slope's soil is an imperative factor with regards to preventing slope failure. Distinctive sorts of soils will have altogether different qualities with regards to frictional resistance from erosion and cohesion among the grains. For example, loose soil or sand, has low cohesion and will effectively erode when immersed in water. Soils that have a lot of clay, then again, will in general enlarge when saturated by water; this makes them heavier and progressively tends to motion. (Aaron & Mcdougall, 2019).

1.5.4 Vegetation

The quantity and type of vegetation in a slope is also proportional to that slope's strength. Vegetation (especially its roots) holds the soil in position and makes it more erosion resistant. The more widespread of vegetation, the more roots are so the more it can hold the soil in position. The more vegetation there is, also, the more steady the slope is probably going to be. This is the reason behind why slopes that have had their vegetation removed or annihilated by fires are prime reason for slope failures in the rainy season (Huvenne, Croker, & Henriet, 2002).

1.5.5 Bedding planes

A bedding plane is fundamentally a surface that isolates a stratified rock layer or bed from another layer (Mercier et al., 2017). It seems like margarine spread between two pieces of bread because of their nature, there is also a high risk of slope failure in exposed beds in a slope. This risk is exacerbated if the bed contains a weak rock layer sandwiched.

Imagine placing a glass panel on a slide and a block of wood on top of it to illustrate. The surfaces of contact between the slide, glass and wood are angled downward bedding planes. Although the frictional force that keeps the block of wood on the glass strong, the connection of glass slide is weak, causing the whole structure to erode downwards (Sinai, 2012).

1.5.6 Joints and fractures

Joints and fractures are natural cracks that occur in rocks slope. These are caused by natural rock expansion due to cooling or erosion-related removal of overlying rocks. The cohesion between the rocks that make up the slope is greatly reduced for these cracks, increasing the likelihood of a slope landslide (Aaron & Mcdougall, 2019).

1.5.7 Sudden shocks

Finally, sudden shocks such as hurricanes, earthquakes, blasting, heavy truck passage, volcanic eruptions, and others can trigger soil's sudden mass movement in the slopes (Mercier et al., 2017).

1.6 Types of Slope Failure

1.6.1 Planar failure

Planar failure happens when an intermittence hits almost parallel to the seat of the slope and the slope of the seat converges at a lower point allowing the material to slide over the irregularity as shown in Figure 1.2. Variety can arise in the procedure if the slipping plane is a mixture of joint sets that build up a straight path.

Analyzing of a planar failure involves analyzing the slope's geometry and consideration of two cases:

A) Slope with tension crack in the upper face

b) Slope for tension crack in the face of the slope.

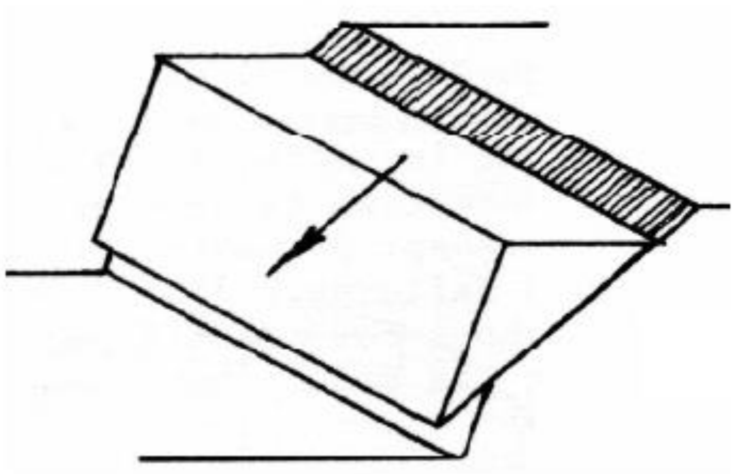

Figure 1.2: Planner failure (Louis N.Y. Wong, 2014)

1.6.2 Wedge failure

The 3D wedge failures happen when two cutouts overlap so that the material wedge formed over the cutouts can slide out in a way parallel to the intersection line between the two cutouts. It is particularly prevalent in the individual bench scale but may also provide the mechanism of failure for a large slope where structures are very continuous and thorough. At the point when two cutouts strike at a slant over the slope face and their line of convergence in the slope, the rock’s wedge resting on these cutouts will slip down over the line of crossing point as long as the decrease of the line is significantly greater than the friction angle and the shearing part of the plane of the discontinuities is less than the total downward force. The total force of downward is the downward component of the wedge's weight, and the wedge's external forces acting along the wedge.

In this type of failure there is two forms

a) Slant wedge failure as shown in Figure 1.3

b) Straight wedge failure as shown in Figure 1.4

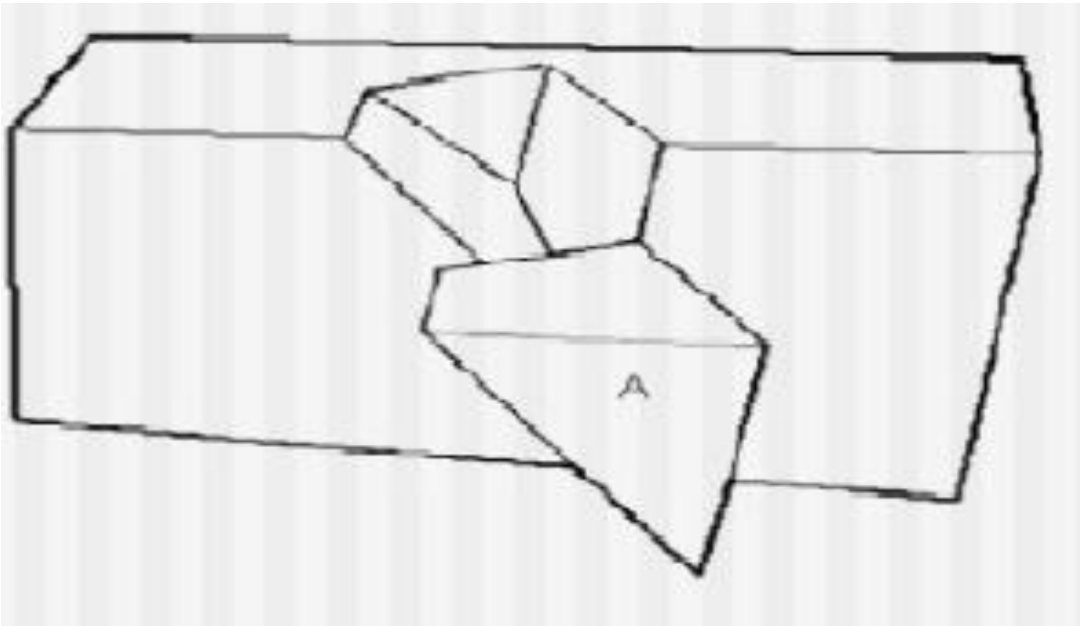

Figure 1.3: Slant **w**edge failure (Prajapati, 2017)

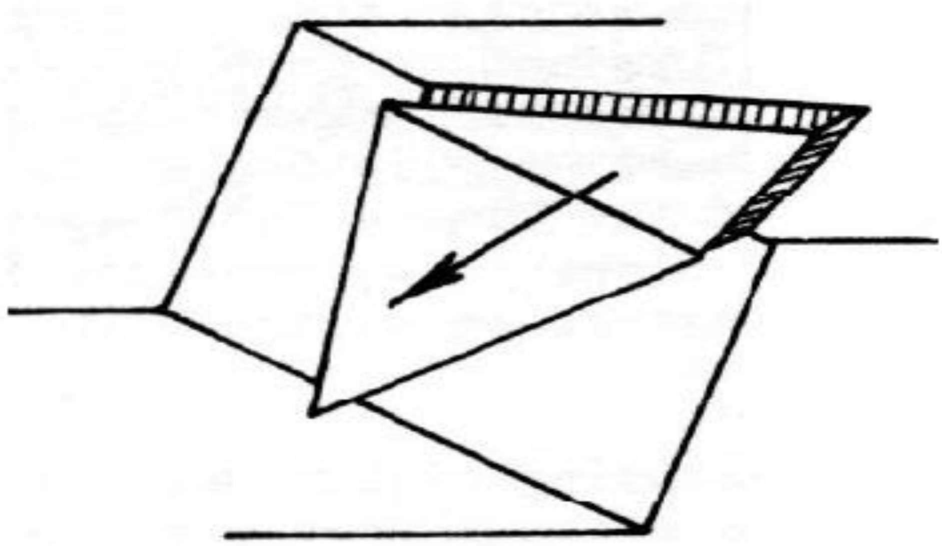

Figure 1.4: Straight wedge failure (Louis N.Y. Wong,2014)

1.6.3 Circulars failure

The great work in Sweden at the starting of the century assured that the shape of a circular arc resembles the failure surface in spoil soil slopes or dumps as shown in Figure 1.5. This failure may occur in soil slopes, when the joint sets are not defined very well the circular method occurs. If the material of the slopes of the spoil dump is weak, like soil, heavily joined or broken rock mass, a single discontinuity surface defines the failure but tends to follow a circular path. The circular failure conditions are as follows:

a. When compared to the slope, the individual soil or rock mass particles comprising the slopes are small.

b. Because of their shape, the particles are not locked and tend to behave as soil.

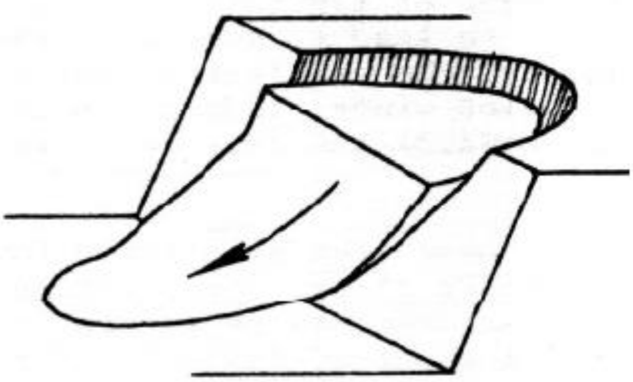

,

Figure 1.5: Circular failure (Louis N.Y. Wong, 2014)

Types of circular failure

A) Slope failure: in this kind the rupture surface arc meets the slope above the slope toe, this occurs when the angle of the slope is very high and the soil near the toe has the high resistance.

B) Toe failure: the rupture surface arc meets the slope of the toe in this kind of failure.

C) Base failure: the arc of the failure passes underneath the toe and into the slope base in this type of failure. This happens when the angle of the slope is low and the soil under the base is more plastic and softer than the soil which is above the base.

1.6.4 Two block failure

These types of failures are significantly less rife way of slope failure of rock than single square failures, for example, the planes and the 3 dimensional wedge and, thusly, are just quickly thought to be here. A few techniques for solution exist and each might be proper at some dimension of examination.

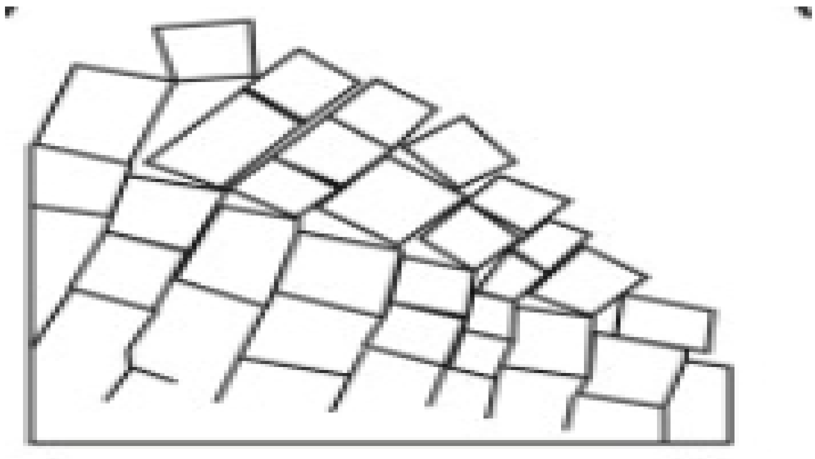

Figure 1.6: Two block failure (Stefano Utili, 2015)

1.6.5 Toppling failure

Overturning or toppling was recognized as a mechanism for failure of rock slope by several investigators and was postulated as the cause of several failures ranging from small to large. Very often, stability depends on the stability of one or two key blocks in slopes with near-vertical joints. The system may collapse once they are disturbed or this failure was assumed to be the reason of several failures ranging from small to massive as shown in Figures 1.7. This type of failure involves rotation around some fixed base of rock blocks as shown in Figure 1.8. In general, when the slopes of the hill are very steep this type of failure occurred.

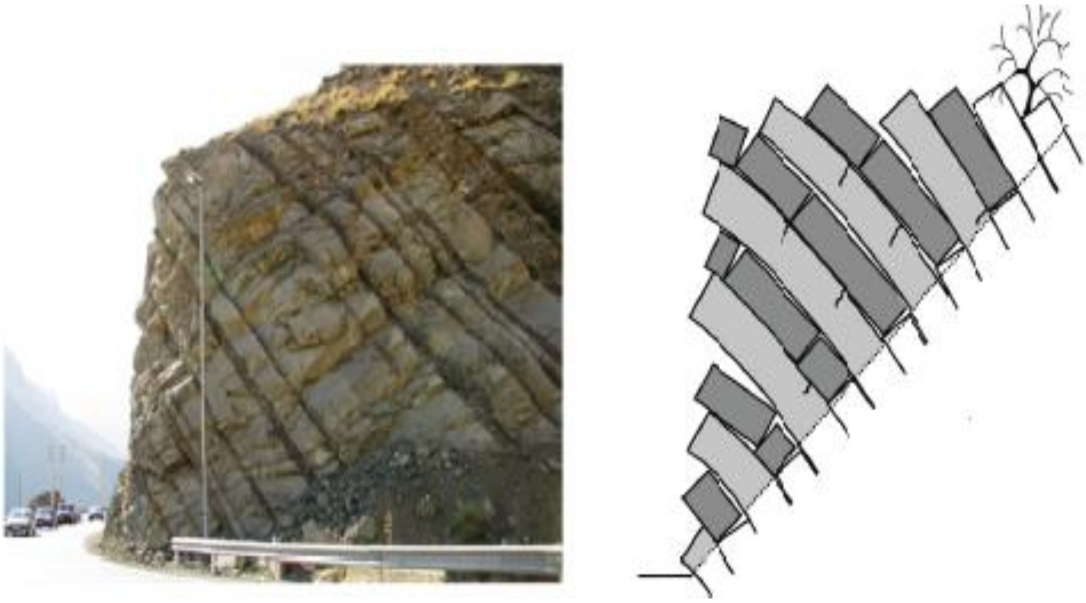

Figure 1.7: The rotation in toppling failure (Louis N.Y. Wong, 2014)

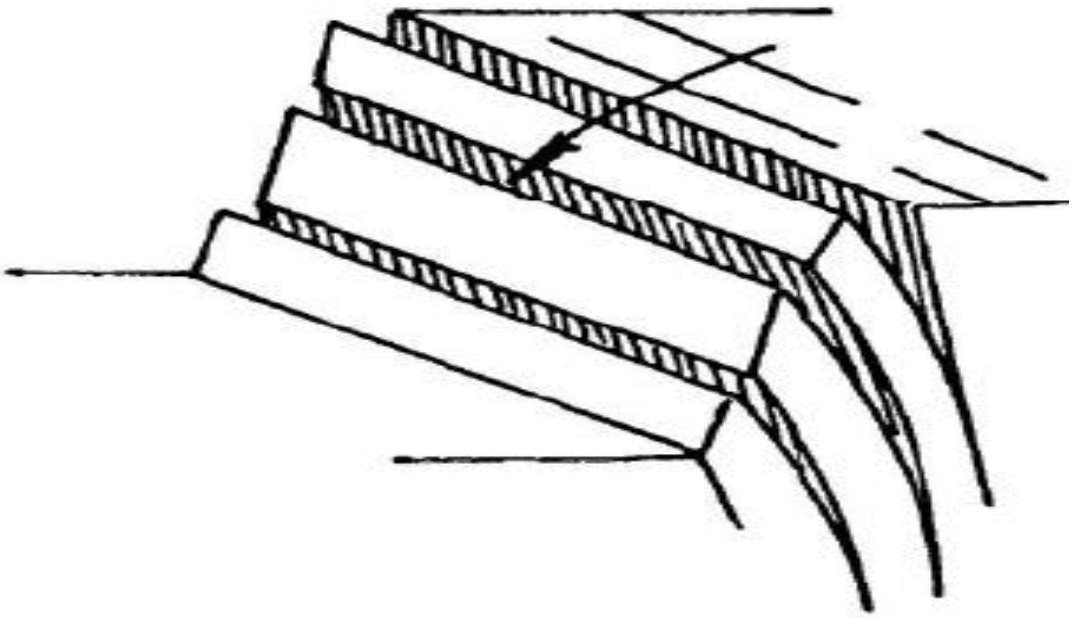

Figure 1.8: Toppling failure (Amini & Ardestani, 2019)

1.7 Factors Affecting Slope Stability:

1.7.1 Slope geometry

Height, the overall angle of slope and surface area of failure are the basic parameters of the geometric design of the slope. Stability of the slope decreases sharply when the slope height increases. The chances of failure at the rear of the crest increase when the overall slope angle is increased and it must be considered in order to avoid any kind of ground deformation at the periphery of the slope structure. An overall angle of the slope 45 ° is considered safe for mines under normal circumstances. The slope's curvature also has a strong impact on the instability. Convex slopes section in slope design should be avoided. The slope is higher and steeper, the stability is lower.

1.7.2 Geological structure

The main geological structure in any structure (building, mines, railways, etc) affecting the stability of the slopes is:

1. Dip quantity and direction.

2. Zones of shear intra-formational

3. Joints and interruptions

a. Reduce strength of the shear

b. Permeability change

c. Acts as sub-surface drain and failure plains

4. Faults

a. Weathering and changing along with faults

b. Act as conduits of groundwater

c. Provides a likely failure plane

If strata dip in the excavations, instability may occur. Faults provide a very low strength lateral or rear release plane and therefore the strata are greatly disturbed. If there is some kind of clay or soil band between two rock bands, the stability will be greatly impeded. Joints and bedding planes also add weakness to the surface. Stability of the slope also depends on the available strength of the shear along the surface, its orientation towards the slope and the action of the water pressure on the surface. The shear strength that can be deployed along the joint surface based on the surface's functional properties and the stress that is transmitted to the surface as normal. Joints can make a situation where a combination of joint sets creates a surface cross.

1.7.3. Lithology

Rock materials that form a pit slope determine the strength of the rock mass modified by, faulting, weathering, discontinuities, past operations and folding. The strength of low rock mass is characterized by circular; stability is restricted by ravelling and rock falling, such as the slope formation in a massive sandstone. Pit slopes with weathered rocks or alluvium on the surface have low shear strength, and if water flows through them, the strength will be further reduced. These kinds of slopes have to be flatter.

1.7.4. Ground water

Following modifications, the existence of ground water is the reason:

a) It alters the parameters of cohesion and friction.

b) It decrease the normal stress

It can cause increased thrust or even deriving forces and has a extremely adverse impact on the stability of the slopes. Both physical and chemical effects of water in joints can change the friction and cohesion of the surface of discontinuity. Physical influence decrease the shearing resistance along a failure plane by elevating reducing the frictional resistance and the joints so thus decreasing the normal stress.

1.7.5 Dynamic forces

Due to the vibration induced by the blasting process, shear stress is increased, maximizing the dynamic acceleration for the material, which in turn creates slope plane instability. That accelerates ground motion resulting in rock fracturing. Because of the blasting process, the angles of the bench face also increase. The impacts of poor blasting methods are caused by bench instability. Because of back break and blast damage, these variables also influence rock mass failure i.e. bench face angle, blasting vibrations. Many soft blasting methods have been implemented to decrease these implications for small-scale slopes. In the event of bigger slopes, blasting has less adverse effects on the general stable slope angle due to back break and blast harm of benches. The high frequency waves generated as a result of the blasting 12 P a g e method ban big rock masses in the displacement method. Blasting-induced defects are therefore a tiny issue for large-scale slopes.

1.7.6 Internal friction angle

It is the angle between the resulting force and the normal force when the shearing stress causes the failure to occur. Internal friction angle is a measurement of any material capable of withstanding shear stress amount. The factors are responsible about soil grains roundness, quartz content and particle size.

1.7.7 Cohesion

Cohesion is the property of material that measures to resist deforming or breaking force. As a result of the loading process, it is also caused by negative capillary pressure and pore pressure or by electrostatic forces for over-associated clay. Slopes with less strength of cohesion are less stable.

Cohesive force factors are:

a. Friction.

b. Particular stickiness.

c. Grains cementation by silica or calcite.

d. Artificial reinforcement.

e. Content of water.

f. Repeated wetting and drying expansion or contraction.

g. Downhill in slopes.

h. Earthquake or blast vibrations.

1.8 Factor of Safety

Simply FOS is the ratio of resisting force of driving force F = $\frac{S}{\tau}$ (Duncan, Wright, & Brandon, 2014), or ratio of shear strength to that needed to keep the slope stable in case only stable slope without any structure on it.

The collapse of any slope is due to the inability of the shear resistance of the sliding block to overcome the shear stresses. Safety action is the value through which the stability state of the slopes is checked.

As it is mentioned before there are two types of slopes, soil slopes and rock slopes. In this study the soil slopes are modeled and analyzed, but rock slopes will be discussed as well. Analysis of rock slopes stabilization is a branch of rock engineering that is extremely likely to be treated with probabilism. Probabilistic assessment of rock slope stabilization was used as an efficient tool for assessing uncertainty in variables and gained significant attention in the literature.

Figure 1.9 illustrates planar sliding rock slope and its parameters. The equation for determining the factor of safety can be articulated for this type of sliding failure as:

$$FOS = \frac{cA+(W(\cos\psi_p-\alpha \sin\psi_p)-U-F_w\sin\psi_p)\tan\emptyset}{W(\sin\psi_p+\alpha\cos\psi_p)+F_w\cos\psi_p} \quad (1.1)$$

$$Z = H(1-\sqrt{cot\psi_f\ tan\psi_p}\ ) \quad (1.2)$$

$$W = \frac{\gamma H^2}{2}[(1-(\frac{Z}{H})^2)\ cot\psi_p - \cot\psi_f \quad (1.3)$$

$$U = \frac{\gamma_w Z_w A}{2} \quad (1.4)$$

$$F_w = \frac{\gamma_w Z_w^2}{2} \quad (1.5)$$

$$A = \frac{H-Z}{sin\psi_p} \quad (1.6)$$

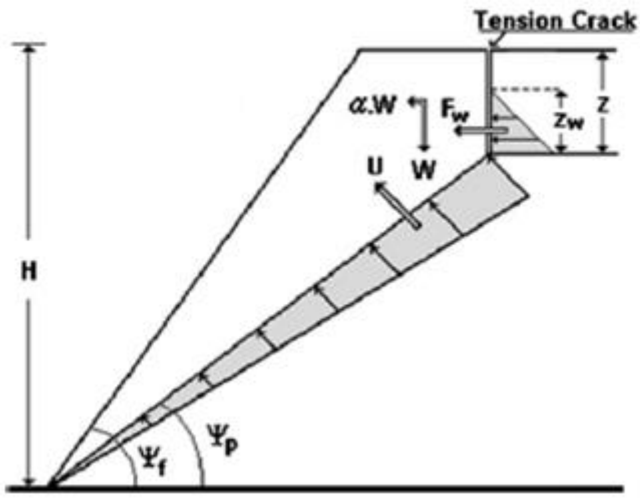

Figure 1.9: Rock slope geometrical definition with plane slipping. (A.Johari et al 2013)

Where;

FOS; the factor of safety contra slipping

Z; tension crack depth

Z_w; water in tension crack depth.

A; wedge area

W; rock wedge weight resting on failure surface.

H; the overall height of the slope

U; uplift force due to water pressure for failure surface

F_w: the horizontal force for water in crack, a is the acceleration of horizontal earthquake

C; cohesive strength over sliding surface

Ø; sliding surface friction angle

ψ_p; failure surface angle (measured from horizontal)

ψ_f; slope face angle (measured from horizontal)

γ_r; rock's unit weight

γ_w; water unit weight

Factor of safety guidelines values for different cases are shown in Table 1.1

Table 1.1: Factor of safety values guidelines (Suman, 2015)

Factor of safety value	**Details of the slope**
FOS < 1.0	Unsafe
FOS between 1.0 and 1.25	Questionable Safety
FOS between 1.25 and 1.4	Satisfactory for routine cuts and fills but questionable for dams, or where failure would be catastrophic
FOS > 1.4	Satisfactory for dams

For extremely unlikely loading conditions, factor of safety can be as small as 1.2-1.25, even for dams. E.g. situations based on seismic impacts, or where the water level in a reservoir is rapidly declining. (Suman, 2015).

Mitchell et al., 1993 and Duncan (1992) found that factor of safety which calculated by using 3D analyzes will always be higher than or equal to the factor of safety calculated by using 2D analyzes. There are various methods for formulating factor of safety, usually each of the techniques of analysis has its own formula for FOS, but the most popular formula assumes that the FOS is constant and can be divided into two types: Moment equilibrium and Force equilibrium (Cheng & Lau, 2008).

1.9 Organization of Thesis

This thesis is made up of 5 chapters:

Chapter 1: This chapter gives the general information regarding slope stability in addition to its factors, types and common cases of slope failure. The aims, objectives, scope and limitations of research are also stated.

Chapter 2: This chapter presents literature review which it discussed stability of the slope analysis methods, a general view about infinite slopes and slip surface seeking approaches, comparison between slope stability analysis methods, relationship between soil strength parameters, location of failure surface, and overview about some previous studies about 2D and 3D analyzing methods.

Chapter 3: This chapter is the methodology which it introduces and discusses software programs and methods that were used in this thesis.

Chapter 4: This chapter presents the results of thesis which it studies the effect of each soil strength parameter, cohesion, unit weight and internal friction angle (c, γ, and ϕ) on the factor of safety FOS, both together and separately. In the first part of this study, in order to determine the trend of changes in FOS and failure surface, the number of models have been studied is limited, and in the second part, to find an accurate relationship between the strength parameters of soil and the surface of failure, various number of models were analyzed. After all the models were generated and analyzed, figures were drawn to show the effects of the variables on factor of safety and failure surface. In addition, the reasons for these different behaviors were discussed.

Chapter 5: This chapter presents the conclusions and recommendations for future actions to be taken.

At the end in the references part the resources used for this study are presented.

CHAPTER 2

LITERATURE REVIEW

2.1 Introduction

In this part a studies will be presented on stability of the slope analysing methods, a general view about infinite slopes and slip surface seeking approaches and relationship between soil strength factors and location of failure surface.

As it has mentioned recently there're two types of slopes

Finite slopes

Infinite slopes

2.2 Infinite Slopes

This part shows the similar infinite slopes development descriptions and equations of different cases to calculate FOS for infinite and long slopes. The reason this study stems from a renewed interest in the dynamics of deep landslides and the require for a more basic method to long slope studies for depth variation in soil properties. The Standard utilize of infinite slopes equations for both cohesive and frictional soils provides a factor of safety Assuming a critical failure plane and a homogeneous soil profile parallel to the surface of the soil at the full depth of the soil (Griffiths et al., 2010).
Some of the earlier studies on this topic concentrated on shear stress mechanisms and stress in an infinite slope, and also analysing of displacements and strains 1D and 2D.

More specific, (Runesson & Wiberg, 1984) and (Wiberg. 1990) presented a finite element method to infinite slopes on the basis of the principle of strain softening behavior and limit equilibrium. Another group of researchers like (Iverson, 1990) and (Bromhead & Martin, 2004) found the impact of streams of groundwater and lateral (3D) streams on landslides and estimated the effect of infiltration on surface slope stability using an infinite slope analysis (Cho & Lee, 2002) and (Tsai & Yang, 2006). More previously, (Yang. 2007) considered the impact of horizontal acceleration on land slide seismic stability through the equations of slope stability.

2.2.1 Dry condition

Dry condition happen when the level of water table lower than shear plane, to find the shear and normal forces by equations down below and the details of the slope's cross section shown in Figure 2.1.

$$N = W^{*}\sin\alpha \text{ (stable the slope)} \tag{2.1}$$

$$T = W^{*}\cos\alpha \text{ (cause the failure)} \tag{2.2}$$

Where: W: the weight of the slope section.

α: the angle between the slope and horizon.

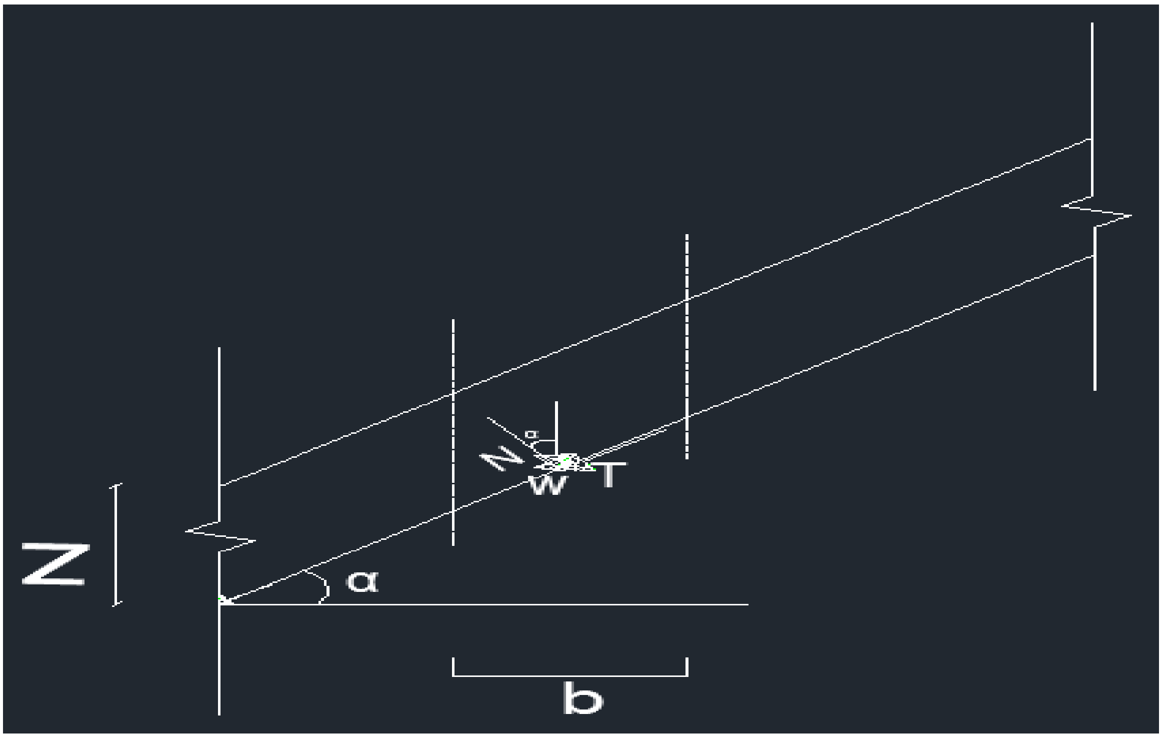

Figure 2.1: Details for infinite slope

$$W = ɤ*A = ɤ*b*Z \quad (2.3)$$

$$Ơ = \frac{N}{A} = \frac{ɤ*b*z*cos\alpha}{\frac{b}{cos\alpha}*1} = ɤ* Z*cos^2\alpha \quad (2.4)$$

$$Ƭ = \frac{T}{A} = \frac{ɤ*b*z*sin\alpha}{\frac{b}{cos\alpha}*1} = ɤ*Z*sin\alpha*cos\alpha \quad (2.5)$$

A is the area resist the collapse.

The max stress soil can resist is $Ƭr = C + \sigma \tan Ø = C + ɤ* Z*cos^2\alpha*\tan Ø$ (2.6)

$$FOS = \frac{C + ɤ* Z*cos2\alpha*\tan Ø}{ɤ*Z*sin\alpha*cos\alpha} \quad (2.7)$$

$FOS = \frac{C}{ɤ*Z*sin\alpha*cos\alpha} + \frac{\tan Ø}{\tan\alpha}$ this formula for C-Ø soil.

For Ø-soil (C=0) $FOS = \frac{\tan Ø}{\tan\alpha}$ (2.8)

This formula is very important for site work because by finding the internal friction angle of the soil needed to build on we can determine the slope angle by giving the factor of safety value of 1, so the slope angle (α) will be equal to internal friction angle Ø.

2.2.2 Condition with seepage

FOS for infinite slopes in seepage case is the same of dry case but multiplied by the value $\frac{ɤ(sub)}{ɤ(sat)}$ as presented in equations down below.

$$FOS = \frac{C}{ɤ*Z*sin\alpha*cos\alpha} + \frac{\tan Ø}{\tan\alpha}*\frac{ɤ(sub)}{ɤ(sat)} \quad (2.9)$$

Example: by giving specific gravity, Gs and water content, Wc to find void ratio,e, use the equation

$$e*Sr = Gs*Wc \quad (2.10)$$

since the soil is saturated, Sr = 1, so we can determine the value of e.

Then find $ɤ_{sat}$ and $ɤ_{sub}$ by the formulas

$$ɤ_{sub}= ɤ_{sat}- ɤ \quad (2.11)$$

$$\gamma_{sat} = \frac{Gs+e}{1+e} * \gamma_w \quad (2.12)$$

2.3 Finite Slopes

There are numerous methods available to select from and use to analyze the slope stability. As nowadays, no method of analysing is prioritize atop other methods, so the engineer is entirely responsible for the reliability of any solution (Albataineh, 2006).

The techniques are divided in two main types according to their procedure:

Limit equilibrium methods

Finite element methods

2.3.1 Difference between LEM and FEM

Although limit equilibrium techniques are easier to utilize, consumes less time, and is useable for hand calculations, the limitations arises when it comes to calculating forces specially in the slope’s parts that localized stress focusing is high so because of the limitations, factor of safety in limit equilibrium techniques become a little higher (Arryal, 2008; Khabbaz, Fatahi, & Nucifora, 2012), furthermore, some executors think that finite element techniques are more powerful especially in states with compound conditions. (Duncan, 1996).

While also, many of the executors think that the outputs of LEM and FEM are almost the same (Azadmanesh&Arafati, 2012, Wright G, 1969, Wright, Kulhuwy, & Dumcan, 1973) also Chang thinks this convention, except phi that is greater than 0 (Chang, Lansivara & Wei, 2007). Although both LEM and FEM have their disadvantages and advantages , neither of them are routinely analyzed is ascendant to the other one (Cheng, Lansivara, & Wei, 2007). Each one of those techniques are divided into two groups depend on their numbers of dimensions to two dimensional methods and three dimensional methods.

2.3.2 Finite element methods

The FEM is a numerical analysing method to obtain accurate solutions for various engineering troubles although it had originally been developed to be used `in the study of stresses on structures of complex aircraft structures(Oghli, 2011), but from that time it has been developed to be widely applied in different engineering fields.

Although the finite element method appeared in 1960 when it was used before by Clough to solve flat flexibility issues, the ideas of finite element analysis date back to a date beyond. In 1943 Variant Courant used the Vibrational methods, then in 1956 Martin, Topp and Clough used the finite element method for calculating stiffness (Oghli, 2011).

Analysis using finite element method

Finite element analysis depends on the following idea that: any complex form can be divided into a group of small elements to make it easy to deal with, a very simple and common idea used everywhere in the working life as in engineering.

The solution is using the finite element method by following the steps.

1. Divide the structure to be studied using the finite element method to a number of the limited geometric forms as shown in Figure 2.2.

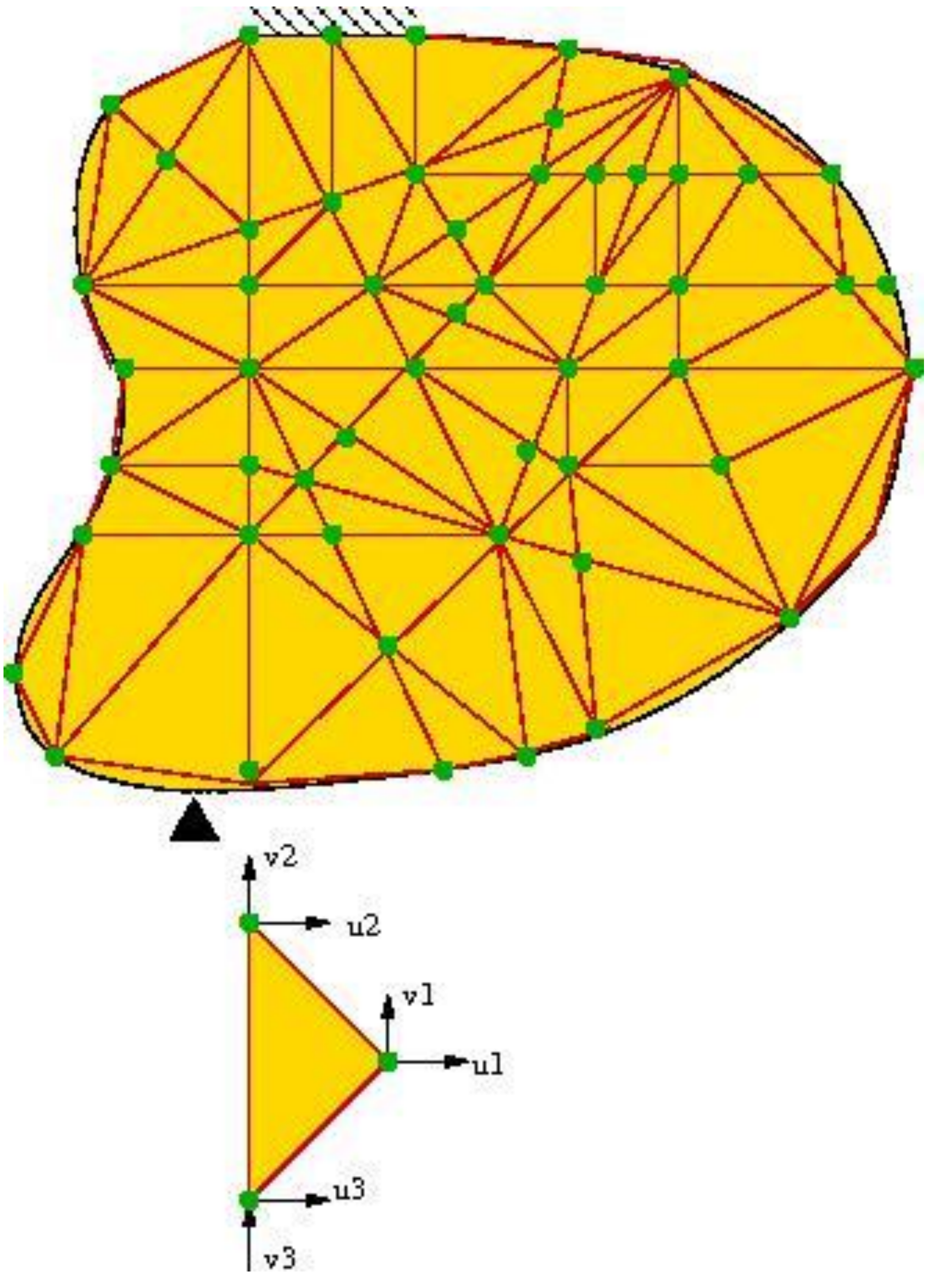

Figure 2.2: Divide the structure to many geometric forms (Oghli,2011)

2. Start by solving each of the limited elements using the local coordinates grid for each element.

3. Compiling solutions on the network of local coordinates to solutions on the network coordinates.

4. Checking solutions If the solutions are not convergent, the 2 and 3 steps must be repeated.

5. Evaluating the solution when solutions converge.

Before starting the solution, it is necessary to define the element: a small piece of body that is characterized by:

a- Elements’s type, if the element is structure span, pillar or slope.

b- Elements’s dimensions if it is a linear element, one deminsional,1D such as spring, triangle and tube. Or a standard element (2D) such as cortical, plate, membrane. Or a volume element (3D) such as finding transitions, stresses, and flow velocity.

c- The number of degrees of freedom for each nodes, transitions androtations.

d- The shape of the element.

Finite element technique uses a similar mechanism of failure to limit equilibrium methods and the major difference between those procedures is the use of FEM capacity, which does not require simplification of the presumptions.

In general, this procedure firstly proposes a slip surface failure, and then FOS which will be calculated, is implemented to compute the ratio of usable forces of resist to the deriving forces.

There are two more useful methods of FEM:

Shear reduction method

Increase gravity method

Shear reduction method (SRM)

Since the factor of safety doesn’t defined by a single definition, the most important one is the definition it presented by Duncan (1996) which it “the ratio of actual shear resistance to the minimal shear resistance that necessary to prevent breakdown”, or the factor that makes the shear resistance fall to the point where the slope becomes the edge of the failure.

Shear reduction method (SRM) based on the slope stability analysis studied using the method of finite elements, which depends on the analysis of the stresses and displacements of the slope by reducing the shear resistance values from cohesion and friction (Oghli, 2011).

The slope will reach a point where it cannot be achieved analysis of its stability using finite element method where the transitions will be large on the slope and the collapse of the slope will occur, therefore we will get the value of FOS of the modeled slope without the need to determine the shape or the surface of the sliding surface, as well as the side forces affecting the slides and slopes.

In SRM, the soil strength parameters will be reduced till the slope fall so the FOS become the ratio between real strength parameters and critical parameters. The factor of safety definition in SRM is the same as that of limit equilibrium method (Griffiths & Lane, 1999).

Increasing gravity method is more frequently favored to test the slope stability in the construction cases, as its results are more credible, meanwhile SRM is more effective to test the existed slopes. (Matsui & San, 1992).

Gravity increase method

In this method, gravity forces increases little by little until slope fails. This force value is called the failure gravity, g_f.

Factor of safety in this method is the proportion of failure gravitational acceleration and the actual acceleration of the gravity (Swan & Seo, 1999).

$$\text{FOS} = \frac{gf}{g} \qquad (2.13)$$

When: gf ⟶ The raised gravity at the failure level

g ⟶ The main gravity

2.3.3 Limit equilibrium methods

As it has mentioned before there are two types of methods, two-dimensional methods and three dimensional methods and since this study work on two dimensional methods so will start with it.

Two dimensional methods also subdivided in three different groups:

1. Circular Methods

2. Non-Circular Method and

3. Methods of Slices

Circular methods

Swedish circle

The Swedish Circle method is the simplest procedure used in analyzing the short term stability of slopes disrespect to its inhomogeneous or homogeneous state.

This is a method that analyze the slopes stability by considering two simple assumptions, a rigid cylindrical block of soil can fall by rotating round its center with assuming Phi is 0. For that, the only resist moment or force is going to be the cohesion and the driving moment simply will be cylindrical failure soil’s weight.

From this method, the FOS was defined as ratio of resist (holding) force over driving force (Abramson, 2002). The figure 2.4 demonstrates the holding forces and driving forces applying on the soil block.

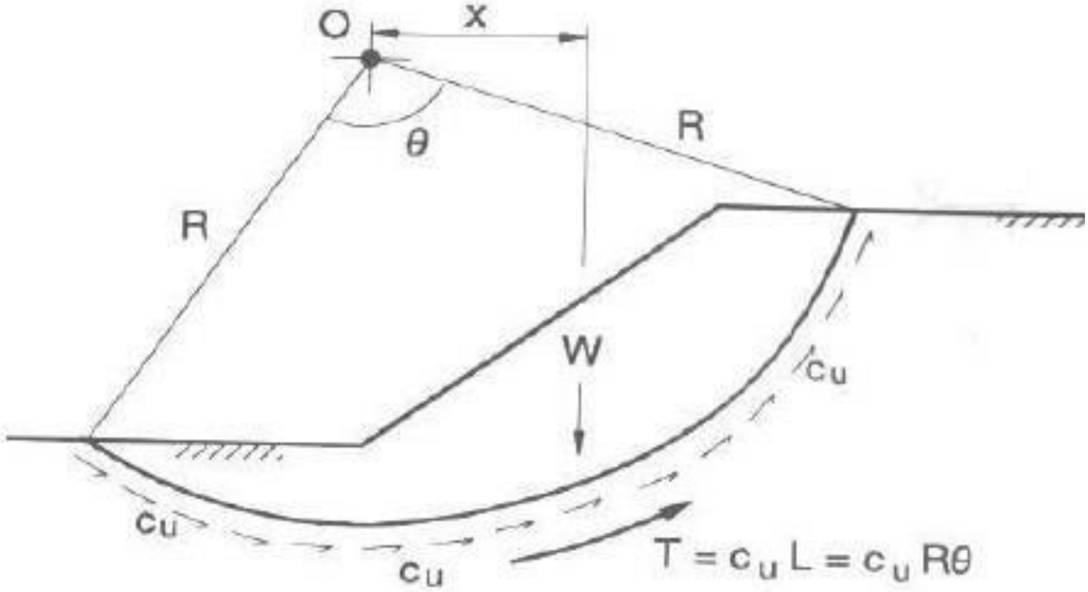

Figure 2.3: Swedish circle's details (Abramson 2002)

The algorithm about Swedish method presented in the following equations

$Z = C + \sigma \tan\text{Ø}$ (2.14)

$C = C'{*}l$ (2.15)

Frictional force = $\sigma \tan\text{Ø} = N \tan\text{Ø}$ (2.16)

Resisting force = $\sum (C'{*}\,l) + \sum (N \tan\text{Ø})$ (2.17)

Disturbing force = $\sum T$ (2.18)

Resisting moment: $R\ \{\sum (C'{*}\,l) + \sum (N \tan\text{Ø})\}$ (2.19)

Disturbing moment: $\sum T{*}R$ (2.20)

$$\text{FOS} = \frac{\text{Resisting force}}{\text{Disturbing moment}} = \frac{R\{\sum (C'{*}l)\ + \sum (N \tan\text{Ø})\}}{\sum T{*}R} = \frac{\sum (C'{*}l)\ + \sum (N \tan\text{Ø})}{\sum T} \quad (2.21)$$

Where: $T = W \sin\alpha$ (2,1)

$N = W \cos\alpha$ (2,2)

$$FOS = \frac{\sum (C' * l) + \sum (W.\cos\alpha.\tan\emptyset)}{\sum W \sin\alpha} \quad (2.21)$$

The friction circle method

This procedure was developed in order study of homogeneous soils with internal friction greater than 0. In this procedure the resulting shear strength (frictional and normal forces) affect on the failed slip surface to form which is named as friction circle (FC), with a radius of R_f. Figure 2.6 demonstrates the FC. R_f could be deduced by using the equation below (Abramson 2002):

$$R_f = R \sin \emptyset_m \quad (2.21)$$

Where: R → radius of failure circle.

$\emptyset_m$ → the affected friction angle, could be computed by using.

$$\emptyset_m = \tan^{-1} \frac{\emptyset}{F\emptyset} \quad (2.22)$$

Where: F_φ is factor of safety contra the resistance of friction.

This precedure utilizes a repetitive computation. Abramson et al. (1996) recommended the following methodology to find FOS

1) Finding out the slip weight (W).

2) Finding out the greatness and direction of the resultant pore water pressure (U).

3) Finding out the perpendicular length to the action's line, C_m, R_c that could be found using:

$$Rc = \frac{Lasssrc}{Lchord} . R \quad (2.23)$$

The lengths are these the lengths of circular cord and arc define the mass of failure.

4) Computing the effective weight resulting from U and W forces and the intersection of

Cm at A.

5) Assuming a value for F_{φ}

6) Calculating φ_m

7) Using to draw the frictional angle.

8) Drawing the polygon force with w, suitably raised, and pass over A

9) Drawing the direction of P, resulting from the friction circle's frictional and normal forces tangential

10) Drawing Cm direction, according to the chord inclination joining the end points of the surface of the FC

11) Then the closed polygon gives the value of Cm

12) By finding the value of Cm, finding the value Fc

$$F= \frac{cLchord}{Cm} \tag{2.24}$$

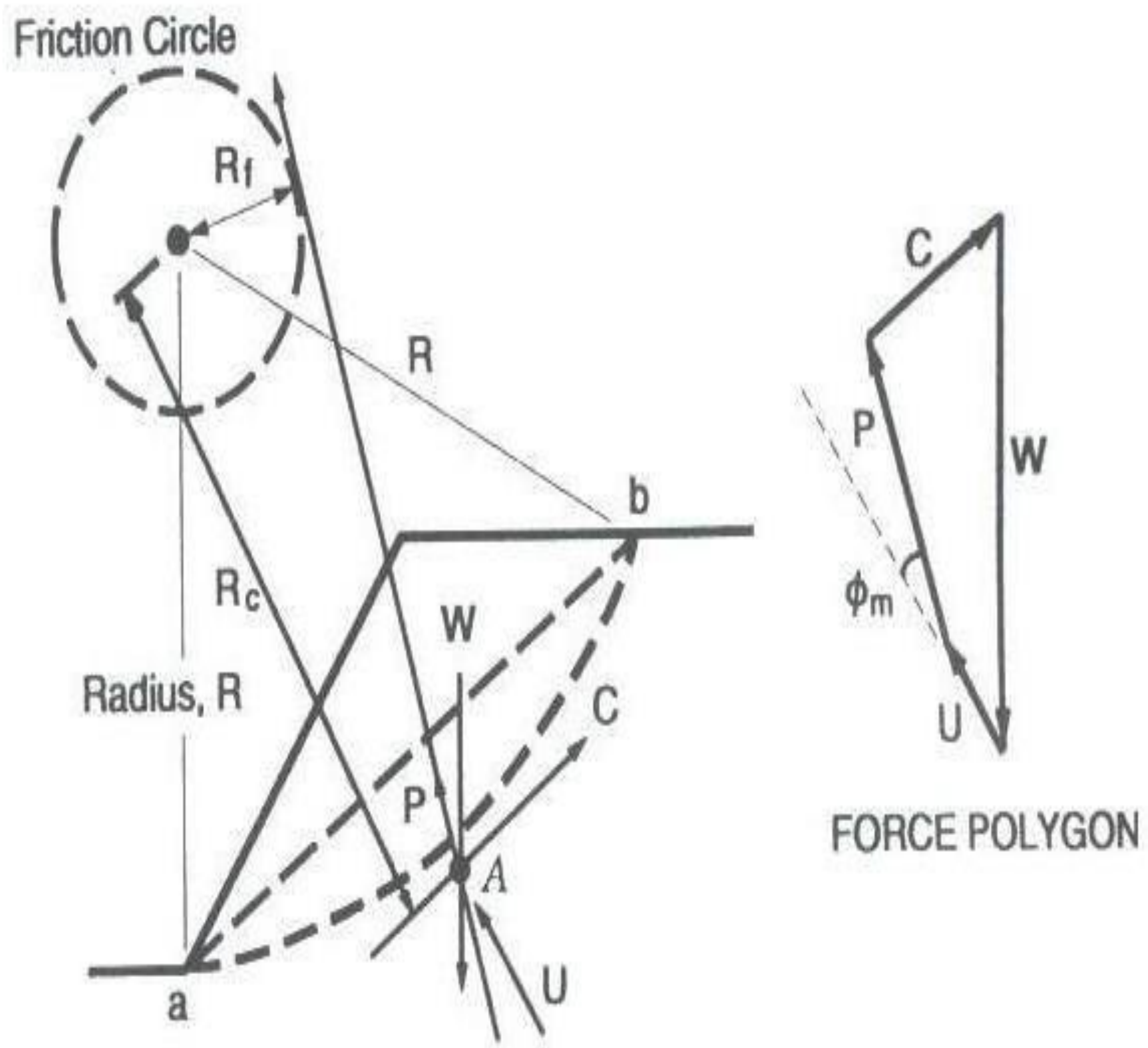

Figure 2.4: Friction circle method (Abramson 2002)

Non circular methods

Log spiral procedure

In this method, the failure surface will be assumed and use the equation below to deduce the radius to have a logarithmic composition.

$$r = r_0 e^{\theta \tan Ø d} \qquad (2.25)$$

Where r_0 → The initial radius

θ → Angle between r and r_0

φ_d → The transposal Phi

The normal and shear strengths on the slip can be computed using the equations below:

$$\tau = \frac{C}{F} + \sigma \frac{\tan Ø}{F} \qquad (2.26)$$

$$\tau = c_d + \sigma \tan Ø_d \qquad (2.27)$$

Where c, φ → the shear strength parameters

c_d, φ_d → the developed friction angle and cohesion

F → factor of safety

Assuming this particular shape shown in Figure 2.8, frictional force and normal force will pass from the center of the spiral, so there will be no momentum about the center. The developed cohesion and soil weight will therefore be the only moment producing forces.

Having the developed friction presented in the r equation (2.25). This procedure is also a repetitive process, therefore to achieve a FOS that satisfies the formula (J Michel Duran & Wight, 2005) several trials should be done.

$$F = \frac{C}{Cd} = \frac{tan\varphi}{tan\varphi d} \quad (2.28)$$

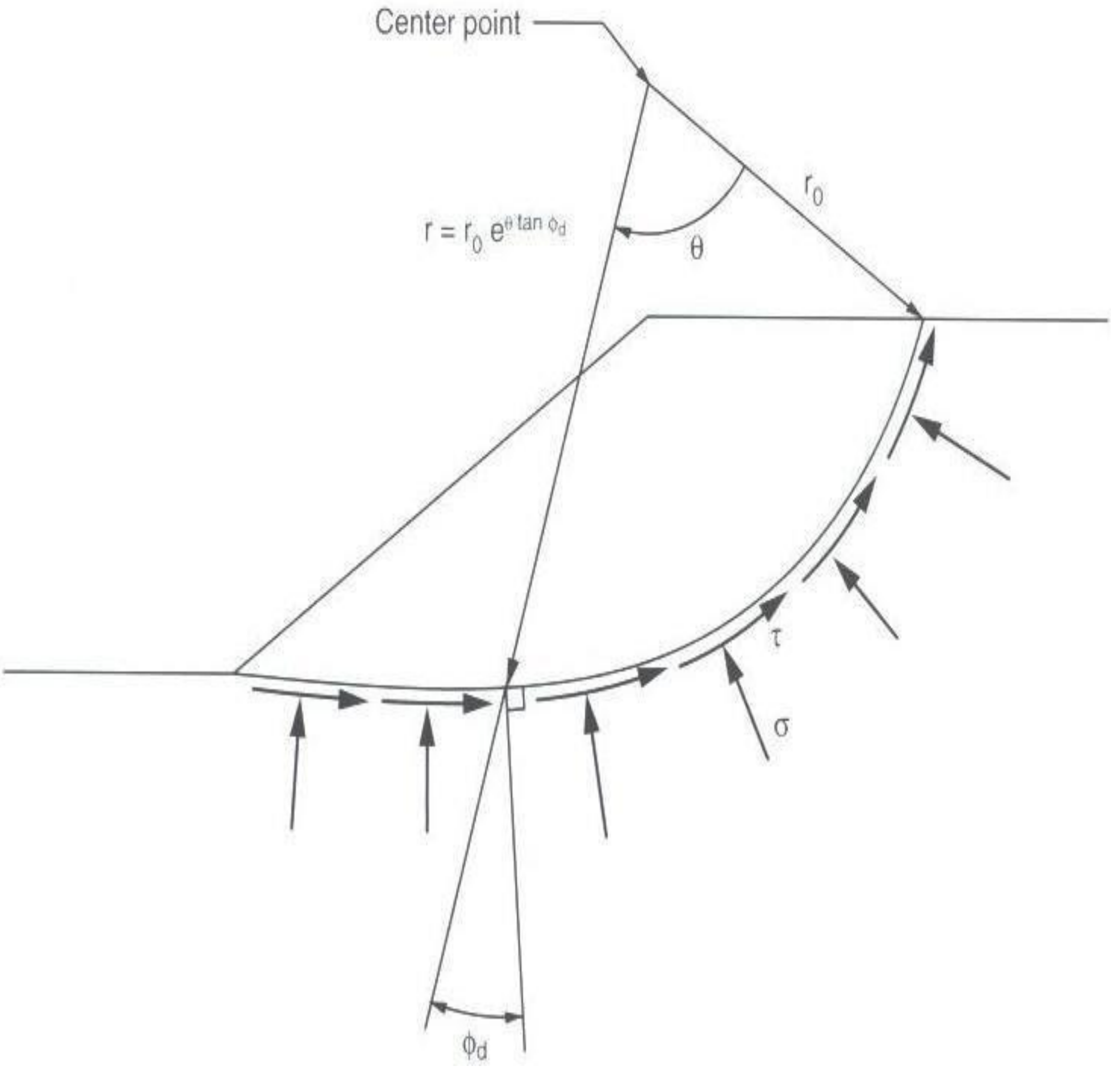

Figure 2.5: Log Spiral procedure (Duran and Wight, 2005)

In this procedure, knowing the slip fail surface is very influential cause the method begins by finding a center of the spiral and an R_0.

Methods of slices

In this method soil density over the fail area will be subdivided in many slices vertically and the balance of every slice will be studied individually. However, the splitting of a static trouble in many parts doesn't make it statically found, therefore, to make it solvable, an assumption is needed. These methods will be distinguished by classifying these hypotheses.

Again, the important issue here is that knowing the surface of failure is important in these methods as those techniques are primarily focused on the soil mass division of the slip. Number of more realistic techniques for this sort would be discussed.

Ordinary method of slices

This method assume this the resulting inter slice forces in every vertical slice are parallel to their basement and are therefore ignored and satisfied only at the balance moment.

Researches (Whitnan, Baley, 1967) showed that FOSs computed using this technique is sometime as conservative as 60 % compared to more accurate techniques, so this procedure isn't much used nowadays.

In order to the slice shown in Figure 2.9, the Mohr Coulomb fail criterion is:

$$s = c' + [\sigma - u] \tan\emptyset' \quad (2.29)$$

Use FOS, $t = s / F$, $P = s \times$, $T = t \times l$, the formula becomes:

$$T = \frac{1}{F}[c' l + [P - ul]] \tan\emptyset' \quad (2.30)$$

Having neglected inter slice force leads to make the normal forces at the basement of the slice as follows:

$$P = w * \cos\alpha \quad (2.31)$$

Where w ⟶ the weight of slice

α ⟶ the angle between center of slide base tangent and the global vertical.

The moment will be around the center of the shape of the slope failure:

$$\sum W * R * \sin \alpha = \sum T * R \qquad (2.32)$$

Therefore:

$$FOS = \frac{\sum(c' l + \{w * \cos \alpha - ul\} * \tan \emptyset')}{\sum \quad W * \sin \alpha} \qquad (2.33)$$

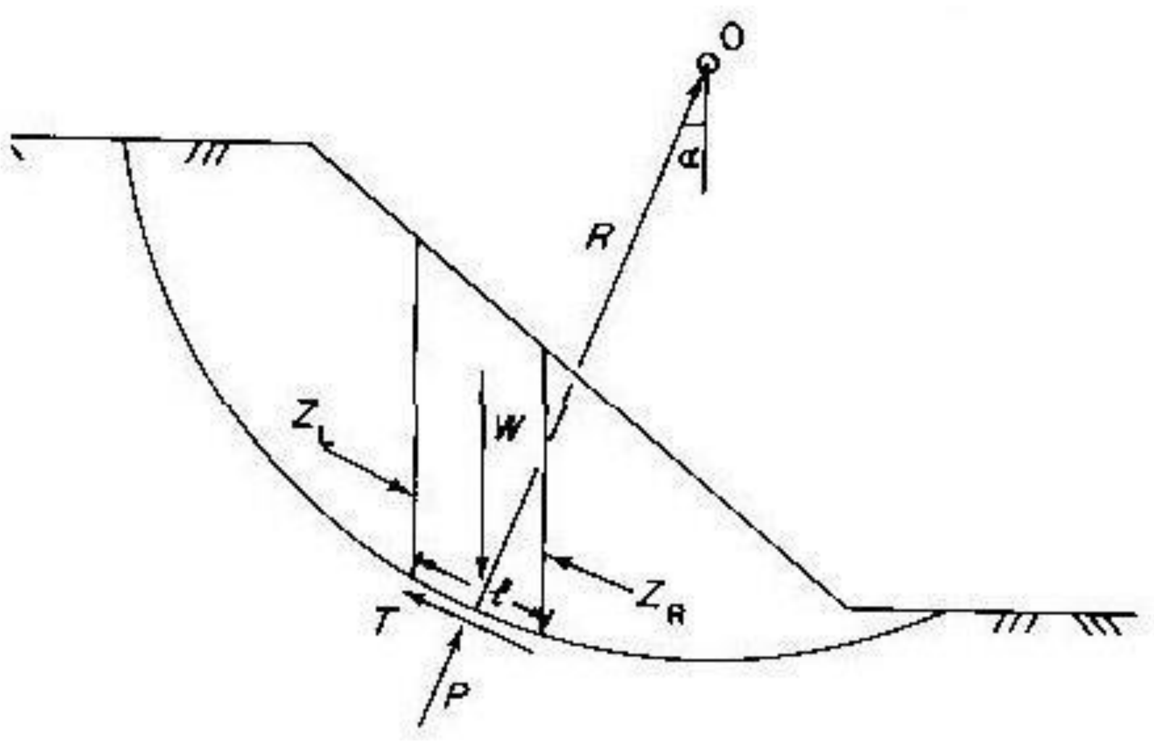

Figure. 2.6: Ordinary method of slices (Anderson, M. G., & Richards, K. S. 1987)

As shown in this method, calculating FOS hiring this method again requires knowing the surface of the failure (Anderson & Richards, 1987).

Simplified bishop method

By using this technique to find FOS, we assume the fail occurs as shown in Figure 2.10 by rotating the soil circular mass. Meanwhile the forces in-between all the slices are regarded horizontally, between them there is no active shear stress. Each slice's normal force (P) is supposed to behave on the center of every base. Using equation this stress can be calculated.

$$P = \frac{[W - 1/F(c' * l * \sin\alpha - ul * \tan\emptyset' * \sin\alpha]}{Ma} \quad (2.34)$$

Where:

$$Ma = \cos\alpha + \frac{(\sin\alpha * \tan\emptyset\prime)}{F} \quad (2.35)$$

By taking moment around the center of circle:

$$F = \Sigma \frac{c' * l * \cos\alpha + (w - ul * \cos\alpha)\tan\emptyset\prime}{\cos\alpha + (\sin\alpha * \tan\emptyset'/F)} / \Sigma W\sin \quad (2.36)$$

This forces us to solve it iteratively, As the equation demonstrates, F is on both sides. This method is generally fast and gives-out a relatively accurate response, with a 5% variation in FEM, so it is appropriate for hand computations (Andresen and Richard, 1987).

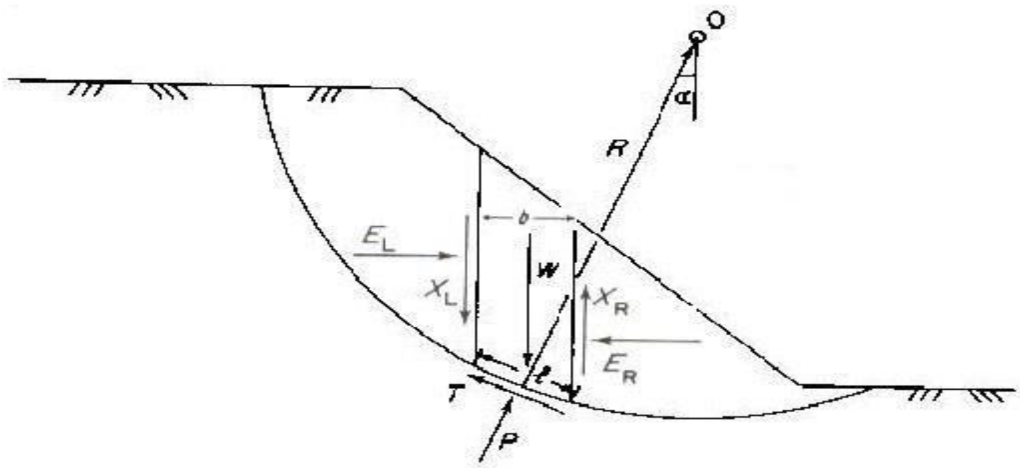

Figure 2.7: Simplified-Bishop procedure (Anderson, M. G., & Richards, K. S. 1987).

Like the other methods, the failure surface needs to be assigned at the beginning.

Spencer method

Even though the Spencer technique was described for the surface of circular failure, by assuming a frictional center of rotation it was easily extended for non - circular slips. They will have the same tendency by assuming parallel inter slices forces:

$$\tan\theta = \frac{X1}{E1} = \frac{Xr}{Er} \quad (2.36)$$

Where: $\theta \longrightarrow$ the angle of the inter slices forces horizontally

The force at the base of the every slice is going to be as below by the summation of forces perpendicular for the inter slices.

$$P = \frac{W-(Er-El)\tan\theta-1/F(c'l\sin\alpha-ul\tan\text{Ø}'\sin\alpha)}{m\alpha} \quad (2.37)$$

Where

$$m_{\alpha} = \cos\alpha\,(1+\tan\alpha\,\tan\text{Ø}'/F) \quad (2.38)$$

Two different factor of safetys will be extracted by supposing the total moment and force equilibrium in Figure 2.10, this is due to the over-specified maximum assumptions.

From the moment of equilibrium to find FOS, by taking moment around O:

$$\Sigma W*R*\sin\alpha = \Sigma T*R \quad (2.39)$$

Where:

$$T = \frac{1}{F}\,(c'l+(p-ul)\tan\text{Ø}' \quad (2.40)$$

$$Fm=\Sigma(c'l+(p-ul)\tan\text{Ø}'\Sigma W\sin\alpha \quad (2.41)$$

FOS from force equilibrium, while $\Sigma F_{H0}=0$ in consideration:

$$T\cos\alpha-P\sin\alpha+E_R-E_L=0 \quad (2.42)$$

$$\Sigma E_R - E_L = \Sigma P \sin\alpha - 1 F_f ⁄ \Sigma(c'l + (P - ul)\tan\varnothing') \cos\alpha \qquad (2.43)$$

Using the Spencer's assumption ($\tan\theta = XlEl = cte$) and $\Sigma XR - XL = 0$, in surface loading absence:

$$F_f = \frac{\Sigma(c'l + [P - ul]\tan\varnothing')\sec\alpha}{\Sigma(W - (XR - XL))\tan\alpha} \qquad (2.44)$$

The method of trial and error should be used to evaluate the factor of safety that meets both formulas.

Spencer studied this technique and demonstrates that both the FOS values achieved from both of equations will be equal at a precise angle for inter slice forces, and that this value will be regarded as the factor of safety (Spencer, 1967).

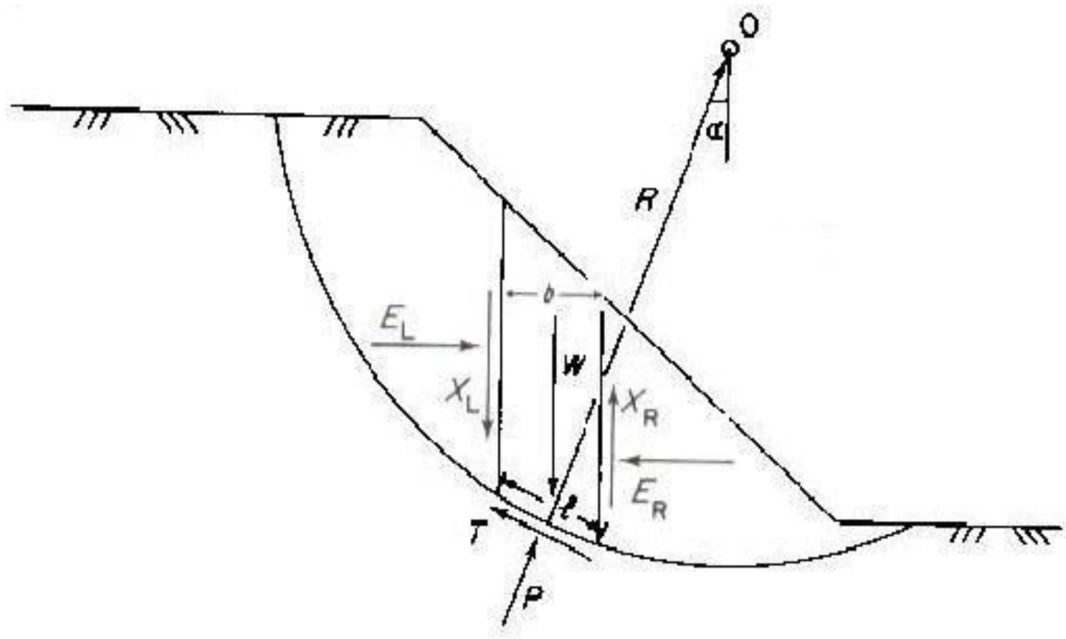

Figure 2.8: Spencer method (Andresen, M. G., & Richards, K. S. 1987)

And again, it is important to have the correct surface of failure in this method.

2.3.4. Previous studies on analyzing 2D slope stability

Table 2.2 shows some studies on 2D slope stability analyzing have done by researchers and students.

Table 2.1: Previous studies analyzing 2D slope stability

Author	Method	Software
(Chok, 2008)	Limit Equilibrium method, The random finite element method (RFEM)	Neuframe SLOPE/W
(Adams, 2015)	the Swedish method of slices	HOBO Micro Station HOBOware
(Ekstrand & Nylander, 2013)	Method of slices	SLOPE GeoSuite
(Nor, 2010)	Ordinary, Bishop, Janbu dan Morgenstern-Price methods	GeoStudio 2007
(Xiao, Yan, & Cheng, 2011)	Limit Equilibrium method (Spencer method	ANSYS
(Oghli 2011)	Limit equilibrium method (Bishop method), FEM (SRM)	Slide5 Phase2
(Hammouri, Husein Malkawi, & Yamin, 2008)	Limit Equilibrium Method Finite element method	PLAXIS SAS-MCT
(Naderi 2013)	FEM LEM	GEO5,SLOPE/W FLAC/Slope
(Amini & Ardestani, 2019)	Finite element method	Dips Phase2

Author	Method	Software
(Kang, Han, Salgado, & Li, 2015)	Monte Carlo simulation Gaussian process regression (GPR)	MATlab (experiments)
(Suman, 2015)	LEM	FLAC/SLOPE
Farah, Ltifi, & Hassis, 2011)	LEM FEM	-
(Oh & Lu, 2015)	LEM FEM	-
(Widger, 1976)	Bishop's simplified method	-
(Xing, 1988)	LEM	-
(Zeroual Née Dadouche, Lazhar, & Zennir, 2011)	kinematic method of rigid solids	-
(Marquez D. V. Griffiths, 2007)	methods of columns, method of slices Limit equilibrium method	-
(Li, Li, Zhang, Yang, & Wang, 2015)	Least squares support machine algorithm	-

Chok, (2008) focuses on researching and quantifying the impacts on the stability of natural slopes of soil variation and vegetation. The soil variation is quantified by the parameters called coefficient of variation (COV) and fluctuation scale (SOF), while a slope's safety is evaluated using failure probability. Chok used the ANN and random finite element method, RFEM, to explore the COV and SOF impact on the probability of a cohesive slope failure (i.e. undrained clay slope) with distinct geometries. The findings acquired from the parametric research are then used to develop probabilistic stability charts. These charts can be used for a preliminary evaluation of a spatially random cohesive slope's probability of failure.

Adams, (2015) presented a study by using HOBOware software , the objective of his study was to determine the circumstances on softly sloped terrain resulting in regular slope instability. A perched water table, produced by excessive or intense precipitation events, was hypothesized to affect the slope stability in the region and result in intermittent landslide motion. Data collection operations included precipitation surveillance. Measurement of the height and magnitude of the perched water table that used a piezometer array, interpretation of the place and morphology of impermeable boundaries with radar penetration and assessment of relative slide movements. Field measurements indicate a correlation between the quantity of rainfall received and the shift in height over the impermeable surface of the water.; A slope stability analysis was conducted to quantify the likely stability conditions. Conditions leading to slope instability on gentle slopes were recognized in this research as precipitation falling on soils with high ambient moisture conditions, resulting in a perched water table being formed, The height of the perched water table need for motion is encountered seasonally, according to the safety assessment factor. Movement happened slowly because of the gentle slopes.

Ekstrand & Nylander, (2013) designed a probabilistic slope stability model. The probabilistic model questions the ordinary assumptions taken when assessing a slope's stability. These assumptions contain the size of traffic loads, how to apply water concentrations and how to calculate the impacts of underlying structures. Their research involves an investigation of the impact on stability measurements of anisotropic clay characteristics. Their study gathered the information needed for the model from Previous stability studies and soil investigation reports. The model was intended with fundamental statistical ideas and Swedish geotechnical guidelines from distinct geotechnical engineering fields. The final result shows which assumptions have the biggest effect on a slope's calculated stability. The findings suggest that underlying buildings and anisotropic clay behavior are often neglect main factors when it comes to calculating a slope's factor of safety.

Nor, (2010) presented in his study which happened in Malaysia sites to Determine the adequate cost for the slope protection chosen and compare the different slope stability analysis techniques used and thus. His research was conducted using Ordinary, Bishop, Janbu and Morgenstern-Price techniques based on two chosen slopes at Lot 4189, Bandar Tanjong Bungah, Jalan Selari Pantai Utara, Pulau Pinang. The analysis was conducted using GeoStudio (GEO/SLOPE) software. The evaluation result showed that the Morgenstem-Price technique was the realistic and acceptable technique that can be used to analyze both of the chosen slopes while the Reinforced concrete holding wall provides the optimum cost for both chosen slopes.

Xiao, Yan, & Cheng, (2011) described an accurate technique that combines LE and numerical analysis to identify prospective slide surfaces on slopes of soil . In this method, the direction of the critical surface at any point in a slope is defined by the use of the Coulomb strength principle and the extreme concept predicated on the ratio of the shear strength to the shear stress at that point. Once the soil slope stress field is acquired, the ratio, which is regarded as an evaluation index, can be calculated. His paper provides examples of the feasibility of the suggested technique programmed by macro instructions in ANSYS software.

Hammouri, Husein Malkawi, & Yamin, (2008) have used the main Both techniques are used to analyze homogeneous and inhomogeneous slopes, taking into consideration the condition of rapid drawdown, tension cracks, and undrained clay soils. PLAXIS (finite element technique) and SAS-MCT 4.0 (limit equilibrium technique) were used to perform the analyzes. Comparison is made between the factor of safety and place of the critical slip surface acquired from both techniques.

Amini & Ardestani, (2019) presented a study after A failure occurred in the Daralou copper open pit mine's north-eastern slope, in the 2015 season. Geological and geotechnical ground and sub-surface studies explained the mechanism of this instability. Next, the latest analytical method for evaluating the static slide-toe-top pling failure has been updated also new formulas have been made for dynamic failure analysis. After that a computer's code has been developed to test the instability on the basis of the new formulas. The failed slope was analyzed in the next step using the system of code and FE tecnique, and the results of those analyzes have been compared to real conditions. The analysis demonstrated that the theoretical, statistical and real tests were satisfactorily accepted. Thus, these approaches were used in static and dynamic conditions to expect the final slope's behavior. Such analyses showed this if relocated materials are fully dug up and taken out of the mine, the total dip of the slope will be decreased, the final slope gainst "slide toe toppling failure" will be stable. This study summarized the outcomes and concluded that a slope can be analyzed against the secondary toppling mode by both the adjusted analytical procedure and the FEM. In addition, the research shows this resloping and unloading are two effective approaches that could be used to stabilize the failure.

Farah, Ltifi, & Hassis, (2011), presented a solution of the slope stability problem analysis procedure and studied slope stability reliability analysis with soil spatial variability. By assuming till yield criteria, the elastic soil attitude assessed stresses mobilized through the slip surface to evaluate the efficiency function and analyzed the outcomes of SFEM (Stochastic FEM) and the LE method , such as the simplified method used by Bishops to check their efficiency and accuracy. They conducted an optimization strategy to search for critical slip surfaces, and also conducted sensitivity studies to examine the impact of random field variables used in soil spatial variation modeling.

Naderi (2013) Used FLAC/Slope, SLOPE/W and GEO5 software programs to determine the critical failure surface, analyze the slope stability problems and investigated the effectiveness and validity of these programs, by giving values of shear strength parameters: soil unit weight (γ), cohesion (c) and internal friction angle (ϕ) and investigate their effect on FOS value. Comparison and discussion of the results that obtained from different software programs. The study results showed that the slope's FOS changes with varying cohesion, internal friction angle and the unit weight. his results showed that, compared to SLOPE/W, GEO5 is more conservative slope stability analysis software. It gives 5% less factor of safety than SLOPE/W. In contrast to GEO5 and FLAC/Slope usually gives greater value for FOS.

Suman (2014) used the software program FLAC to carry out numerical models for rock slopes on his thesis “Soil Slope Stability Techniques: A Comprehensive Analysis ” by having different rock properties and various dimensions. The numerical modelling is performed for finding out the factor of safety. For each slope, the parameters are varied and the factor of safety calculated for each step. To find out how the factor of safety changes with changing parameters, these values are correlated with the bench parameters.

Oghli (2011) studied slope stability by Bishop based on LEM and Shear Strength Reduction SSR based on FEM and used the software packages SLIDE5 and PHASE2. So she applied on the homogeneous slope in two sides. First is a design side on the slope and the extent of the effect on ratio H/L on factor of safety by using the method SSR, second is mechanically by change the five parameters to the FOS by using finite element method (cohesion, friction, density, elasticity factor, Poisson factor) and the extent of the effect on FOS .The results obtained were merged to a mathematical model, through this model the factor of safety could be calculated for a homogeneous slope which the values of the factors affecting on FOS change by using the experimental design method.

Fei Kang et al (2014) evaluated the probability of slope stability based on system called Regression of the Gaussian method (GPR) and sampling of Latin hypercube. The analysis consists of three sections. Firstly, Latin hypercube sampling is used to create s amples to build the surface's response. Then, on the basis of the samples. Gaussian process regression, which is a common machine learning method for nonlinear system simulation, is used to evaluate the reaction of surface to estimate the limiting of state function. Monte Carlo simulation is conducted via e GPR surface's response to determine the slope’s probability system failure.
(Zevgolis et al, 2019) presented the landslide that happened on 12 June 2017 which was definitely an unprecedented occurrence in Greek lignite mining history and is possibly one of the biggest lignite mine landslides in the world. The slipping mass shifted from south to the north and occupied a huge area estimated to be between 2,98 and 3,56 km^2 depending on satellite images. Two independent committees (one by the Ministry of Environment and

Energy and the other by PPC) have been requested to evaluate the event, given the disastrous effects of the landslide. The two committees' findings were not yet released publicly. Nevertheless, a recent report released by the Greek Ombudsman's Independent Authority discusses the main conclusion of the studies of the two committees.

Three dimensional methods

Such procedures are centered on observing a fault surface 3D structure that is beneficial for more geometrically complicated slopes or meanwhile the material of the slope is strongly anisotropic or inhomogeneous.

Alike two dimensional technique, extra equations or in some situations both to obtain a statically defined situation,. In general, almost all of those techniques belong to the two dimensional methods. Even though the author won't debate about them in this research, it will introduce some of the most useful methods by name in Table 2.2. Please check the references in this thesis ' reference section for more information about them.

Table 2.2: 3-D analyzing methods for slope stability (Duncan, 1996)

Author	**Methods**
(Anagnosti, 1969	Extended Morgenston and Price
(Baligh and Azzouz, 1975	Extended circular arc
(Giger and Krizek, 1976	Upper bound theory of perfect plasticity
Baligh, Azzouz, & Ladd, 1977	Extended circular arc
Hovland, 1979	Extended Ordinary method of slices
A. Azzouz, Baligh, and Ladd, 1981	Extended Swedish Circle
Chen and Chameau, 1983	Extended Spencer
A. S. Azzouz and Baligh, 1983	Extended Swedish Circle
D Leshchinsky, Baker, & Silver, 1985	LE and variational analysis
Keizo Ugai, 1985	LE and variational analysis
Dov Leshchinsky & Baker, 1986	LE and variational analysis
R Baker & Leshchinsky, 1987	LE and variational analysis
Cavoundis, 1987	LEM
Hungr, 1987	Extended Bishop's modified
Gens, Hutchinson, & Cavounidis, 1988	Extended Swedish circle
K Ugai, 1988	Extended ordinary technique of slices, Janbu and Spencer, modified Bishop's
Xing, 1988	LEM
Michalowski, 1989	Kinematical theorem of limit plasticity
Seed, Mitchell, & Seed, 1990	Ad hoc 2D and 3D
Dov Leshchinsky & Huang, 1992	Limit equilibrium and variational analysis

2.4 Soil Slope Failure Surface Searching Methods

There are many variant methods utilized in analyzing soil slopes stability, either natural slopes or artificial. Every one of them leads us to a variant FOS. Several ones are quite precise, alike FEM, some are more conservative, such as that of ordinary method of slices. But such variations apply for only those of one slip fail, and this must be the critical one. The method for finding this critical surface of fail has multiple techniques as well, many of them are complex whereas others are less complicated, but most often they could be accomplished only by using software programs and they are very hard to use for hand computations. The FOS is also very empathetic to the exact location of the critical solution with a thin soil's layer for complicated problems, and there are large differences between different methods of global optimization. (Cheng, Li, Lansivaara, Chi, & Sun, 2008).

To optimize this procedure, most of those techniques have been made on basis on trial and error techniques so far. Different methods of optimization have been developed, such as genetic algorithm (GA), annealing, and so on.

Some more recent methods are discussed in this section

2.4.1 Simulated annealing method

Optimization was accomplished in this method by implementing a method of annealing to accomplish the lowest possible global for FOS. It is focused on two first points identified by the user (that fully defined as follows) and an additional upper limit.

2.4.2 Simple genetic algorithm

This procedure provides a clear form of Calculation based upon Morgenstern Price's slope stability analysis system for noncircular surfaces with pseudo-static's earthquake loading (McCombie, Wilkinson, 2002). That's simpler version of the genetic algorithm (Sengupta, Upadhyay, 2009). In order to obtain the critical noncircular slip surface, this method used a simple genetic algorithm (SGA). The following figure (Figure 2.11) demonstrates the technique utilized by this method to locate the slip (Zolfghari, Heath, & Mccombie, 2005).

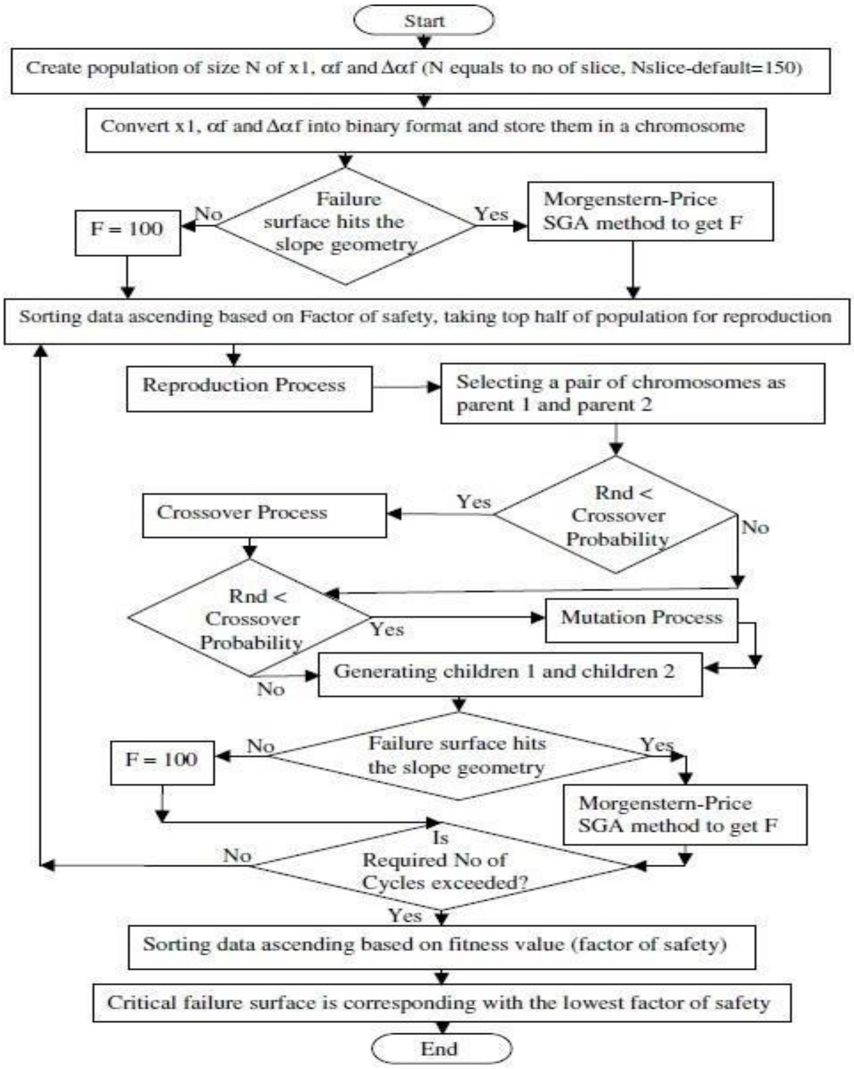

Figure 2.9: Algorithm of simple genetic (Zolfghari, Heath, & Mccombie, 2005)

2.4.3 Leapfrog algorithm method

This approach is based on the methods used by Janbu and Spencer to analyze the stability of the slope. The cause the researchers used these techniques for their studies is that they do not need any main geometry statement, and the initiation of slip termination points is not restricted in those techniques. This allows the technique to generate a general form of the slip surface.

The author then claims that the most efficient procedure was the Leapfrog algorithm after testing a number of optimization methods.(Bolton, Heymann, & Groenwold, 2002).

2.4.4 Other methods

From other methods, it is possible to count "Monte Carlo techniques" (Malkawi, Hassan, & Sarma, 2001) and Particle swarm optimisation theory (Cheng, Li, Chi, & Wei, 2007) which in this thesis would not be considered.

2.5 Potential Slope Failure Surface and Soil Strength Parameters

There have been numerous studies on the effect of soil strength parameters on factor of safety, But their impact on the surface of the slip was seldom taken into account. One of a handful studies (Lin & Cao, 2011), discusses the relationship in-between those parameters and the potential surface of the slip and their impact on the surface of the failure, this paper studies a function of Phi, cohesion c, unit weight and slope's height (h) as follows:

$$\lambda = c/(\gamma * h * \tan \emptyset) \qquad (2.45)$$

This study debates this once the value of Lambda (λ) stays unchanged, the surface of the failure stay the same, this is consistent with a previous study (Jiang & Yamagami, 2008), which shows a special correlation between $\frac{c}{tan\varphi}$ and the slip surface. In addition, the higher λ shows a deeper failure slip and the lower value of λ makes the surface of fail nearer to the surface of the slope (Lin & Cao, 2012).

CHAPTER 3

METHODOLOGY

3.1 Introduction

In this chapter, software programs and methods that will be used in this thesis will be introduced and discussed.

3.2 Methodology

As it has discussed before, for each slope, there are resisting forces and driving forces which should be considered. Driving forces are mostly a result of the weight of the soil formed the slope that is in a direct proportion with the unit weight of the soil, and resisting forces are mostly a result of internal friction angle and cohesion of the soil. In the first part of the study, the effect of cohesion (c), internal friction angle (ϕ) and the unit weight (γ), of the soil will be studied to compute the factor of safety FOS.

In the second part of this study, an adequate numbers of slopes will be analyzed and modeled with different soil shear strength parameters, cohesion, unit weights and internal fraction angle in addition to slope geometry by changing the angles, length and height of the slopes in order to make a database of failure surfaces for these slope parameters. In these first two parts, the study will be analyzed by using the educational license of the software package SLOPE/W.

Finally reanalyze the previous models with the same properties and conditions on another software packages PLAXIS and FLAC and compare the results between them then compare the outputs with the results of SLOPE/W in order to check and control the accuracy of SLOPE/W results

The results data of the failure surface's circle (center, entry, exit and radius) of the models will be used to draw the slope by the version of Automatic Computer Aided Design (AutoCAD) software 2014 to measure the length of the failure arc and locate the slip surface entry and exit points by measuring the arc between them.

The results of analyzing each model will be used by enter it into the version of Microsoft Excel 2010. After this step, using the software, various figures are going to be generated. And find some equations of the results by this software. The methodology appointed in treating this thesis involves:

1-Investigate the factor of safety variations by change soil unit weight (ɤ), cohesion (c), and , internal friction angle (ϕ) and their effect on the factor of safety.

2- Create detailed scenarios including the geometry, details and soil properties.

3- Studying the background of the methodology for the 3 software programs ; PLAXIS, FLAC and SLOPE/W. (Finite Element Method, Limit Equilibrium Method).

4- Cognize which software packages could be used in geotechnical stability for research scenarios.

5-Analyse after Create the concepts for each scenario.

6- Research soil properties and each scenario's parameters.

7- Familiarise with each software and its ability.

8- Analyze each scenario after modeling by using PLAXIS, FLAC and SLOPE/W and discuss the results and benefits.

9- From all the above steps discuss the benefits and limitations of each of the software packages and make notes and recommendations.

3.3 Materials

3.3.1 Soil

More than 100 soil types with different strength parameters have used in this study to be modeled and analyzed. In order to generate models with a good accuracy in finding the relationship between the factor of safety and the soil strength parameters for different soil types with small changes in soil parameters have been selected, modeled and analyzed.

Soil strength parameters

The range of soil strength parameters chosen for this study in the Table 3.1 below

Table 3.1: Soil strength parameters

Soil strength parameters	The range	The unit
Cohesion	15~32	kPa
Unit Weight	15~31	kN/m^3
Internal Friction Angle	15~32	°

3.3.2 Water level

In thus study the soil has assumed dry because of time limitation thus effect of water hasn’t studied, deny its effect has done by assuming the water level being far away below the slope level.

3.4 Software and Programs

3.4.1 FLAC/SLOPE

FLAC/Slope is a mini-version of FLAC specifically designed to conduct slope stability factor of safety calculations (ITASCA Consulting Group, 2011).

This software is a two dimensional express limited distinction program for building mechanics calculation. This program recreates the conduct of a structure worked of soil, rock, or different materials that may experience plastic stream. FLAC finds the static answers for an issue utilizing the two-dimensional plane-strain model. In any case, the dynamic conditions of movement are incorporated into the plan to help model the unstable and stable forces with the model; this guarantees the scenario of an unexpected collapse with the model is represented. The required soil properties present in Table 3.2

Table 3.2: Required soil properties for FLAC/SLOPE

Definition	**Property**	**Symbol**	**Units**
Unit weight of the soil	Density	γ	kg/m^3
The cohesion component of the shear strength	Cohesion	c	Pa
Friction angle of the soil	Phi	Ø	°
Dilation angle of the soil	Psi	Ψ	°

The dilation angle has been set to zero in this study, suggesting no volume change during output. The role of the dilation angle was discussed in details elsewhere like Griffiths & Lane (1999).

Methodology of FLAC/Slope Analysis :

To draw the model insert the coordinates needed for each point by using “input” button under the window “sketch” as shown in Figure 3.1, after draw the slope divide it and cut the edges and merge the points make a text for the model if there is any mistakes during the drawing as shown in Figure 3.2.

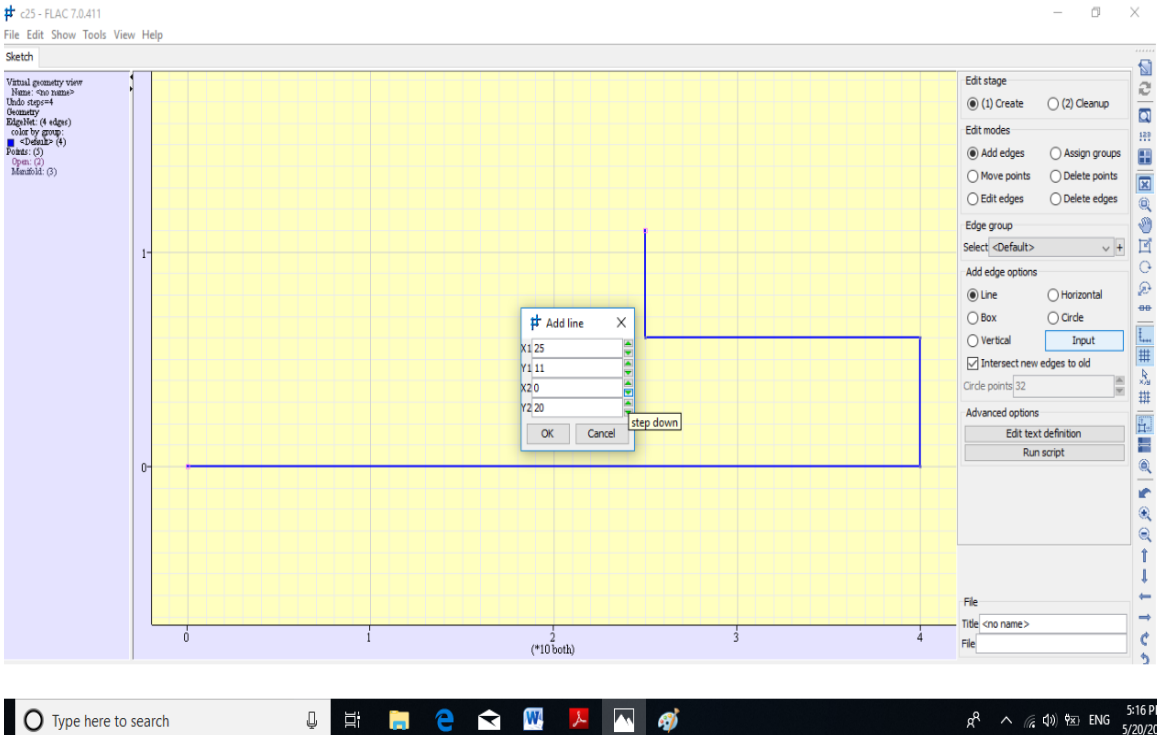

Figure 3.1: Insert slope’s coordinates on FLAC/SLOPE

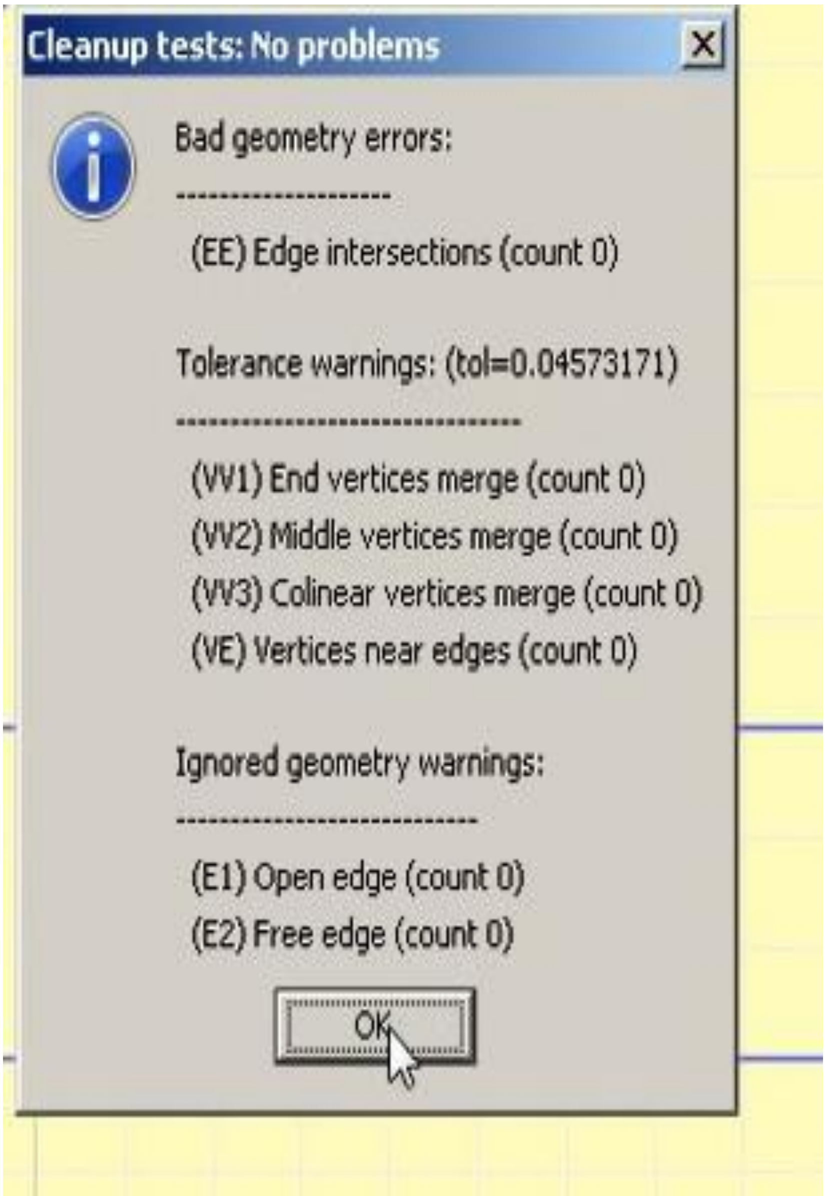

Figure 3.2: Check on slope's drawing

Assign and create the properties of materials is needed. It has to be noted that FLAC requires the density and Cohesion of the material inputted in kg/m^3 and Pascal respectively as presented in Figure 3.3.

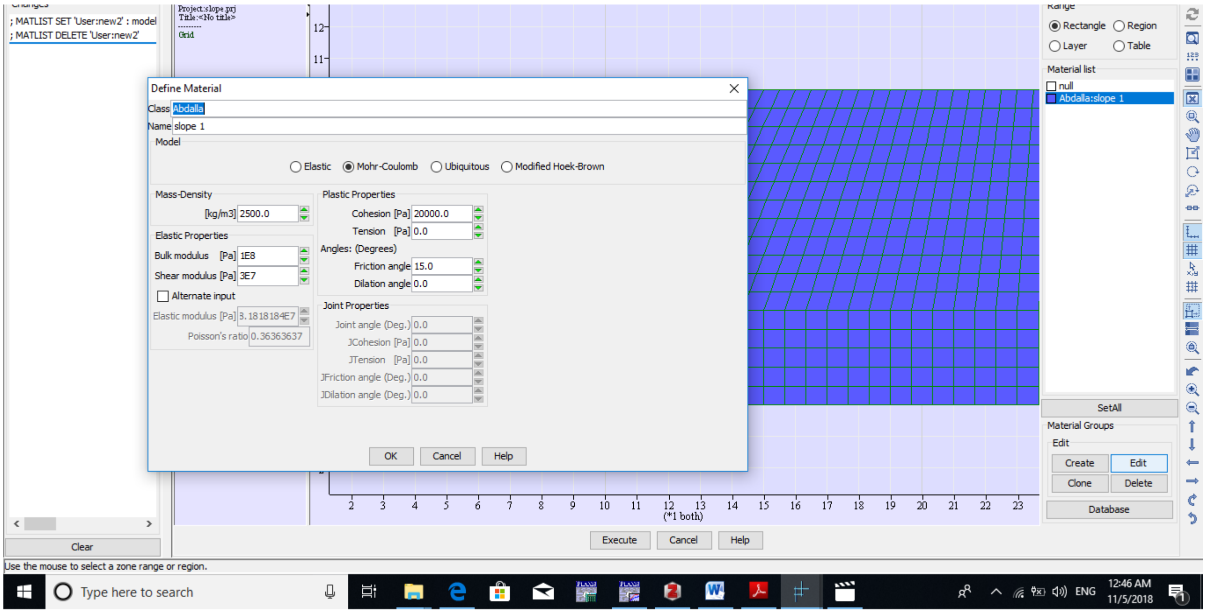

Figure 3.3: Assign material properties on FLAC/SLOPE

Assign a mesh to the slope is required. A medium mesh has been chosen in this thesis for FLAC as it shown in Figure 3.4 down below. In order to achieve the optimum size suitable for meshing, both fine and medium size mesh was tried for few models, it was found that the final result difference between fine and medium meshes for factor of safety are about 0.007 which could be neglected as it makes less than 1% difference (Figure 3.5).

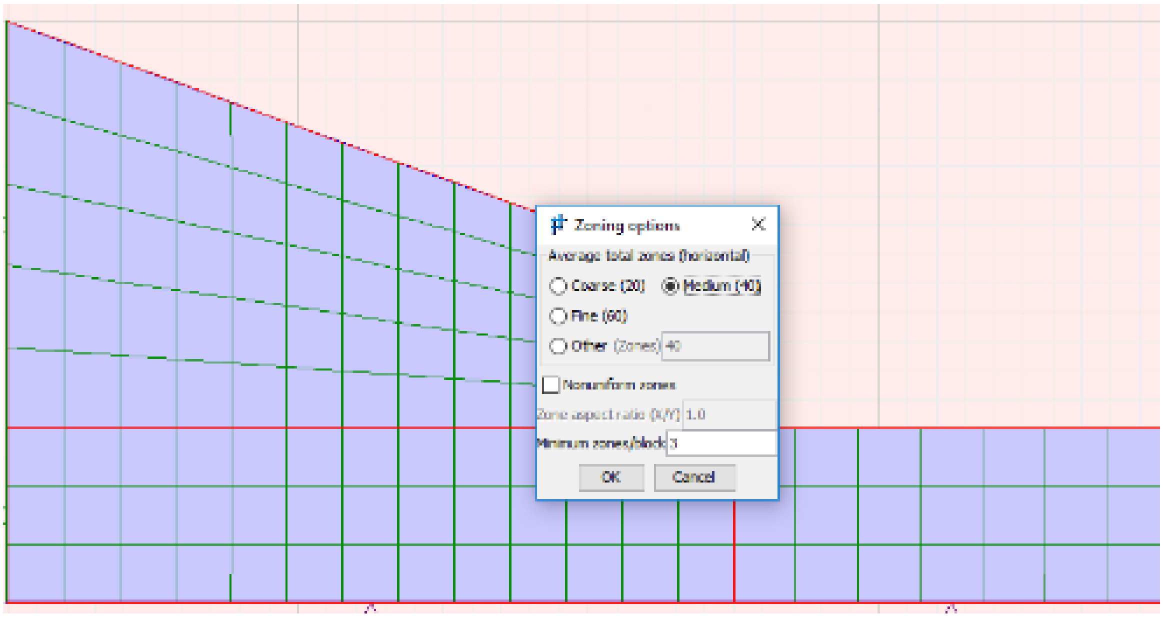

Figure 3.4: FLAC/SLOPE Assign mesh

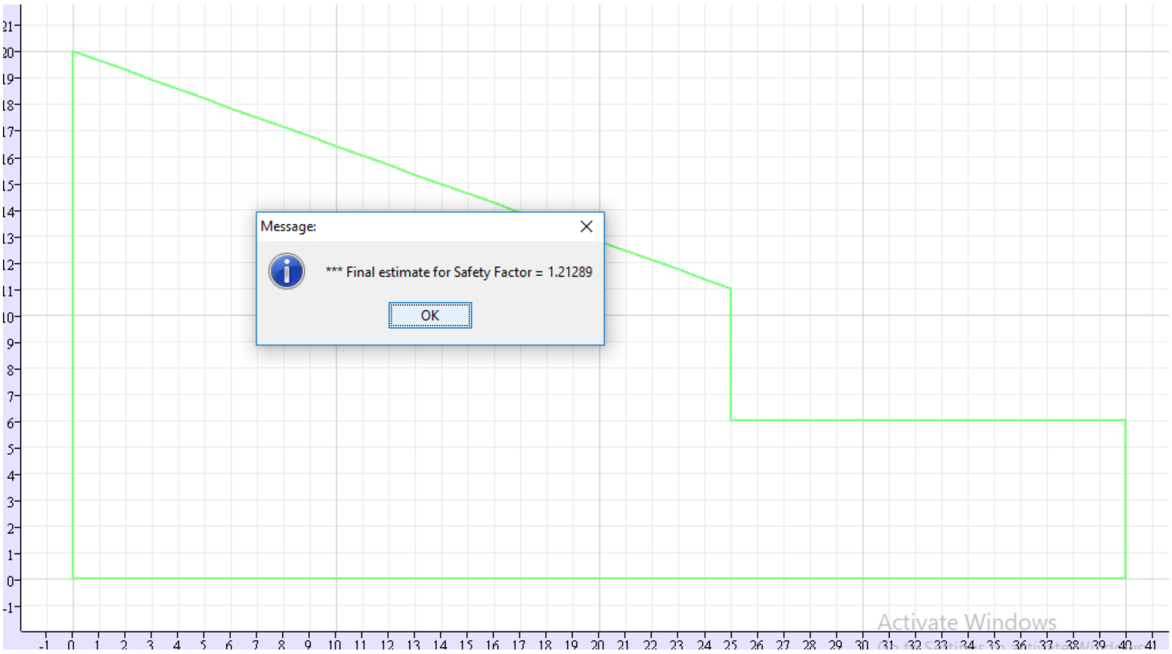

(a)

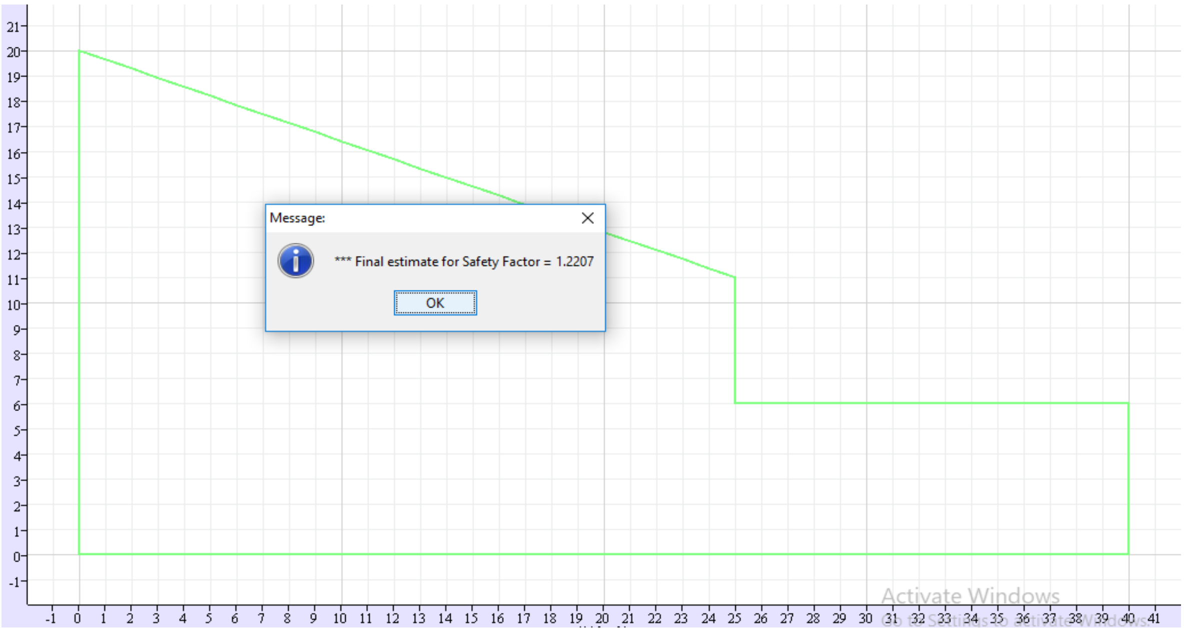

(b)

Figure 3.5: The difference between fine and medium meshes for the value 17 kN/m^3 of unit weight. (a) Fine mesh, (b) Medium mesh

Finally the result of factor of safety will be given in small box and a shape of the slope's displacements as shown in Figure 3.5

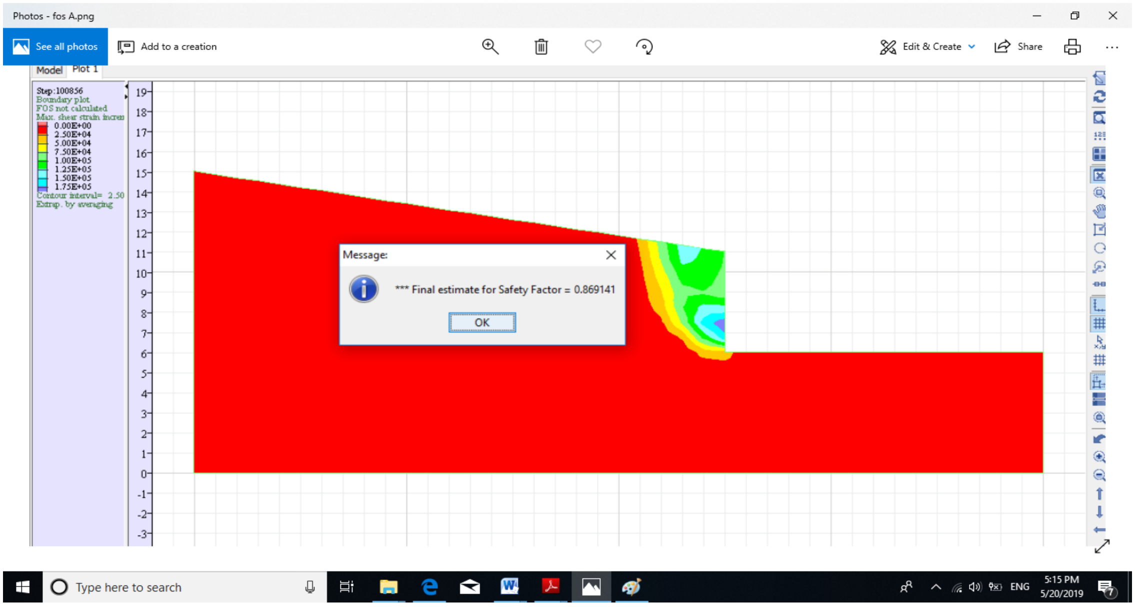

Figure 3.6: Factor of safety value on FLAC/SLOPE

3.4.2 SLOPE/W

SLOPE/W is software that uses LE method to compute the factor of safety FOS of rock and soil slopes and earth. The user of SLOPE/W must have a background and knowledge of the concepts and principles of geotechnics involved in the judgment and analysis is required to assure that realistic soil properties are used to compute an accurate FOS. The version SLOPE/W 2012 has been used in this study. Although this software based on LE method but it uses finite element method too for some slopes (GEO-SLOPE International., 2015). For the number of increments 15 have been used for modeling the slopes for entry and exit ranges. The required soil properties presented in Table 3.3.

Table 3.3: Required soil properties for SLOPE/W

Definition	**Symbol**	**Property**	**Units**
Soil's Total Unit Weight	ɤ	Unit Weight	kN/m^3
Soil's Cohesion	*C*	Cohesion	kPa
Soil's Friction Angle	Ø	Phi	°

The Methodology of SLOPE/W Analysis

Start SLOPE/W by setting the units and some properties of the slope and slip surface draw scale for the model so we can draw the axes after that as shown in Figure 3.6.

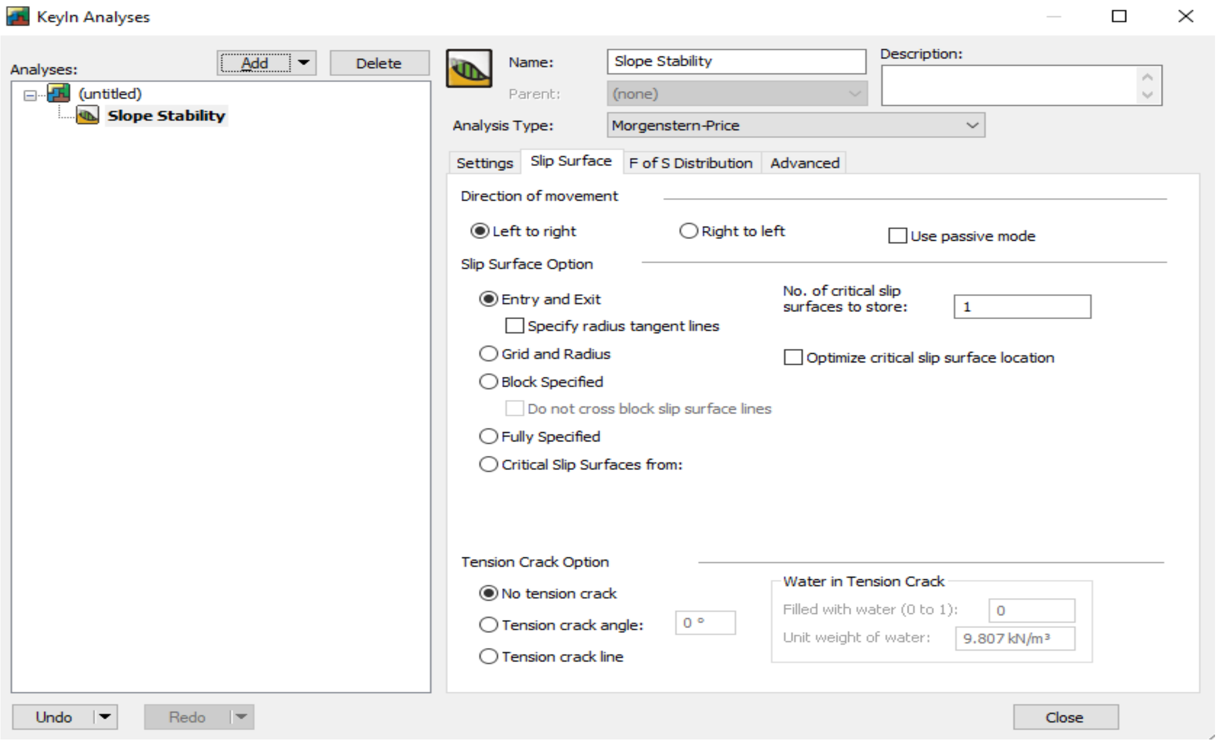

Figure 3.7: SLOPE/W set units

To draw the model using the inbuilt CAD is needed alike PLAXIS and unlike FLAC which it needs to input the coordinates (X, Y) of each point of the drawn slope

Assign and create the properties of material is needed which can be found under the menu “Keyln”, as cohesion, unit weight and internal friction angle, material dialogue box presented in Figure 3.7.

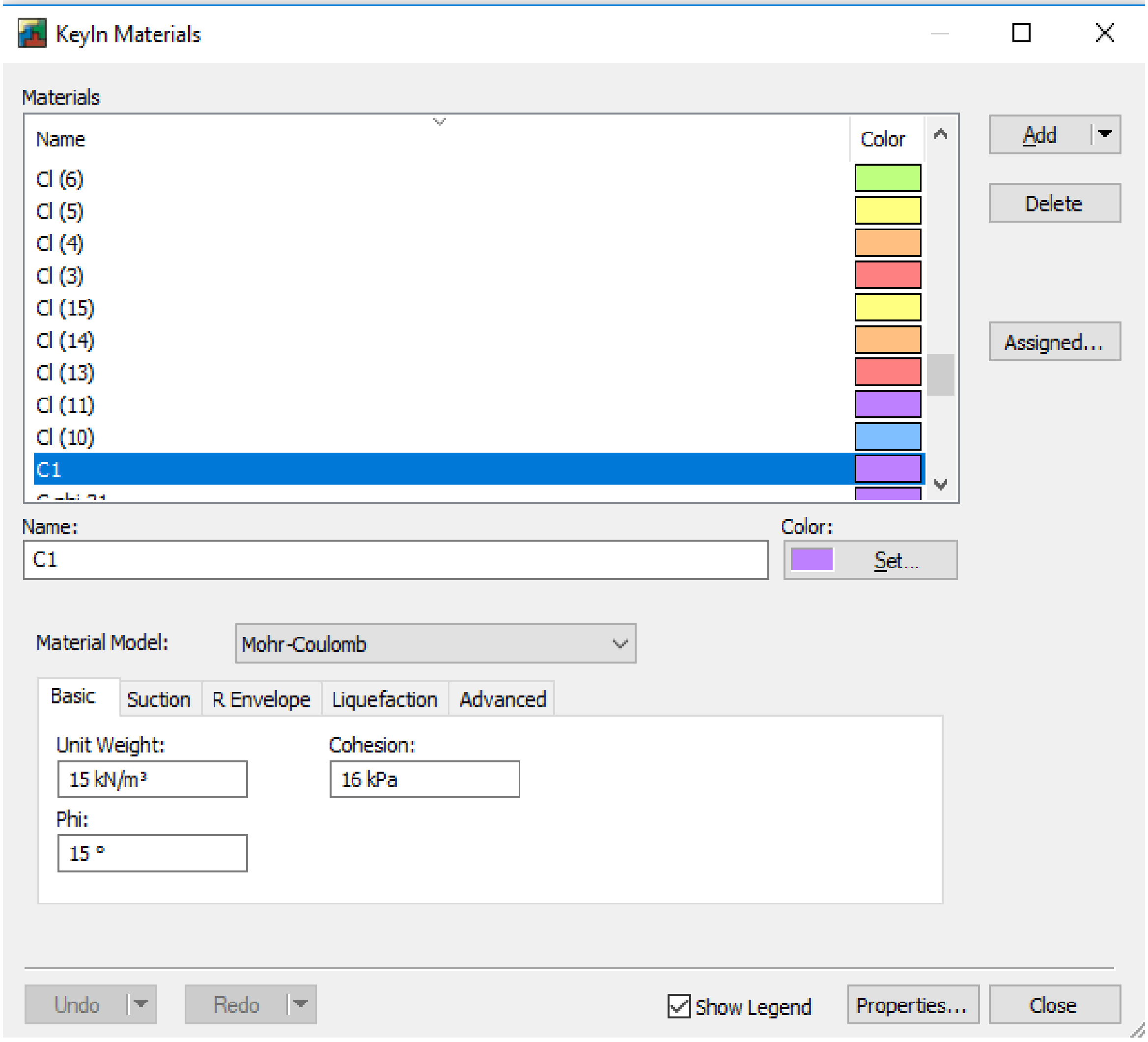

Figure 3.8: Assign and create the properties of material on SLOPE/W

After defining soil strength parameters in the software and all inputs start calculate the minimum factor of safety of the slope by clicking on "start" button, the program will take time to analyze the slope and that depends on the number of increments and the type of mesh that chosen for the slope the computed model shown in Figure 3.8 show the case of cohesion and internal friction angle both 16 kPa and ° respectively and unit weight 15 kN/m³.

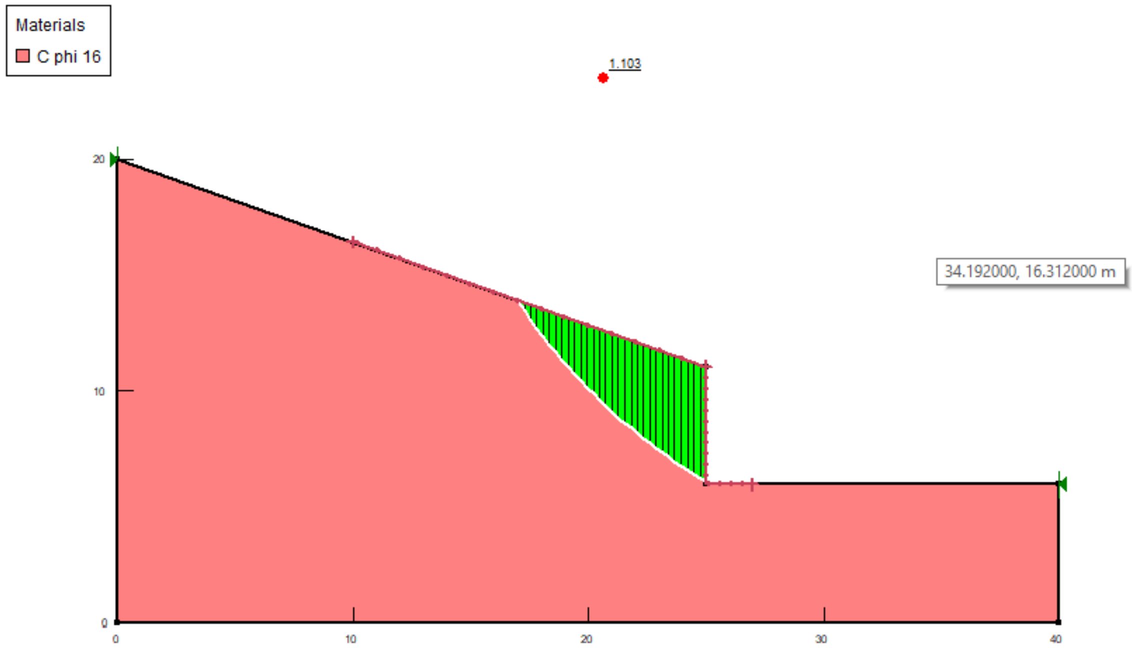

Figure 3.9: SLOPE/W factor of safety value

3.4.3 PLAXIS

PLAXIS is described as a finite element FE package for geotechnical analysis that can use both three-dimensional and two-dimensional analysis in determining the moment of inertia and shear forces of slopes stability, deflection , displacements and deformation experienced by slopes. PLAXIS provides itself to modeling more complex geotechnical scenarios as it has the ability to simulate inhomogeneous soil properties and time dependent scenarios. The required Soil Properties presented in Table 3.4.

Table 3.4: Required soil properties for PLAXIS

Definition	**Property**	**Symbol**	**Units**
Soil's Total Unit Weight	ɤ	Unit Weight	kN/m^3
Soil's Cohesion	*C*	Cohesion	kPa
Friction angle of the soil	Phi	Ø	°
The ratio of lateral strain to linear strain	Poisson's Ratio	ν	-
Elastic modulus at the reference depth	Reference Elastic Modulus	Eref	kN/m^2

The Methodology of PLAXIS Analysis

Start PLAXIS by setting the units and draw scale and slope limits (right, left, bottom, down) and grid spacing for the model as presented in Figure 3.9 so the axes can draw after that.

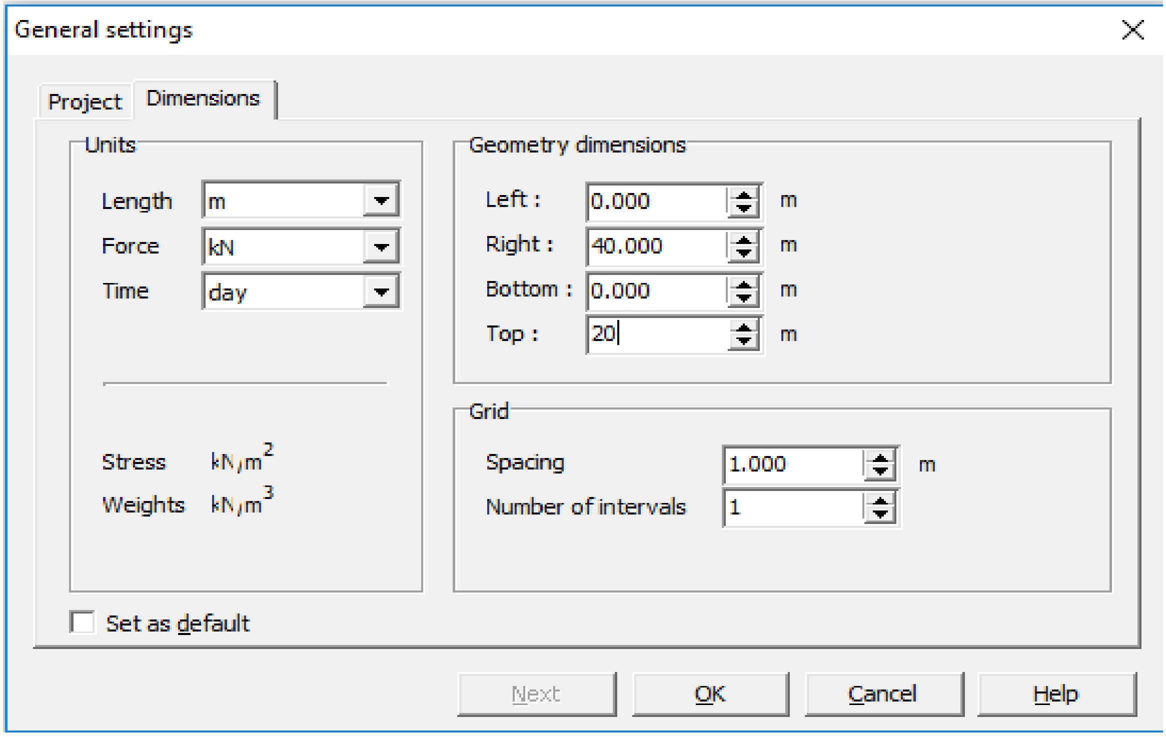

Figure 3.10: Set units on PLAXIS

Drawing in PLAXIS is easy because drawing the model can be done by using the inbuilt CAD interface as shown in Figure 3.10 alike SLOPE/W and unlike FLAC which it needs to input the coordinates (X, Y) of each point of the drawn slope.

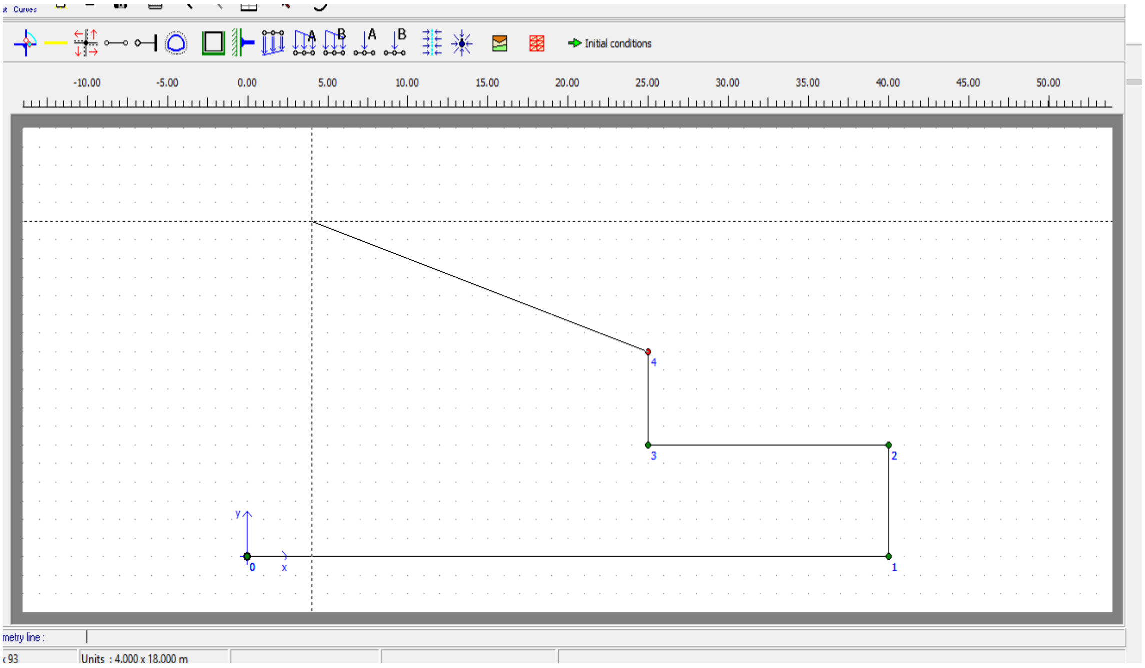

Figure 3.11: Drawing in PLAXIS

The model need to be fixed by hitting the button "standard fixties" from the tool bar so the slope unmovable from continues sides (bottom and left sides) as shown in Figure 3.11.

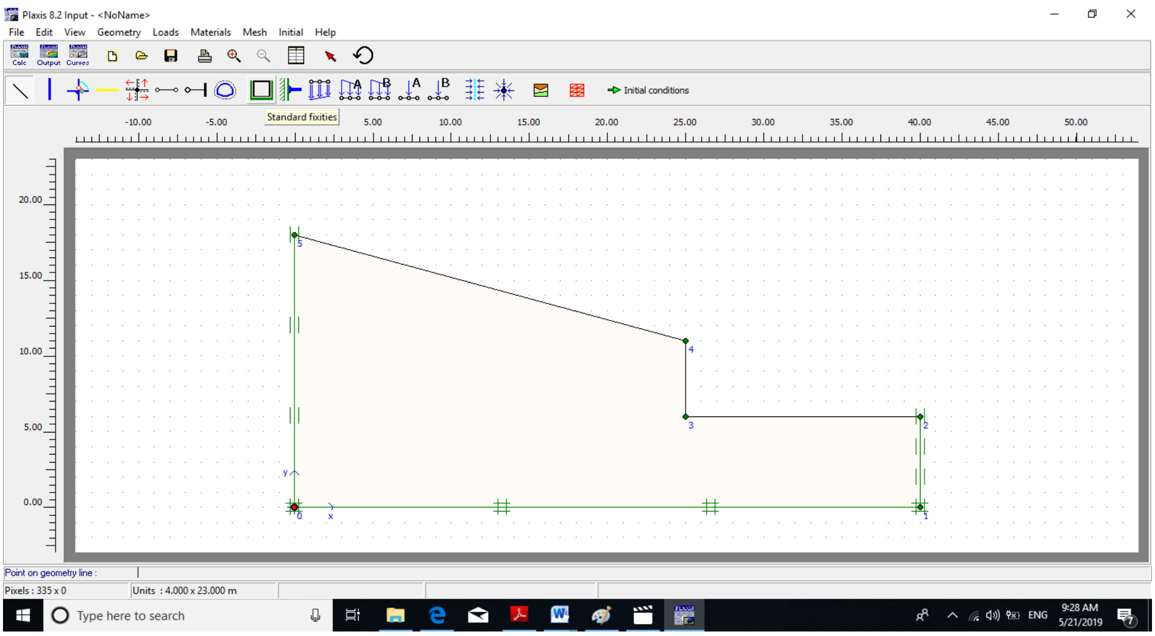

Figure 3.12: PLAXIS standard fixities

Assign and create the properties of material are needed but PLAXIS need advanced properties the elastic parameters Young's modulus and Poisson's ratio were allocated nominal values of 100 kN/m^2 and 0.3 respectively, as they have little impact on the computed factor of safety (Hammah, Yacoub, Corkum, & Curran, 2005) as shown in Figure 3.13.

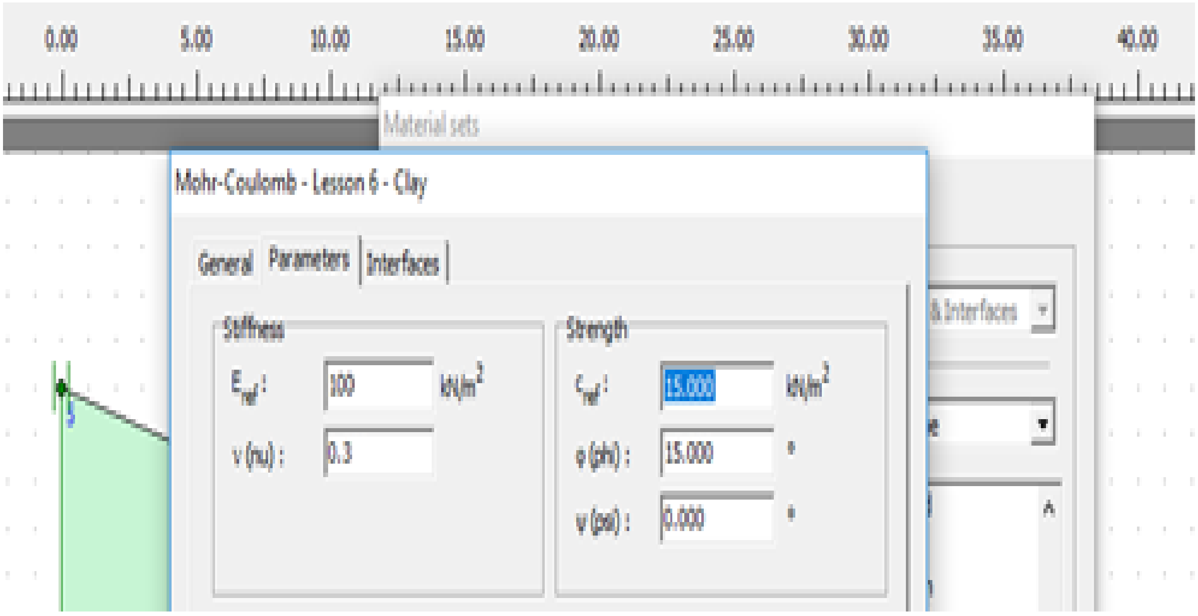

Figure 3.13: Assign and create the properties of material on PLAXIS

Generating the mesh is needed in this software. A medium mesh is being used in this study to help improve accuracy as shown in Figure 3.14. The mesh is presented in Figure after generating in Figure 3.15.

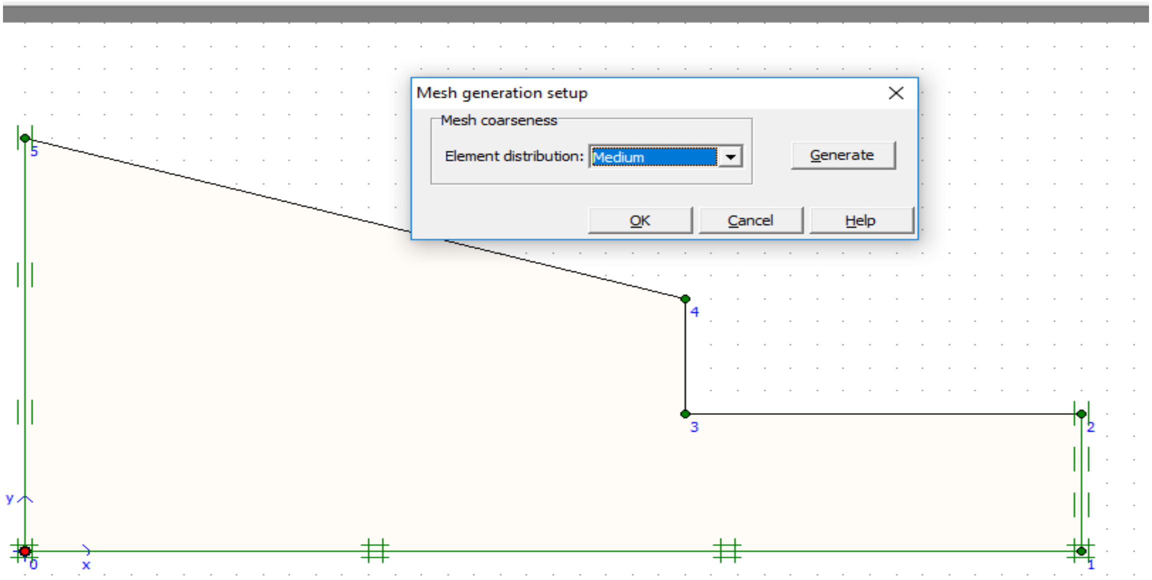

Figure 3.14: Determine the mesh size on PLAXIS

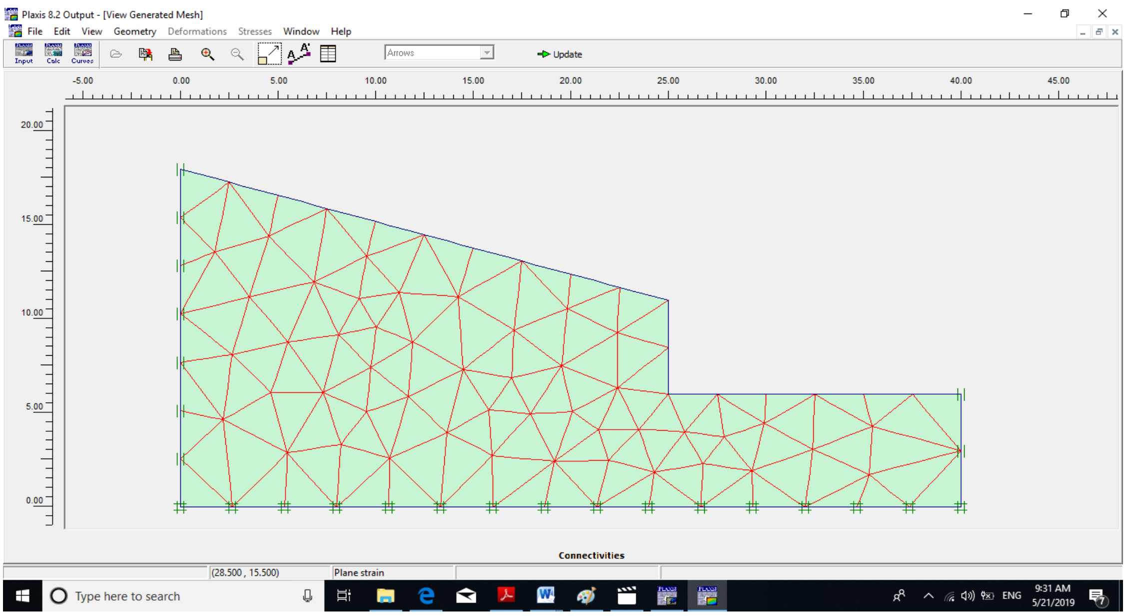

Figure 3.15: PLAXIS before generating mesh

By hitting calculate button in tool bar the program will ask to determine some points in the slope for the expected failure surfce then calculte the fctor of safety after that as shown in Figure 3.15.

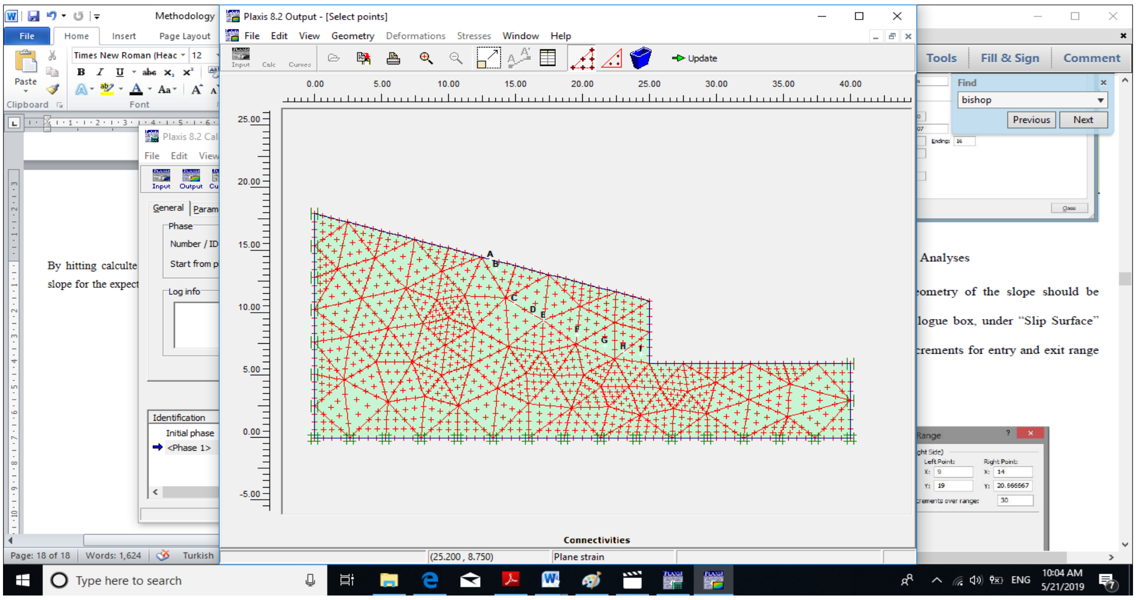

Figure 3.16: PLAXIS after generating the mesh

By hitting calculate button the software will show the deformed slope as shown in Figure 3.16 and calculate the factor of safety.

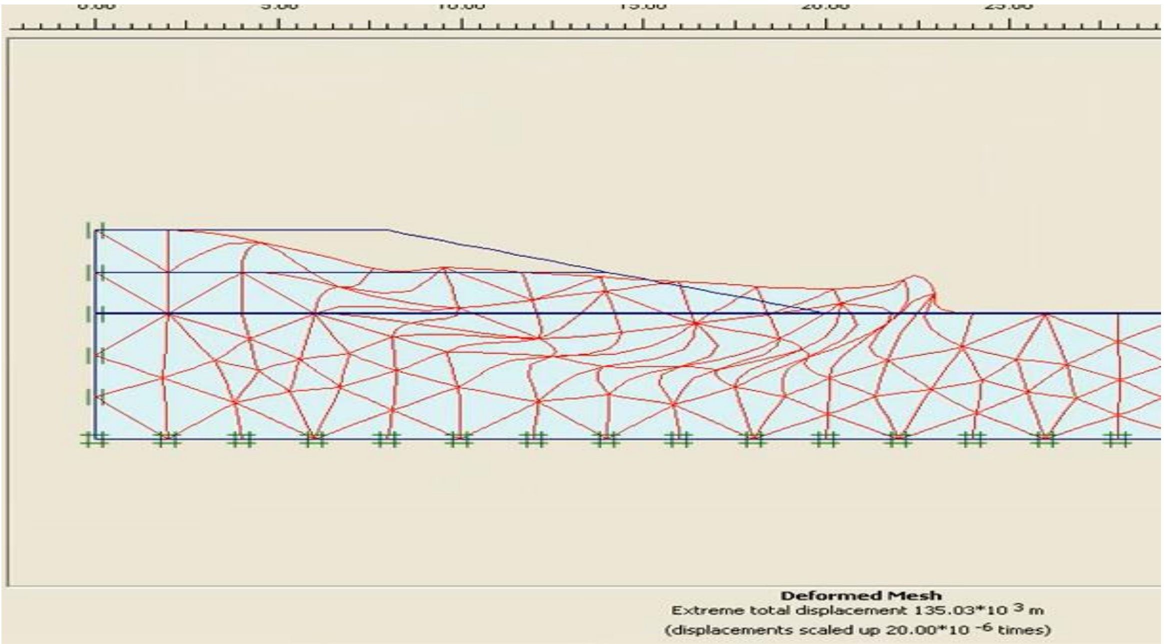

Figure 3.17: Slope displacement on PLAXIS

CHAPTER4

RESULTS AND DISCUSSION

4.1 Introduction

In this chapter, the effect of every soil's strength parameter, cohesion, unit weight and internal friction angle (c, γ, and ϕ) has been studied on factor of safety FOS and failure surface, both together and separately. In the first section of the results, in order to determine the varying in FOS and slip surface, a number of models were analyzed, while in the second section, to find an accurate relationship between the strength parameters of soil and the surface of failure and an adequate number of models were analyzed. After all the models were generated and analyzed the figures were drawn to demonstrate the influences of the variables on FOS and failure surface. In addition, the reasons for these various behaviors were debated.

4.2 Impact of Soil Strength and Slope Geometry Parameters on the Factor of Safety

In this section, three series of analyzing were performed in order to study the feasibility of this study. One of the parameters changed in each set of models while the other two parameters kept constant, these models were studied to see if there is any relation between the position of the surfaces of failure and the soil parameters.

4.2.1 Impact of unit weight on factor of safety

In order to study the influence of unit weight $\boldsymbol{\gamma}$ on FOS, the values of unit weight have been chosen from 15 to 30 kN/m^3 while the internal friction angle and the cohesion have been chosen as 15° and 15 kPa, respectively.

Table 4.1: Effect unit weight on FOS

Model number	Unit weight [kN/m³]	Internal friction angle[°]	Cohesion[kPa]	Factor of safety
1	15	15	15	2.411
2	16	15	15	2.295
3	18	15	15	2.173
4	20	15	15	2.044
5	22	15	15	1.956
6	24	15	15	1.884
7	26	15	15	1.822
8	28	15	15	1.769
9	30	15	15	1.724

In Table 4.1 the values showed that as the soil's unit weight raise, FOS values decrease. This reduction could be explained by weight of the soil as the unit weight increases, weight of soil as the main derivative force behind the failure, increases. Therefore, increasing unit weight causes the slope to become more unstable leading to a reduction in the FOS. Clayey and silty sands represent the value between 17-32 kN/m^3 of unite weight (NAVFAC,1986).

Extensive field experiments for (Feng, S. J et al, 2019) were carried out in conjunction with numerical simulation and LE analyzes to examine the major failure of an unfilled landfill structure in Shanghai, China, The study also found the collapse happened in the sandy silt with silt clay layer which represent 18.2 kN/m^3.

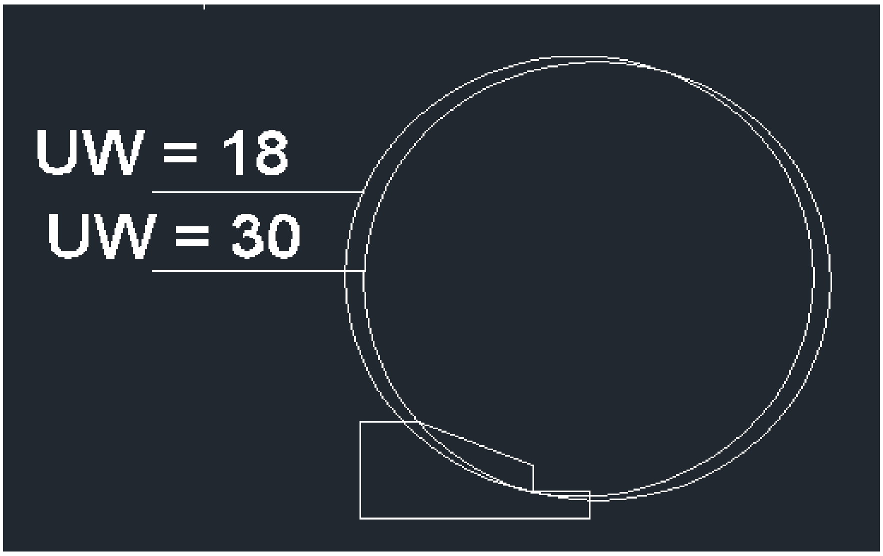

(a)

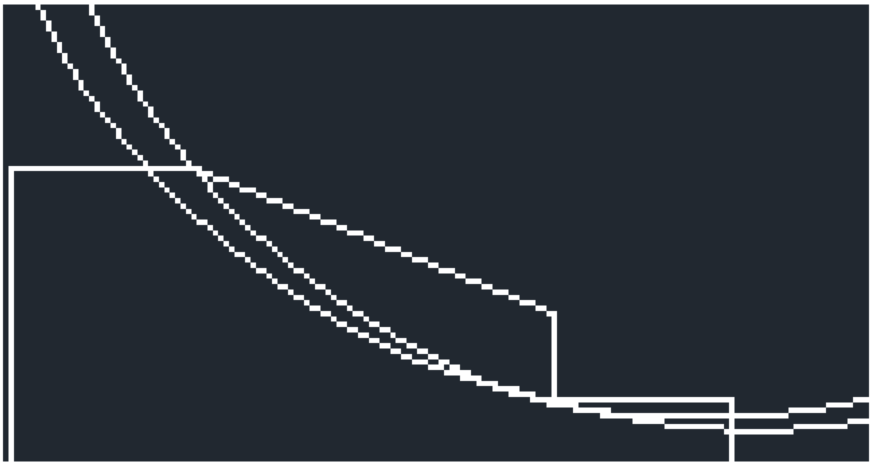

(b)

Figure 4.1: (a) Impact of unit weight on slip surface. (b) cropped portion of (a)

Figure 4.1(a) demonstrates the impact of unit weight on failure surface (whereas Figure 4.1(b) is a cropped variant of (a)). The tests follow a practical rule, by maximizing unit weight of the soil, the failure surface is moved to the right, leading in a smaller volume of soil failure and thus decreasing the slip surface length. Less resistant force is activated due to the smaller surface for holding forces (friction and cohesion). For these reasons, a lower value for safety factor is accomplished.

4.2.2 Impact of cohesion on factor of safety

To study the impact of cohesion on FOS, the cohesion values diverge from 16 to 30 kPa were chosen while the internal friction angle and unit weight of the soil chosen as 15˚ and 15 kN/m^3 respectively.

The calculated values of FOS for different C values are shown in Table 4.2

Table 4.2: Impact C on FOS

Model number	Unit Weight [kN/m^3]	Internal Friction Angle [°]	Cohesion [kPa]	Factor of Safety
1	15	15	16	1.355
2	15	15	18	1.409
3	15	15	20	1.463
4	15	15	22	1.517
5	15	15	24	1.572
6	15	15	26	1.626
7	15	15	28	1.680
8	15	15	30	1.724

The values in Table 4.2 showed that as the cohesion of the soil raised, FOS values increased, this increase is due to the raise up in cohesion value, as mentioned before, since cohesion is one of the resisting forces. Increasing cohesion caused the slope to become more stable leading increasing in factor of safety.

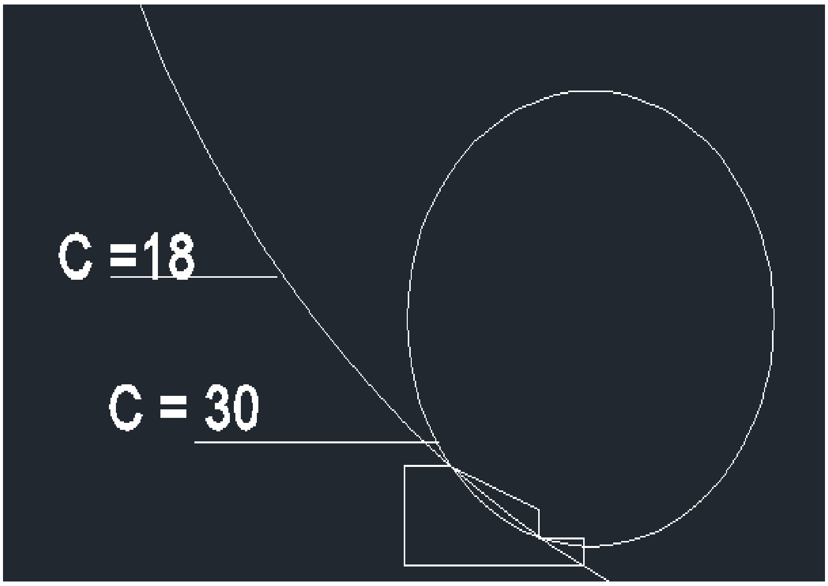

[a]

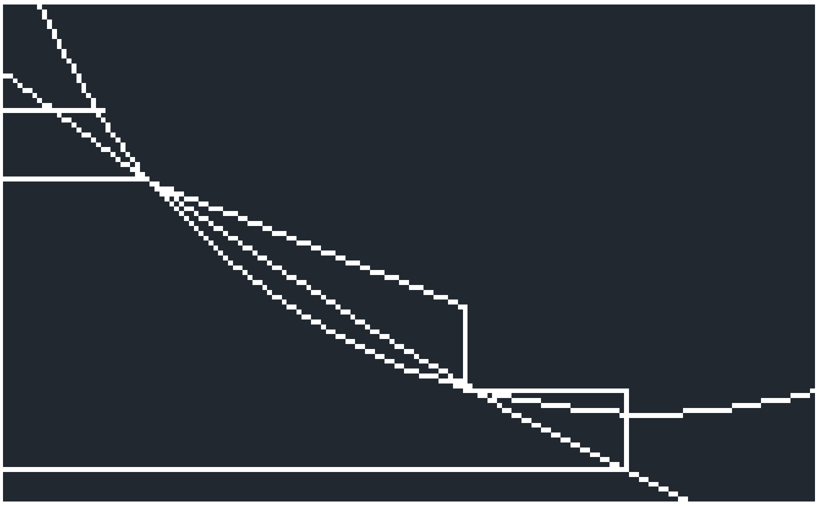

[b]

Figure 4.2: [a] Impact of C on slip surface. [b] cropped portion of [a]

As it shown in Figure 4.2, tests follow a logical order; by maximizing the cohesion value, failure surface and La increase to obtain the same cohesion force value (calculated by multiplying cohesion by failure arc length). In addition, a greater failure surface leads to a greater weight value for the volume of failure (greater derivative force) and a greater friction force value.

Furthermore, as the value of cohesion rises so the fault surface increased (including La), FOS rises. This suggests the increasing in the resistance forces is more prevalent than the increasing in the influence of driving forces.

4.2.3 Impact of internal friction angle on factor of safety

With the aim of testing the impact of friction angle on the factor of safety of the soil, various values of Ø changing from 16 to 30 degrees were selected, meanwhile the soil's unit weight and the cohesion were preserved constant respectively at 15 kN/m^3 and 15 kPa,.

Table 4.3: Effect Ø on FOS

Model number	**Unit Weight [kN/m^3]**	**Internal friction angle [°]**	**Cohesion[kPa]**	**Factor of Safety**
1	15	16	15	1.180
2	15	18	15	1.259
3	15	20	15	1.340
4	15	22	15	1.399
5	15	24	15	1.475
6	15	26	15	1.556
7	15	28	15	1.638
8	15	30	15	1.724

In the Table 4.3 data demonstrates that factor of safety increased by increasing the friction angle value. As mentioned before since friction angle is one of the holding and resisting factors, The results obtained are in line with the concept.

Figure 4.3 (a) demonstrates the impact of friction angle on failed surface (meanwhile Figure 4.3 [b] is a cropped part from [a]).

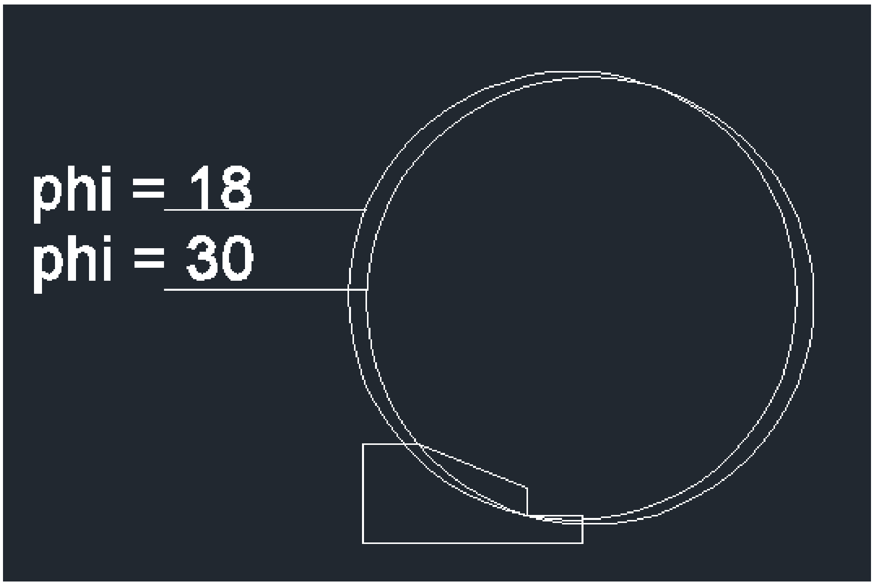

[a]

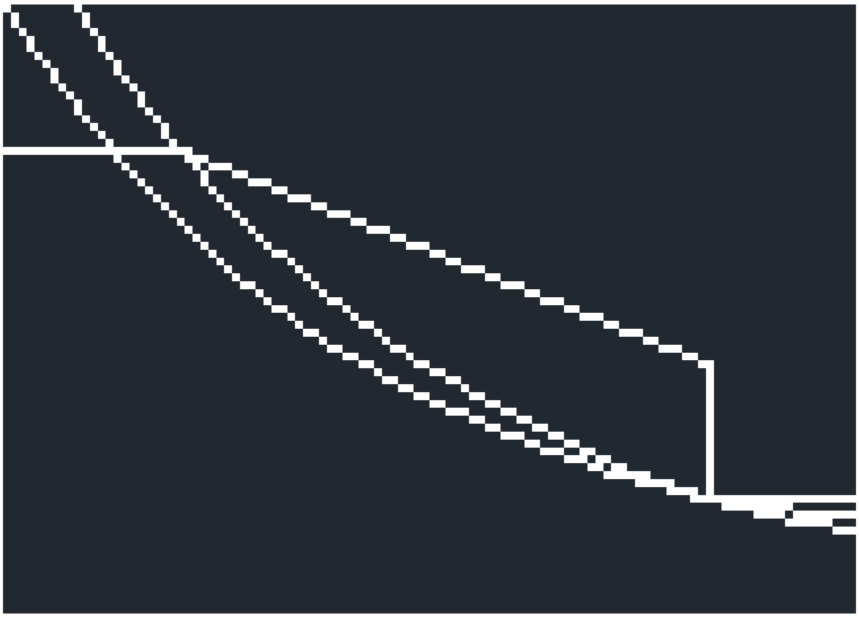

[b]

Figure 4.3: [a] Cohesion impact on slip surface, [b] cropped portion of [a]

As it shown in the Figure 4.2, the same as the unit weight effect, the tests succeed logical trendacy, by maximizing the friction angle.

The failure surface and La decrease to accomplish the same friction force value (calculated by multiplying the tangent of Ø by La). In addition, a small failure surface leads to a smaller failure's weight volume's value (lower derivative factor) and a lower value of the cohesion force.

Furthermore, an increase in internal friction angle (Ø) results in a reduction in the slip surface and La, thus FOS increases. This suggests that, a reducing in the impact of cohesion is more prevalent than reducing in driving factor.

4.2.4 Impact of slope geometry on factor of safety

With constant soil strength parameters, four different slopes shapes were analysed in order to monitor the impact of the slope shape on the factor of safety: c = 15 kPa, ɤ = 15 kN / m^3 and Ø = 15˚.

Taking into account situations numbers 1 and 2 together, 3 and 4 together as shown in Table 4.4, it is obviously noticed that increase the surface soil angle (Alpha) as shown in Figure 4.4) will result the slope to become less stable; this may be due to the fact that this amount of soil added to the upper part will act as an overhead load increase the driving force and resulting in the factor of safety to decline.

On the other hand, taking into account states numbers 1 and 2 together, 3 and 4 with each other, it is observed that increasing the angle of slope (Beta) is going to result the slope to become more stable, this maybe due to the fact that, by increasing that angle and La increases, yield to more resistant force that will raise the factor of safety.

Table 4.4: Impact of slope geometry on FOS

Model No (shape No)	Unit Weight [kN/m^3]	Internal Friction Angle [°]	Cohsion [kPa]	Factor of Safety
1	15	15	15	2.325
2	15	15	15	1.794
3	15	15	15	1.175
4	15	15	15	1.142

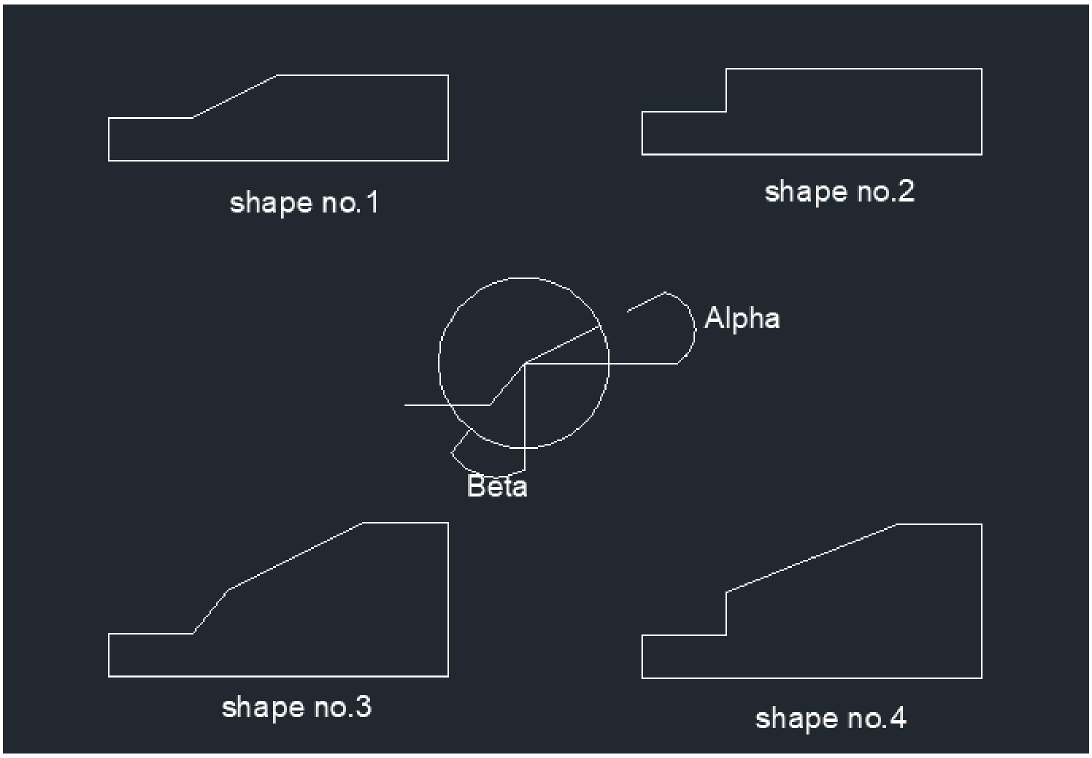

Figure 4.4: Models for effect slope geometry on FOS

4.3 Impact of Geometry and Soil Strength Parameters on the Slip Surface

Based on what was debated in the past part (4.2), it is easy to estimate that a correlation must be existed between the strength parameters of soil and the geometry of the slope and the surface of failure; the following analyzed models will be studied in order to examine this condition.

Many models were generated using SLOPE/W software in this step. The output in this aspect will become the factor of safety and slip circle center coordinates as well as the circular failure surface radius.

The circles have been drawn using AutoCAD software to find out La and locate entry and exit points in the slope failed area.

Figure 4.5 reflects the general shape of the slope geometry that is going to be used in the next 75 models.

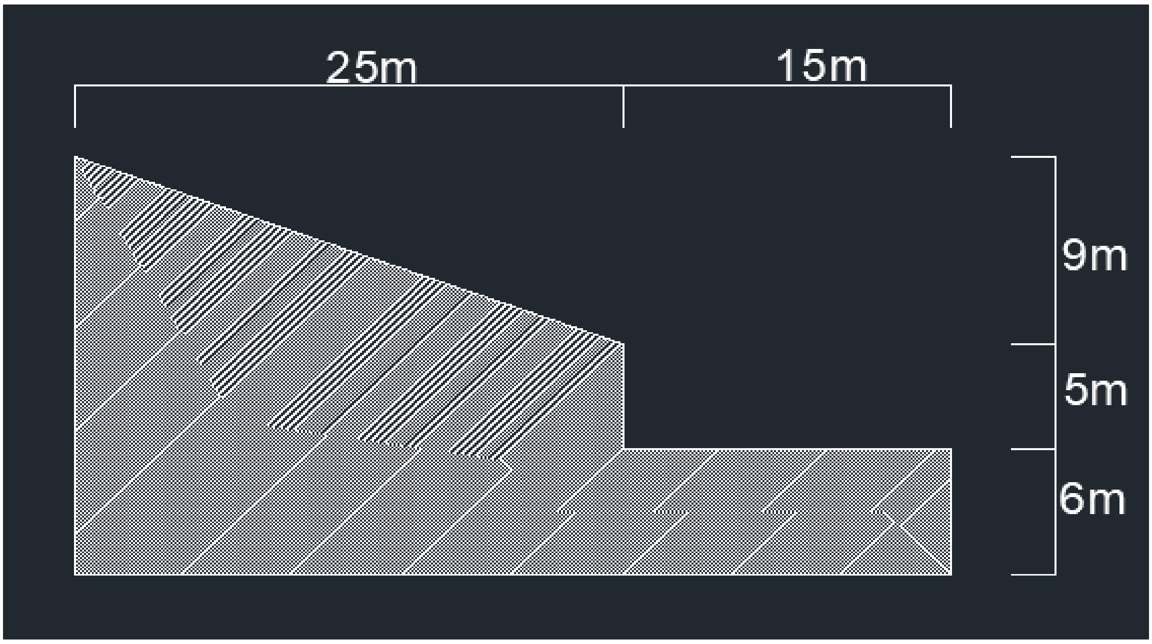

Figure 4.5 Slope model geometry

Various parameters of shear strength and soil unit weight were analyzed for the produced designs. Over the next sections, the specifics of these parameters are given and discussed.

4.3.1 Impact of cohesion, C on slip surface

In this part at 15° and 15 kN/m^3 respectively, the internal friction angle and unit weight of the soil remained constant, and the cohesion changed from 15 to 32 kPa. La and Ø have been referred to length of failure arc and internal friction angle respectively as shown in table 4.5.

Table 4.5: Cohesion impact on the slip surface

Model No	Unit Weight (kN/m^3)	Ø (°)	Cohesion (kPa)	Entry (X,Y) (m)	Exit (X,Y) (m)	Radius (m)	La (m)	Factor of safety
1	15	15	15	17, 13.9	25, 6.08	24.64	10.07	1.033
2	15	15	16	17, 13.9	25, 6.08	24.64	10.07	1.081
3	15	15	17	17, 13.9	25, 6.09	24.64	10.07	1.129
4	15	15	18	18, 13.5	25, 6.09	23.91	10.33	1.158
5	15	15	19	18, 13.5	25, 6.09	23.91	10.33	1.207
6	15	15	20	17, 13.9	25, 6.08	24.64	10.98	1.272
7	15	15	21	16, 14.2	25, 6.07	25.5	12.17	1.340
8	15	15	22	16, 14.2	25, 6.07	25.5	12.17	1.387
9	15	15	23	18, 13.5	25, 6.09	23.9	10.33	1.401
10	15	15	24	16, 14.2	25, 6.07	25.53	12.17	1.483
11	15	15	25	16, 14.2	25, 6.07	25.53	12.17	1.530
12	15	15	26	16, 14.2	25, 6.07	25.53	12.17	1.578
13	15	15	27	16, 14.2	25, 6.07	25.53	12.17	1.626
14	15	15	28	15, 14.6	25, 6.07	26.52	13.20	1.693
15	15	15	29	16, 14.2	25, 6.07	25.53	12.17	1.721
16	15	15	30	15, 14.6	25, 6.06	26.52	13.20	1.787
17	15	15	31	15, 14.6	25, 6.06	26.52	13.20	1.834
18	15	15	32	15, 14.6	25, 6.06	26.52	13.20	1.882

4.3.2 Impact of internal friction angle, phi on slip surface

Unit weight and cohesion kept unchanged in this part at 15 kN/m^3 and 15 kPa respectively, while the angle of friction varied between 16° and 32°. La and Ø have been referred to length of failure arc and internal friction angle respectively as shown in table 4.6.

Table 4.6: Internal friction angle impact on slip surface

Model No	Unit Weight (kN/m^3)	Ø (°)	Cohesion (kPa)	Entry (X,Y) (m)	Exit (X,Y) (m)	Radius (m)	La (m)	Factor of safety
19	15	16	15	18, 13.5	25, 6.09	23.9	10.555	1.033
20	15	17	15	18, 13.5	25, 6.09	23.9	10.555	1.054
21	15	18	15	18, 13.5	25, 6.09	23.9	10.555	1.074
22	15	19	15	19, 13.2	25, 6.1	23.4	9.5583	1.070
23	15	20	15	19, 13.2	25, 6.1	23.4	9.5583	1.089
24	15	21	15	20, 12.8	25, 6.2	127.17	8.6434	1.135
25	15	22	15	19, 13.16	25, 6.07	13.19	9.6773	1.141
26	15	23	15	19, 13.16	25, 6.1	23.42	9.5583	1.148
27	15	24	15	19, 13.16	25, 6.1	23.42	9.5583	1.168
28	15	25	15	19, 13.16	25, 6.1	23.42	9.5583	1.188
29	15	26	15	20, 12.8	25, 6.17	127.17	8.6434	1.215
30	15	27	15	19, 13.16	25, 6.1	23.42	9.5583	1.230
31	15	28	15	20, 12.8	25, 6.17	127.17	8.6434	1.249
32	15	29	15	20, 12.8	25, 6.17	127.17	8.6434	1.266
33	15	30	15	20, 12.8	25, 6.17	127.17	8.6434	1.284
34	15	31	15	20, 12.8	25, 6.17	127.17	8.6434	1.301
35	15	32	15	20, 12.8	25, 6.17	127.17	8.6434	1.320

4.3.3 Impact of unit weight on slip surface

Friction angle and cohesion kept unchanged at 15° and 15 kPa in this part, meanwhile soil's unit weight ranged from 16 kN/m^3 to 31 kN/m^3.

La and ∅ have been referred to length of failure arc and internal friction angle respectively as shown in table 4.7.

Table 4.7: Impact of unit weight on the slip surface

Model number	Unit Weight (kN/m^3)	Ø (°)	Cohesion [kPa]	Entry (X,Y) [m]	Exit (X,Y) [m]	Radius (m)	La (m)	Factor of safety
36	16	15	15	18,13.5	25, 6.1	23.9	10.555	0.967
37	17	15	15	18,13.5	25, 6.1	23.9	10.555	0.927
38	18	15	15	19, 13.2	25, 6.1	23.4	9.5549	0.874
39	19	15	15	18, 13.5	25, 6.1	23.9	10.555	0.860
40	20	15	15	19, 13.2	25, 6.1	13.2	9.2160	0.817
41	21	15	15	19, 13.2	25, 6.1	23.42	9.5549	0.786
42	22	15	15	19, 13.2	25, 6.1	23.42	9.5549	0.762
43	23	15	15	19, 13.2	25, 6.1	23.42	9.5549	0.740
44	24	15	15	19, 13.2	25, 6.1	23.42	9.5549	0.720
45	25	15	15	19, 13.2	25, 6.1	23.42	9.5549	0.701
46	27	15	15	19,13.2	25, 6.1	23.42	9.5549	0.669
47	29	15	15	19, 13.2	25, 6.1	23.42	9.5549	0.640
48	31	15	15	20, 12.8	25, 6.17	127.17	8.6434	0.613

4.3.4 Impact of unit weight and cohesion on slip surface

The friction angle kept unchanged at 15° in this part and the values varied from 16 to 31 for both parameters cohesion and unit weight kPa and kN/m^3 respectively.

La and Ø have been referred to length of failure arc and internal friction angle respectively as shown in table 4.8.

Table 4.8: Impact of cohesion and unit weight on the Slip Surface

Model No	Unit Weight (kN/m^3)	Ø (°)	Cohesion (kPa)	Entry (X,Y) (m)	Exit (X,Y) (m)	Radius (m)	La (m)	Factor of Safety
49	16	15	16	17, 13.9	25, 6.08	24.64	11.474	1.033
50	17	15	17	17, 13.9	25, 6.08	24.64	11.474	1.033
51	19	15	19	17, 13.9	25, 6.08	24.64	11.474	1.033
52	21	15	21	17, 13.9	25, 6.08	24.64	11.474	1.033
53	23	15	23	17, 13.9	25, 6.08	24.64	11.474	1.033
54	25	15	25	17, 13.9	25, 6.08	24.64	11.474	1.033
55	27	15	27	17, 13.9	25, 6.08	24.64	11.474	1.033
56	29	15	29	17, 13.9	25, 6.08	24.64	11.474	1.033
57	31	15	31	17, 13.9	25, 6.08	24.64	11.474	1.033

4.3.5 Impact of unit weight and friction angle on slip surface

Cohesion factor kept unchanged at 15 kPa in this part, whilst the other parameters varied between 15 and 31.

La and Ø have been referred to length of failure arc and internal friction angle respectively as shown in table 4.9.

Table 4.9: Impact of unit weight and friction angle on slip surface

Model No	Unit Weight kN/m^3	Ø (°)	Cohesion (kPa)	Entry (X,Y) (m)	Exit (X,Y) (m)	Radius (m)	La (m)	Factor of Safety
58	16	16	15	18, 13.52	25, 6.09	23.9	11.47	0.988
59	17	17	15	19, 13.16	25, 6.1	23.42	9.520	0.946
60	19	19	15	19, 13.16	25, 6.1	23.42	9.520	0.915
61	21	21	15	20, 12.8	25, 6.17	127.17	8.643	0.895
62	23	23	15	21, 12.44	25, 6.15	23.87	7.741	0.833
63	25	25	15	21, 12.44	25, 6.15	23.87	7.741	0.830
64	27	27	15	21, 12.44	25, 6.2	130.48	7.725	0.820
65	29	29	15	21, 12.44	25, 6.15	23.87	7.741	0.816
66	31	31	15	22, 12.1	25, 6.24	141.04	6.763	0.804

4.3.6 Impact of cohesion and friction angle on slip surface

friction angle and cohesion changed from 16 to 31 in this segment, meanwhile soil's unit weight kept at 15 kN/m^3. La and Ø have been referred to length of failure arc and internal friction angle respectively as shown in table 4.10.

Table 4.10: Impact of cohesion and friction angle on slip surface

Model No	Unit Weight (kN/m^3)	Ø (°)	Cohesion (kPa)	Entry (X,Y) (m)	Exit (X,Y) (m)	Radius (m)	La (m)	Factor Of safety
67	15	16	16	17, 13.9	25, 6.08	24.64	11.215	1.103
68	15	17	17	17, 13.9	25, 6.08	24.64	11.215	1.173
69	15	19	19	17, 13.9	25, 6.08	24.64	11.215	1.314
70	15	21	21	17, 13.9	25, 6.08	24.64	11.215	1.456
71	15	23	23	17, 13.9	25, 6.08	24.64	11.215	1.600
72	15	25	25	17, 13.9	25, 6.08	24.64	11.215	1.745
73	15	27	27	17, 13.9	25, 6.08	24.64	11.215	1.891
74	15	29	29	17, 13.9	25, 6.08	24.64	11.215	2.040
75	15	31	31	17, 13.9	25, 6.08	24.64	11.215	2.190

4.3.7 Impact of slope geometry on slip surface

Slope geometry were shown to have a direct relation with the stability of the slope as well as the soil strength's properties (Namdar, 2011).

In the last models series, strength parameters of soil kept unchanged at the following values, whereas angles ranged from 0 ° to 63.4° for (Beta) angle while (Alpha) angle ranged from 0 ° to 19.8° in slope geometry (shown in Figure 4.4).

Cohesion = 15 kPa, internal angle of friction = 15°, unit weight = 15 kN/m^3.

Table 4.11: Impact of slope geometry on slip surface

Model No	α (˚)	β (˚)	Slope Height (m)	Entry (m)	Exit (m)	Radius (m)	La (m)	Factor of Safety
1	19.8	0	20	16.9, 13.9	25, 6.1	24.4	11.467	1.037
2	17.75	0	19	17.9, 13.2	25, 6.1	22.9	10.285	1.033
3	15.6	0	18	18.9, 12.6	25, 6.2	21.3	9.1261	1.047
4	13.5	0	17	18.9, 12.5	25, 6.18	20.4	9.0438	1.058
5	11.3	0	16	20,12	25, 6.1	105.6	7.4748	1.042
6	9.1	0	15	19.9, 11.8	25, 6.18	18.64	7.7090	1.048
7	6.8	0	14	20, 11.6	25, 6.2	17.9	7.6002	1.052
8	4.6	0	13	20, 11.4	25, 6.17	93.1	7.0123	1.079
9	2.3	0	12	20.9, 11.16	25, 6.2	89.67	6.0907	1.061
10	0	0	11	21, 11	25, 6.15	90.18	5.9075	1.053
11	0	11.3	11	19.3, 11	25, 6.08	15.43	7.6643	1.252
12	0	21.8	11	18.7, 11	25, 6	15.4	8.2403	1.419
13	0	31	11	17.2, 11	25, 6	9.42	9.8461	1.580
14	0	38.75	11	18.1, 11	25, 6.04	8.8	8.9029	1.642
15	0	45	11	17.5, 11	24.9, 6.1	6.53	9.8891	1.774
16	0	50.2	11	16.7, 11	24.7, 6.3	6.58	10.262	1.928
17	0	54.5	11	15.8, 11	25, 6.02	7.16	11.706	1.978
18	0	58	11	14.6, 11	25, 6.03	7.63	13.197	2.088
19	0	61	11	13.6, 11	25.4, 6)	8.2	14.834	2.185
20	0	63.4	11	12.5, 11	27, 6	9.4	18.053	2.302

4.4 Impact of Geometry and Soil Strength Parameters on Factor of Safety

To evaluate the impact geometry and strength parameters of soil on the factor of safety, FOS versus the strength parameters was offered and drawn in the following figures.

4.4.1 Impact of cohesion, C, on factor of safety

The cohesion effect on the factor of safety has been shown in this part. Increasing the value of cohesion as a resistant, holding, force, as expected, raised the value of the factor of safety. Figure 4.6 shows the linear correlation between cohesion and factor of safety. FOS is nearly linear with a R^2 factor of 0.99.

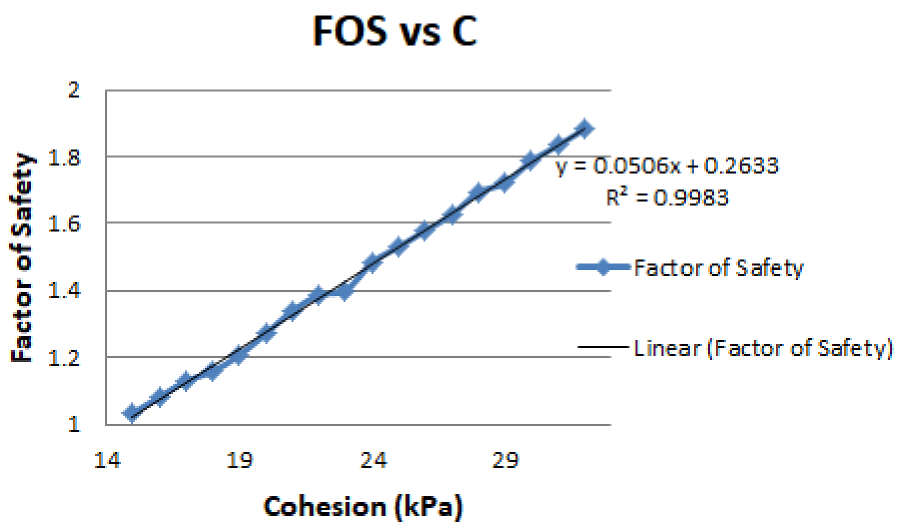

Figure 4.6: Effect of cohesion on the FOS

4.4.2 Impact of internal friction angle on the factor of safety

The effect of the friction angle on the factor of safety was shown in this part. Increasing the internal friction angle value which is also a holding force, as expected, increased the factor of safety value. As it shown in Figure 4.7 the correlation between FOS and the internal friction angle.

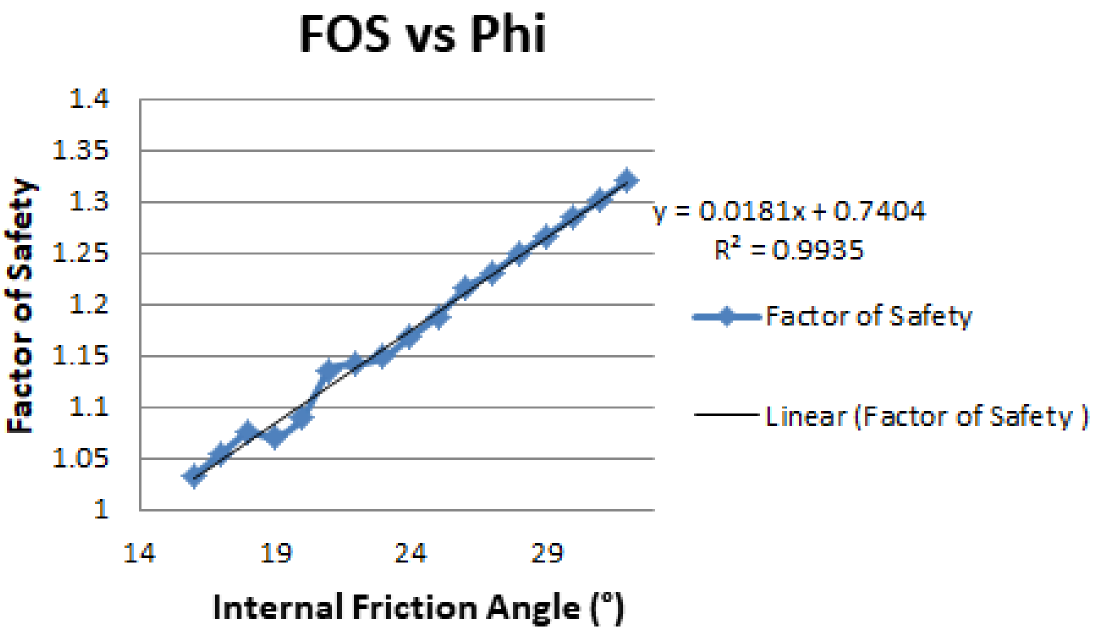

Figure 4.7: Internal friction angle impact on factor of safety

4.4.3 Impact of unit weight, ɤ, on factor of safety

Figure 4.8 shows the influence of soil unit weight, ɤ, on the factor of safety. As could be shown from the Figure 4.8, ɤ is inversely proportional to factor of safety as the major derivative factor, on soil mass was applied.

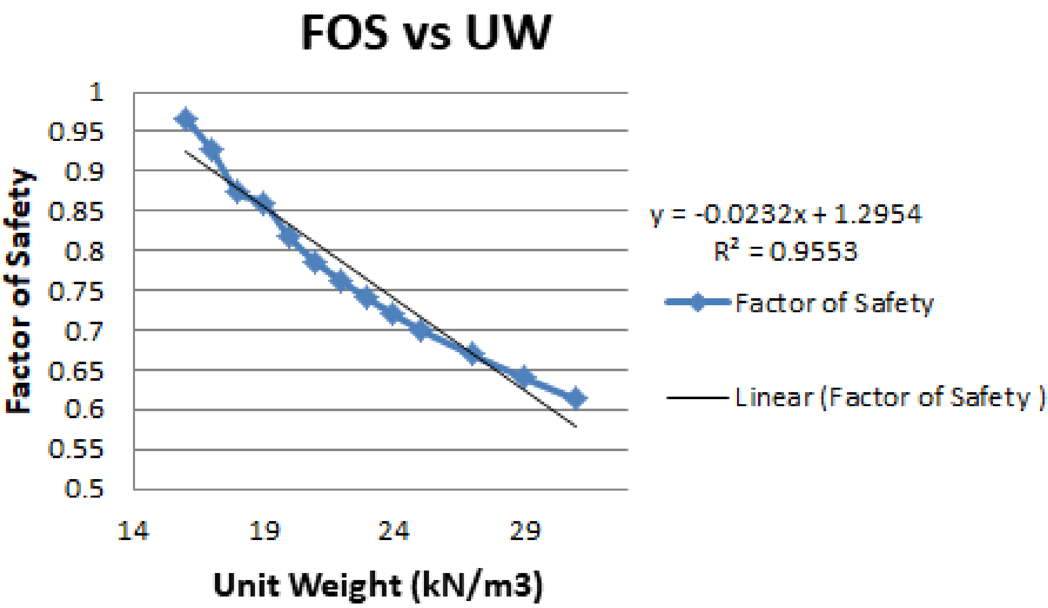

Figure 4.8: Impact of unit weight on the FOS

4.4.4.The combined impact of unit weight and cohesion on factor of safety

In this section, the impact of cohesion and the soil unit weight, ɤ on factor of safety was studied. Cohesion and soil unit weight were raised altogether here, but the ratio kept unchanged. The outputs dictate that the potential surface of the slip is affected by combining of Phi and C, the function which is defined as λ equivalent to:

$$\lambda = C / (\gamma * h * \tan\emptyset) \quad (2.45)$$

Figure 4.9 shows the impact of cohesion and unit weight on FOS while lambda value stays constant.

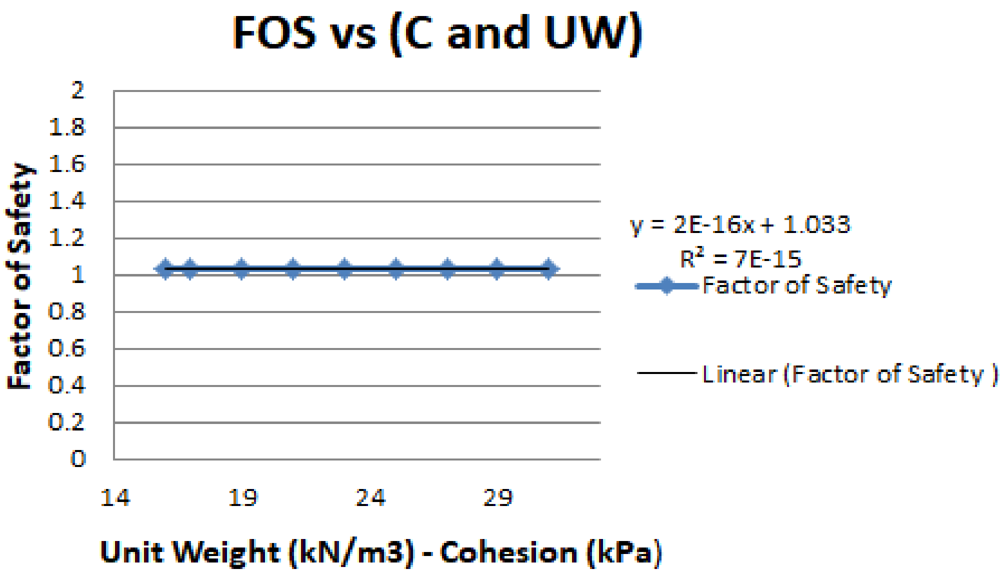

Figure 4.9: The combined effect of unit weight and cohesion the on FOS

4.4.5 The combined impact of friction angle, Ø, and unit weight on factor of safety

In this section, by increasing both, the values of Phi and unit weight, ɤ. Therefore, in Figure 4.10 the factor of safety versus Phi and γ curve was presented.

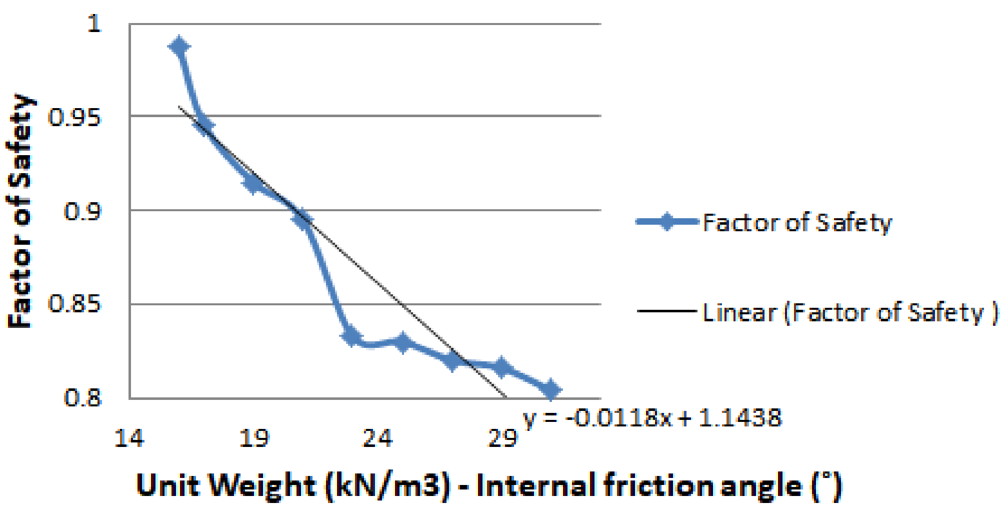

Figure 4.10: The impact of friction angle, Ø, and unit weight on factor of safety

As shown in Figure 4.10, decrease in the value of FOS was achieved by raising the value of Ø and γ. This is due to the failure surface movements to the upper side, thus reducing the La and so reducing the influence of resisting and holding forces.

4.4.6.The combined Impact of friction angle, Phi, and cohesion, C, on factor of safety

In this section, since the surface of potential failure is expected to be influenced by both of C, and Ø values, Figure 4.11 shows the relationship between the factor of safety and C, Ø. Because both of these parameters of shear strength are holding factors, increasing those two parameters results in a raise in the value of the factor of safety. FOS is nearly linear with R^2 factor of 0.9999.

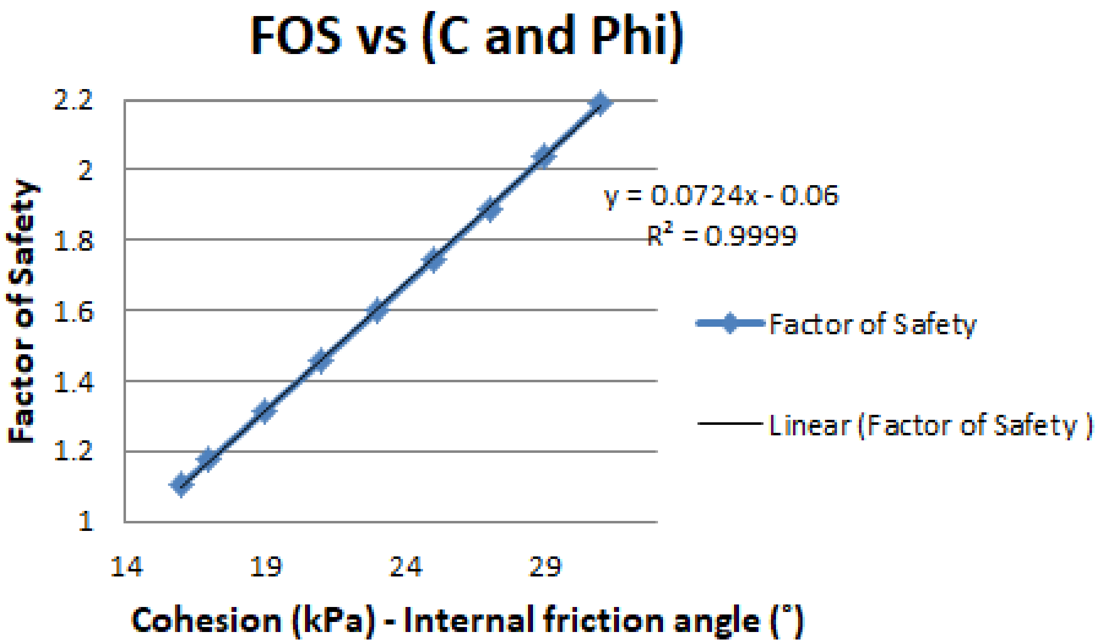

Figure 4.11: The impact of Phi and cohesion on FOS

4.4.7 Impact of the slope geometry on factor of safety

In the methodology section two slope angles α and β were introduced and used to test the impact of geometry on factor of safety and their impact on the factor of safety was observed. The results will be presented in the figures below.

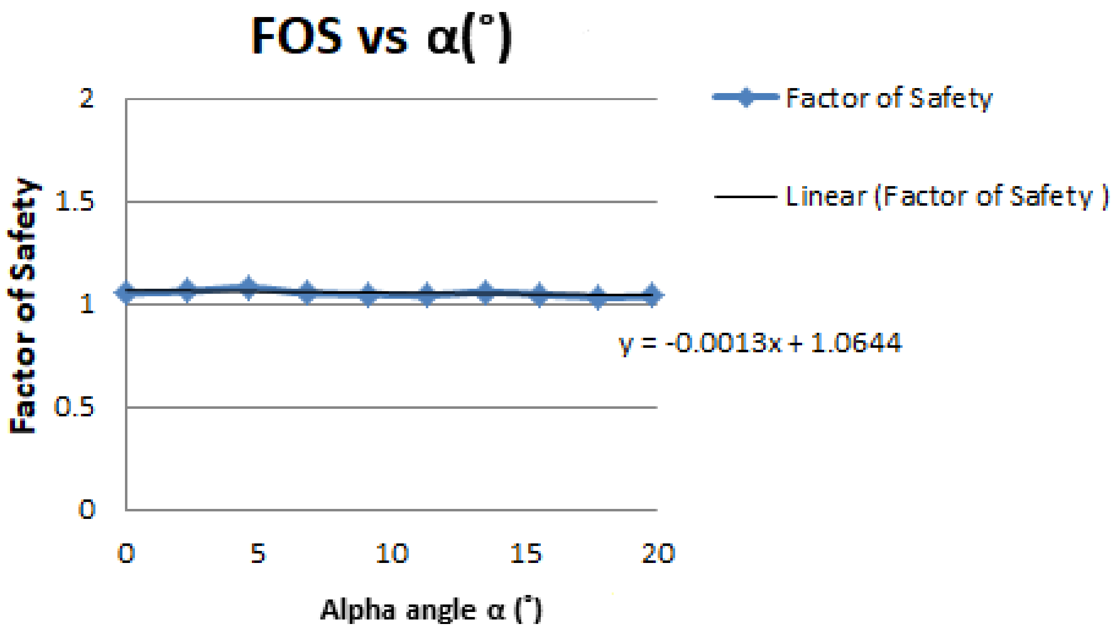

Figure 4.12: Alpha angle impact on factor of safety

Figure 4.12 represents that no noticeable variation is observed in the factor of safety except the value of FOS between angles 4.6˚ and 6.8˚, it decreased unpretentiously after the angle 6.8˚ although it was increasing slightly before that value of Alpha angle. These decrease because it is possible by increase the Alpha angle as if adding an additional overhead load on the surface of the slope. But before the angle 6.8˚ it causes increases the surface of the failure and thus increases the length of the arc, it generates more resistant force and makes the factor of safety constant. While this rise in the surface of failure produces more resistant force, it simultaneously produces an increase in derivative force (weight of the surface of failure). The factor of safety therefore remains constant. For angles more than 6.8˚, the rise in derivative force approaches the value of the resisting force and from this angle value onwards, the derivative force becomes greater than the resisting force, and for that a decrease can could seen in the value of factor of safety.

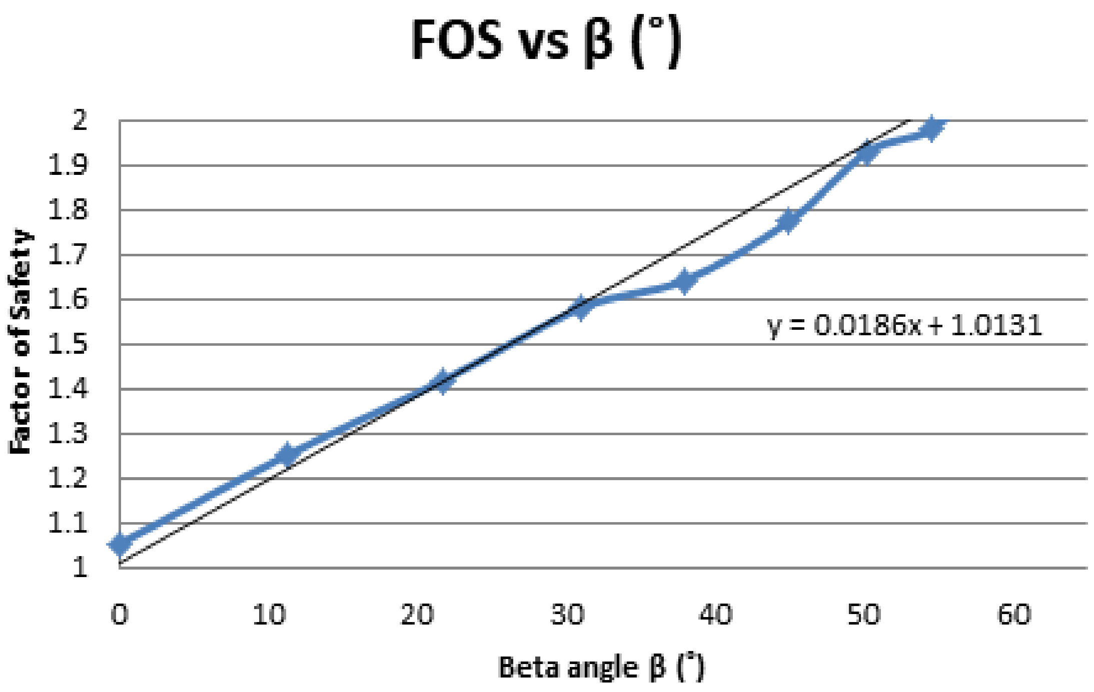

Figure 4.13: Beta angle impact on factor of safety

Figure 4.11 represents the factor of safety significantly increases by increasing Beta angle. The reason for this behavior is that only the failure arc length increases as holding force and the weight of the failure shape as driving force stays constant by increasing the beta angle. For that by increasing the length of the arc result an increase in the resisting force and thus the factor of safety.

4.5 Impact of Soil Strength and Geometry Parameters on Slip Surface

To study the impact of every soil parameter on the slip surface, the length of the failure arc was selected to be studied as a quantitative variable. To demonstrate this impact, the following figures will be provided.

4.5.1 Impact of cohesion on La length of failure arc

The impact of cohesion La is shown in Figure 4.12.

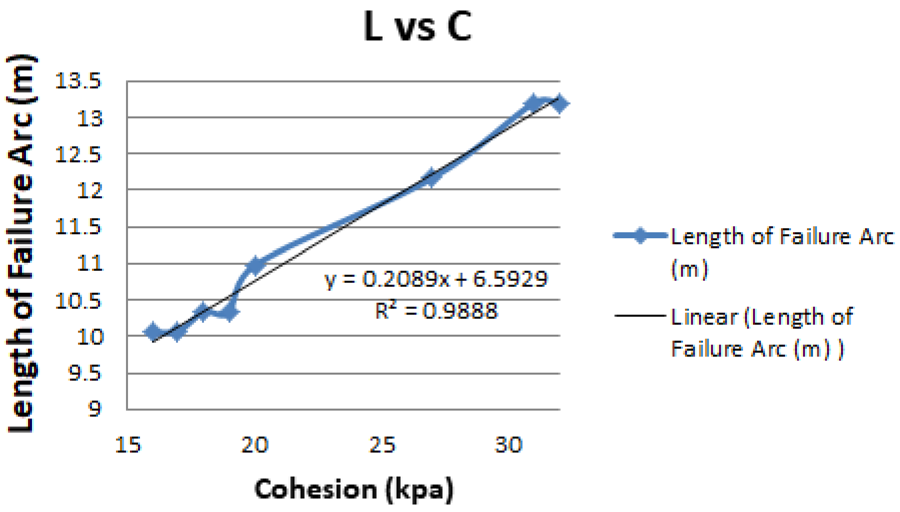

Figure 4.14: Cohesion impact on La length of failure arc

The figure represents that the length of the failure surface will increase with an increase in value of cohesion. The cause is that in the state of the constant location of the failed surface, as the cohesion force raises, the holding force becomes greater the same thing for the FOS. The deriving force must raise, which could be accomplished by increase the area of slope fail, in order to determine the minimum value of FOS (that is initial objective for slope stability analysing). This results in a larger arc failure length and so a greater value of FOS.

4.5.2 Impact of friction angle, Phi, on length of failure.arc

The impact of Phi on failure surface length is shown in Figure 4.13.

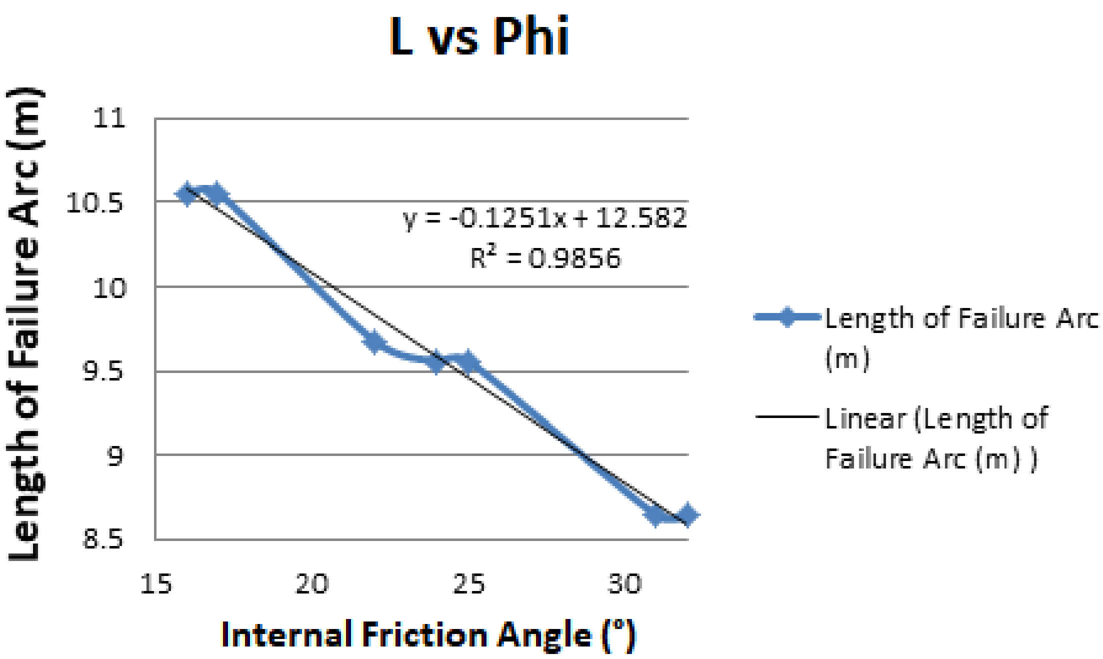

Figure 4.15: Internal friction angle impact on length of failure arc

In the previous section, referring to the same explanation, it could be anticipated that La must be in a proportional correlation with Ø, but as could be seen in Figure 4.13, L and Ø are related inversely.

This inverse relationship is consistent with the study of (Jiang & Yamagami, 2006) that sets that when the distribution of geometry of the slope, unit weight in a homogeneous soil slope is given, the critical slip surface location for specifically slice method is only related to the ratio $\frac{c}{\tan(\varphi)}$ of that slope This study indicates that the slip surface position and therefore La is in the inverse relationship to the angle of the friction.

4.5.3 Impact of unit weight, ɤ, on length of failure arc

In this part the impact of unit weight on failure length arc has been studied.

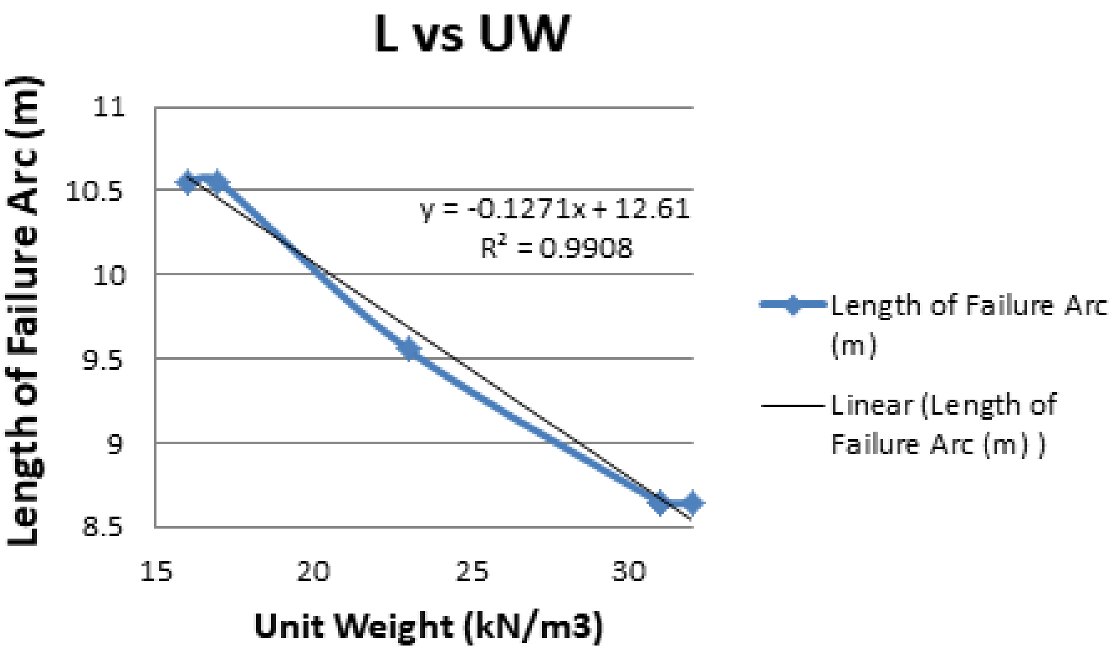

Figure 4.16: Effect of unit weight on La

As shown in Figure 4.14 by raising soil unit weight, the weight of the fallen area rises, resulting a small factor of safety. To say it in another word, by considering lambda the surface of the failure slip shifts towards the face of the slope, while by reducing La, the impact of the friction angle and cohesion as the forces of resistance reduce, thus achieving a smaller factor of safety.

4.5.4. The combined impact of cohesion, C, and unit weight on length of failure arc, La

In this section, unit weight and cohesion increased altogether in a way the ratio remain unchanged. The results shown in Figure 4.15.

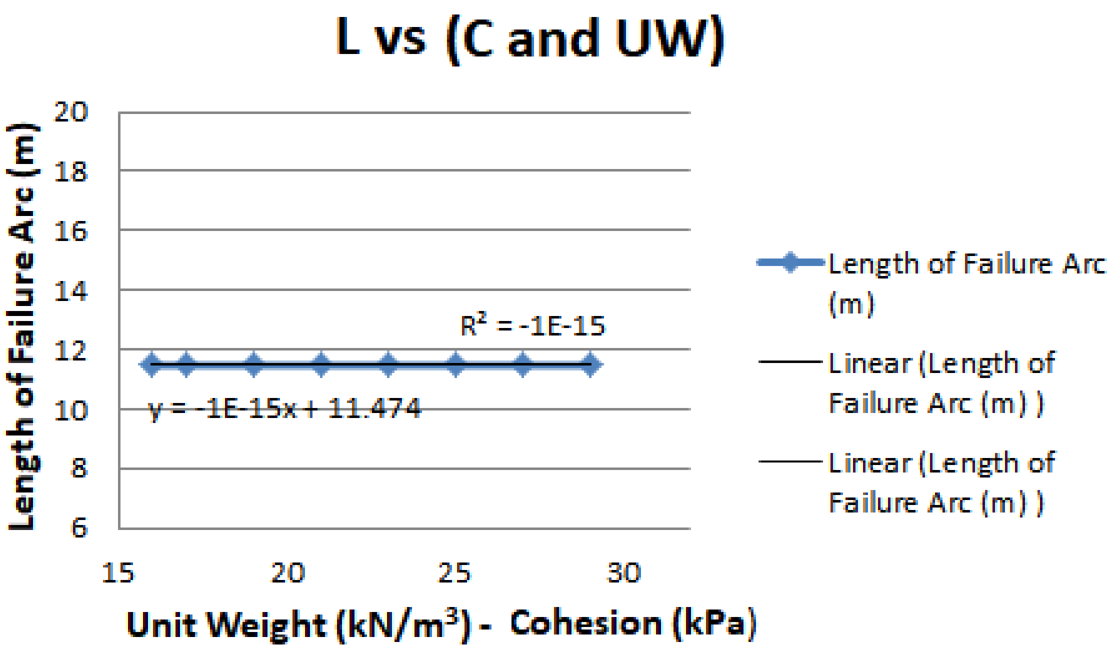

Figure 4.17: The combined impact of cohesion and unit weight on La

Constant c over unit weight ratio, which results in a constant λ. As noted in the study of.(Lin & Cao,.2011) this means the same shape of failure and therefore a unchanged value of La.

4.5.5 The combined impact of friction angle, Phi, and unit weight, ɤ, on La

In this part, unit weight and Phi increased together. The results shown in Figure 4.15 to show the variation impact for both of the strength factors.

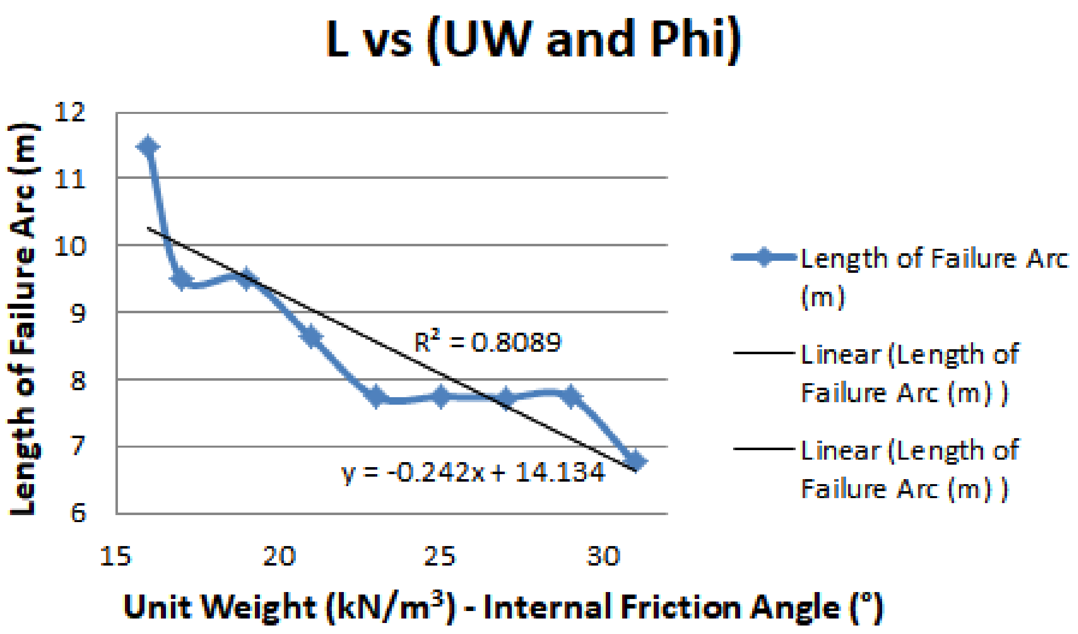

Figure 4.18: The combined impact of internal friction angle and unit weight on the length of failure arc

It can be seen that there will be a reduction in the length of the surface failure by increasing the value of γ and tanφ. It is consists when talking about the λ value, by maximizing this value, λ declines; smaller value of λ means surface of failure nearer to surface of the slope and thus a smaller La.

4.5.6 The combined impact of cohesion and internal friction angle on the length of failure arc

The following figure illustrates the combined impact on the length of the failure arc of variable internal friction angle and cohesion the results have been drawn in Figure 4.17.

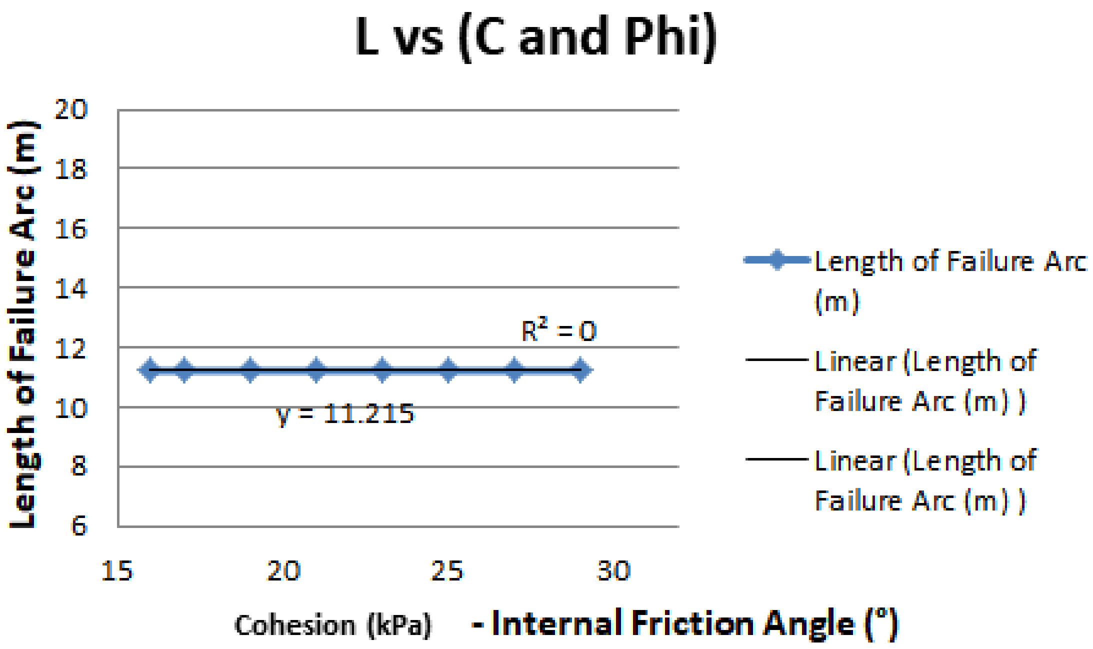

Figure 4.19: The combined impact of cohesion and Phi on La length of failure arc

From the Figure 4.17, it could be seen that La will remain relatively unchanged at value (11.215 m) when both of the factors cohesion and internal friction angle remain constant between the values (16-32). Since constant C and tan(Ø) results in a constant lambda, and constant lambda means a constant surface of failure, the length of the arc also remains constant.

4.5.7 Impact of slope geometry on length of failure arc

In Figure 4.18 and Figure 4.19, La were measured and drawn as a numerical value to show the impact of slope geometry on the surface of the failure.

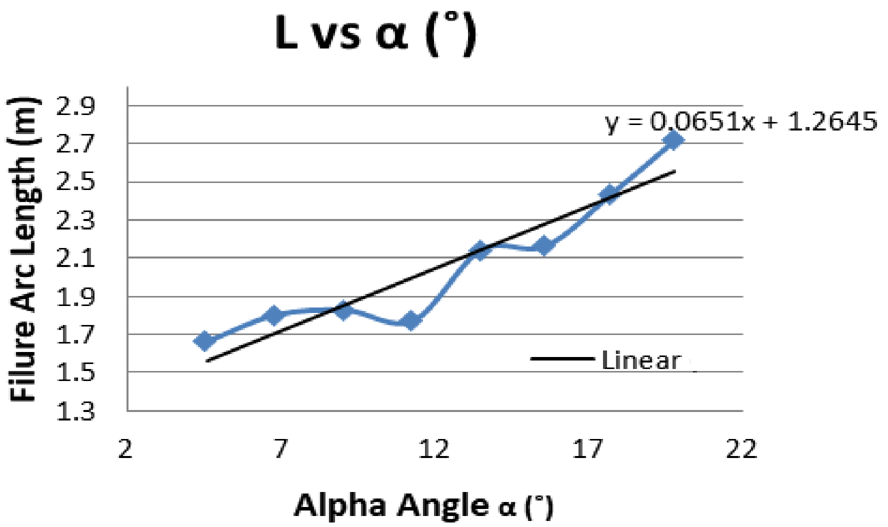

Figure 4.20: The impact of Alpha angle on the La

Results of analysis of the models indicate that the position of the failure surface does not differ significantly by increasing the Alpha angle. The cause for increasing La is only the slope surface motion and therefore the failure arc extension.

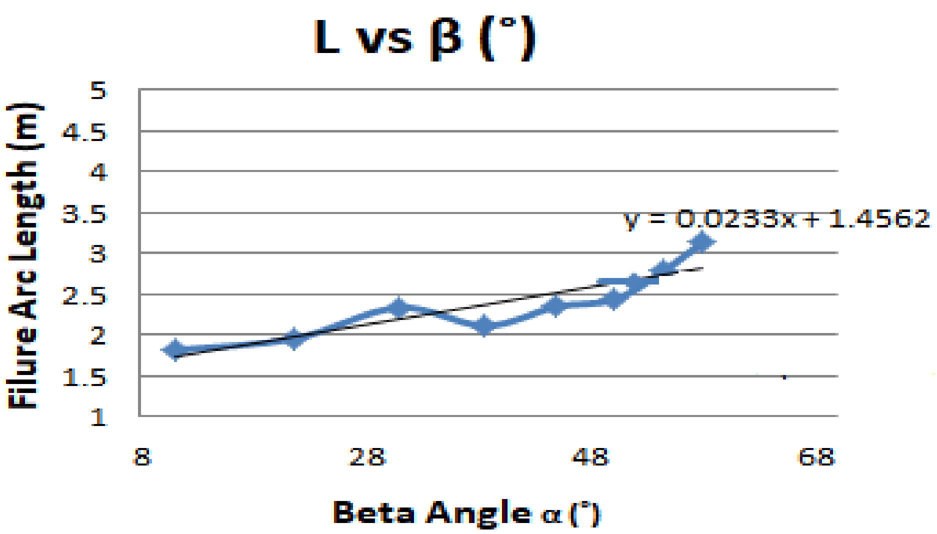

Figure 4.21: Beta angle impact on La

By raising Beta angle value (the other factors in Eq (2.45) will not change and therefore do not affect the value of lambda), the failure surface depth does not change. At the other side, a raise in the Beta angle can shift the surface of the slope to the right so this going to cause the arc to extend as shown in Figure 4.19.

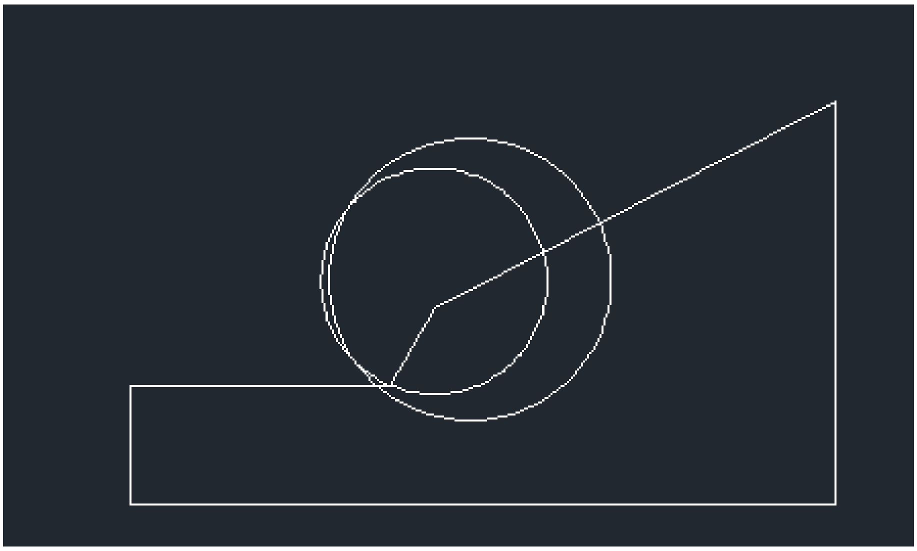

[a]

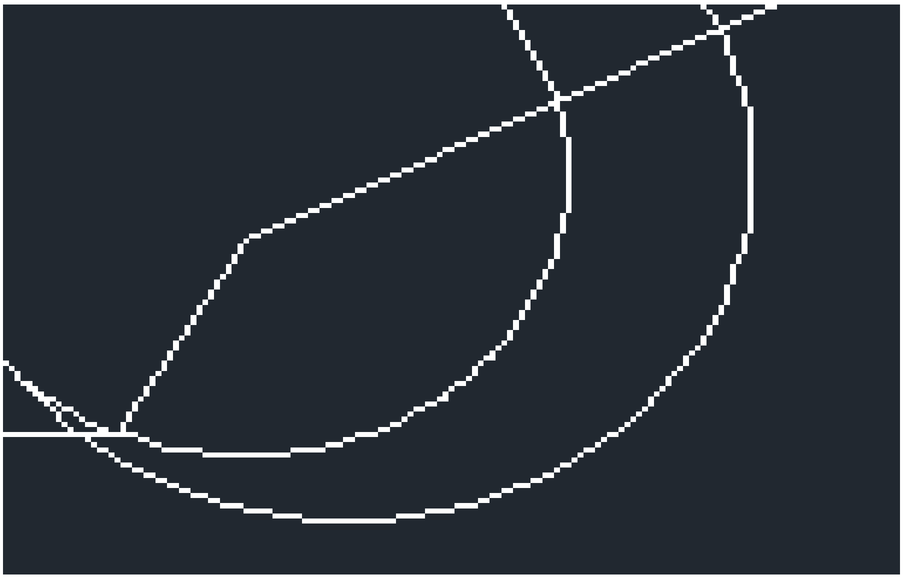

[b]

Figure 4.22: [a] Alpha angle impact on length of Arc and [b] zoomed portion of [a]

4.6 Reanalyzing Models by PLAXIS and Comparison of Results

The studied models were reanalyzed using PLAXIS software program to assure the outputs of SLOPE/W program acquired in part 4.3. Table 4.12 shows the results of these analyzes.

Table 4.12: Models of cohesion values chosen for the factor of safety analysis - PLAXIS

Model number	Unit weight [kN/m^3]	Internal Friction angle [°]	Cohesion [kPa]	Factor of safety
2	15	15	16	1.051
4	15	15	18	1.107
6	15	15	20	1.254
8	15	15	22	1.328
10	15	15	24	1.419
12	15	15	26	1.532
14	15	15	28	1.634
16	15	15	30	1.722

Table 4.13: Models of friction angle, Phi values selected for the factor of safety analysis for PLAXIS software

Model No	Unit Weight (kN/m^3)	Internal Friction Angle (°)	Cohesion (kPa)	Factor of Safety
19	15	16	15	1.047
21	15	18	15	1.061
23	15	20	15	1.073
25	15	22	15	1.108
27	15	24	15	1.152
29	15	26	15	1.237
31	15	28	15	1.271
33	15	30	15	1.316

Table 4.14: Models of unit weight values chosen for factor of safety analysis for - PLAXIS

Model number	Unit weight [kN/m^3]	Internal Friction angle [°]	Cohesion [kPa]	Factor of safety
37	17	15	15	0.867
39	19	15	15	0.796
41	21	15	15	0.752
43	23	15	15	0.713
45	25	15	15	0.689
46	27	15	15	0.635
47	29	15	15	0.608
48	31	15	15	0.594

Table 4.15: Models of unit weight and C values chosen for FOS analysis by PLAXIS software

Model No	Unit weight [kN/m³]	Internal friction angle [°]	Cohesion [kPa]	Factor of safety
49	16	15	16	1.024
50	17	15	17	1.024
51	19	15	19	1.024
52	21	15	21	1.024
53	23	15	23	1.024
54	25	15	25	1.024
55	27	15	27	1.024
56	29	15	29	1.024
57	31	15	31	1.024

Table 4.16: Models of unit weight and internal friction angle values chosen for the FOS analysis for PLAXIS software

Model number	Unit weight [kN/m³]	Internal friction angle [°]	Cohesion [kPa]	Factor of safety
58	16	16	15	0.954
59	17	17	15	0.937
60	19	19	15	0.912
61	21	21	15	0.900
62	23	23	15	0.868
63	25	25	15	0.838
64	27	27	15	0.824
65	29	29	15	0.809
66	31	31	15	0.792

Table 4.17: Models of cohesion, c and friction angle, Phi values chosen for the factor of safety analysis for PLAXIS software

Model number	**Unit weight [kN/m^3]**	**Internal friction angle [°]**	**Cohesion [kPa]**	**Factor of safety**
67	15	16	16	1.048
68	15	17	17	1.120
69	15	19	19	1.224
70	15	21	21	1.391
71	15	23	23	1.493
72	15	25	25	1.617
73	15	27	27	1.803
74	15	29	29	1.947
75	15	31	31	2.113

Table 4.18 summarizes the distinction between the FOS acquired from both programs (PLAXIS and SLOPE/W) and compares these results using the following formula.

$$\text{Difference} = \frac{\text{FOS(SLOPEW)} - \text{FOS(PLAXIS)}}{\text{FOS (PLAXIS)}} * 100 \qquad (4.1)$$

Table 4.18: the difference of FOS between PLAXIS and SLOPE/W

Model No	SLOPE/W FOS	PLAXIS FOS	Difference %
2	1.081	1.051	2.9
4	1.158	1.107	4.6
6	1.272	1.254	1.4
8	1.387	1.328	4.4
10	1.483	1.419	4.8
12	1.578	1.532	3
14	1.693	1.634	3.6
16	1.787	1.722	3.8
19	1.033	1.047	-1.3
21	1.074	1.061	1.2
23	1.089	1.073	1.5
25	1.141	1.108	2.9
27	1.168	1.152	1.4
29	1.215	1.237	-1.8
31	1.249	1.271	-1.7
33	1.284	1.316	-2
37	0.927	0.867	3
39	0.86	0.796	3.2
41	0.786	0.752	1.7
43	0.74	0.713	1.35
45	0.701	0.689	0.6
46	0.669	0.635	1.7
47	0.64	0.608	1.6
48	0.613	0.594	0.95
49	1.033	1.024	0.45

Table 4.18: the difference of FOS between PLAXIS and SLOPE/W

Model No	SLOPE/W FOS	PLAXIS FOS	Difference %
50	1.033	1.024	0.45
51	1.033	1.024	0.45
52	1.033	1.024	0.45
53	1.033	1.024	0.45
54	1.033	1.024	0.45
55	1.033	1.024	0.45
56	1.033	1.024	0.45
57	1.033	1.024	0.45
58	0.988	0.954	1.7
59	0.946	0.937	0.45
60	0.915	0.912	0.15
61	0.895	0.9	-0.25
62	0.833	0.868	-1.75
63	0.83	0.838	-0.4
64	0.82	0.824	-0.2
65	0.816	0.809	0.35
66	0.804	0.792	1.52
67	1.103	1.048	2.75
68	1.173	1.12	2.65
69	1.314	1.224	4.5
70	1.456	1.391	4.6
71	1.6	1.553	3
72	1.745	1.687	3.4
73	1.891	1.803	4.4
74	2.04	1.947	4.7
75	2.19	2.11	3.8

Table 4.19: Effect of slope geometry on the slip surface - PLAXIS

Model number	**α [˚]**	**β [˚]**	**Slope Height (m)**	**Factor of Safety**
1	19.8	0	20	1.013
2	17.75	0	19	1.029
3	15.6	0	18	1.042
4	13.5	0	17	1.061
5	11.3	0	16	1.057
6	9.1	0	15	1.064
7	6.8	0	14	1.052
8	4.6	0	13	1.057
9	2.3	0	12	1.055
10	0	0	11	1.048
11	0	11.3	11	1.216
12	0	21.8	11	1.365
13	0	31	11	1.521
14	0	38	11	1.609
15	0	45	11	1.693
16	0	50.2	11	1.877
17	0	54.5	11	1.951
18	0	58	11	2.029
19	0	61	11	2.129
20	0	63.4	11	2.274

Table 4.21: The difference of FOS between PLAXIS and SLOPE/W for slope geometry

Model No	**SLOPE/W FOS**	**PLAXIS FOS**	**Difference (%)**
1	1.037	1.013	1.2
2	1.033	1.029	0.2
3	1.047	1.042	0.25
4	1.058	1.061	-0.15
5	1.042	1.057	-0.75
6	1.048	1.064	-0.8
7	1.052	1.052	0
8	1.079	1.057	1.1
9	1.061	1.055	0.3
10	1.053	1.048	0.25
11	1.252	1.216	1.8
12	1.419	1.365	2.7
13	1.58	1.521	2.95
14	1.642	1.609	1.65
15	1.774	1.693	4.05
16	1.928	1.877	2.55
17	1.978	1.951	1.35
18	2.088	2.029	2.95
19	2.185	2.129	2.8
20	2.302	2.274	1.4

It can be seen in Table 4.18 that PLAXIS is a more conservative designing program. On average, PLAXIS gives less than 5% lower FOS (except few models) which gave FOS greater than SLOPE/W software that will make PLAXIS more conservative and therefore safer to design and analyze more significant slopes.

By comparison, giving SLOPE/W a higher FOS makes it more beneficial to analyze and design less important slopes.

4.7 Reanalyzing the Past Models by FLAC/Slope

To inspect the results of PLAXIS and SLOPE/W, a sample of the models were chosen up to their properties, and by using the FLAC program these models have been reanalyzed as shown in Tables 4.22 and 4.23. Considering that FLAC is not software with a complete LEM, the results may show a distinction between three software.

Table 4.22: Reanalyze models by using FLAC software (shear strength parameters models)

Model number	Unit weight [kN/m^3]	Internal Friction angle[°]	Cohesion [kPa]	Factor of safety
6	15	15	20	1.029
11	15	15	25	1.221
23	15	20	15	0.932
28	15	25	15	1.049
45	25	15	15	0.607
54	25	15	25	0.842
63	25	25	15	0.764
72	15	25	25	1.436

Table 4.23: Reanalyze models by using FLAC software (slope geometry models)

Model No	α (˚)	β (˚)	Factor of Safety
6	9.1	0	0.869
15	0	45	1.827

Table 4.24: The difference between the three software packages (shear strength parameters models)

Model no	Factor of safety of			Difference between FLAC and	
	FLAC	SLOPE/W	PLAXIS	SLOPE/W (%)	PLAXIS (%)
6	1.029	1.272	1.254	23.6152	21.8659
23	0.932	1.089	1.073	16.846	15.1288
45	0.607	0.701	0.689	15.486	13.5091
54	0.842	1.053	1.024	25.0594	216152
63	0.764	0.83	0.838	8.6387	9.6859
72	1.436	1.745	1.617	21.5181	12.6045

Table 4.25: The difference between the three software packages (slope geometry models)

Model no	Factor of safety of			Difference between FLAC and	
	FLAC	SLOPE/W	PLAXIS	SLOPE/W (%)	PLAXIS (%)
6	0.869	1.048	1.064	20.5984	19.5
15	1.827	1.774	1.774	2.901	-5.3

As shown in Tables 4.24 and 4.25, the average distinction between FLAC/SLOPE and the others programs is less than 1 percent, which is appropriate. In addition, it is noticeable that FOSs obtained from FLAC are lower than the other two programs in 75% of the models.

CHAPTER 5

CONCLUSIONS AND RECOMMENDATIONS

5.1 Conclusions

The conclusions were drawn on the basis of the slope stability analyzes by using the software packages PLAXIS, SLOPE/W and FLAC.

1. Cohesion (c) and friction angle (Ø), as resistance forces are directly related to the factor of safety while unit weight as deriving force is inversely related to the factor of safety.

2. The outputs of this study showed that regarding their friction angle the slopes formed by smaller grains of soil will be more stable; moreover, silty and well-graded soils are more stable than soils with coarse grains such as gravel and sandy soils. Also, slopes with the heavier soil in terms of unit weight have less stability.

3. Slopes made of boulders or the ones with high content of discrete large grains have less stability than slopes formed of gravelly soil.

4. In this study, it is found that clayey and silty sands which represent the soil with unit weight values more than 15 kN/m^3 with constant values of cohesion and friction angle have failed for all slopes. On the other hand, in silty clayey soils with value of cohesion 15 kPa and unit weight and friction angle differing values, the slope would still unstable.

5. According to the dimensionless function λ and the results showed that, an increase in the cohesion value results to higher value for length of failure arc (La). On the other hand, an increase in the friction angle and the unit weight of soil values result to reduce the length of failure arc, (La) value.

6. An increase in the value of Alpha angle to a specific value doesn’t have any noticeable influence on FOS, while, an increase in the value of the Beta angle affects directly on the factor of safety.

7. The greater value of the Alpha angle, leads to a greater value of La. However, varying the value of Beta angle doesn’t affect as much as Alpha does on the value of La.

8. PLAXIS is more conservative software for slope stability studies, comparing to SLOPE/W which it gives about 5% lower value for factor of safety.

9. FLAC/Slope is the most complicated software to deal with and usually gave out the lowest value for factor of safety in comparison with PLAXIS and SLOPE/W.

10. No significant relation between length of failure arc (La) and factor of safety FOS was found.

5.2 Recommendations

The following recommendations analysis can be performed for other studies in connection with this thesis:

1. Analysis and modeling wider range in parameters of soil strength.

2. Including the level of water content and consideration of unsaturated soils and the effect of water pressure.

3. Including more slope geometry variables as the angle of the slope itself and the length of the slope.

4. Conducting a real-scale study to verify the validation of the equations acquired to locate the critical surface of the failure.

REFERENCES

Aaron, J., & Mcdougall, S. (2019). Rock avalanche mobility : The role of path material. *Engineering Geology*, *257*, 105-126.

Adams, C. (2015). *Slope stability analysis of a small intermittent failure* (Doctoral dissertation, California State University, Chico).

Albataineh, N. (2006). *Slope stability analysis using 2D and 3D methods* (Doctoral dissertation, University of Akron, Ohio, USA.

Amini, M., & Ardestani, A. (2019). Stability analysis of the north-eastern slope of Daralou copper open pit mine against a secondary toppling failure. *Engineering Geology*, *249*, 89–101.

Anagnosti, P. (1969). Three-dimensional stability of fill dams. In *Proceeding of 7th International Conference on Soil Mechanics and Foundation Engineering, Mexico* (pp. 275-280).

Anderson, M. G., & Richards, K. S. (1987). Modelling slope stability: the complimentary nature of geotechnical and geomorphological approaches. *Slope Stability: Geotechnical Engineering and Geomorphology*. New York ,John Wiley and Sons, p 1-9.

Aryal, K. P. (2008, October). Differences between LE and FE methods used in slope stability evaluations. In *12th International Conference of International Association for Computer Methods and Advances in Geomechanics (IACMAG)* (pp. 1-6).

Azadmanesh, M., & Arafati, N. (2012). A comparison on slope stability analysis of aydoghmoosh earth dam by limit equilibrium, finite element and finite difference methods. *International Journal of Civil Engineering and Building Materials*, *2*(3), 115-123, (ISSN 2223-487X).

Azimi, S. R. (2016). *Soil slope stability techniques: A comprehensive analysis*, (Doctoral dissertation), Curtin University, Perth, Australia.

Azzouz, A. S., & Baligh, M. M. (1983). Loaded areas on cohesive slopes. *Journal of Geotechnical Engineering*, *109*(5), 724-729.

Azzouz, A. S., Baligh, M. M., & Ladd, C. C. (1981). Three-dimensional stability analyses of four embankment failures. In *Proc., 10th Int. Conf. on Soil Mechanics and Foundation Engineering* (Vol. 3, pp. 343-346).

Johari, A., Fazeli, A., & Javadi, A. A. (2013). An investigation into application of jointly distributed random variables method in reliability assessment of rock slope stability. *Computers and Geotechnics*, *47*, 42-47.

Baker, R., & Leshchinsky, D. (1987). Stability analysis of conical heaps. *Soils and Foundations*, *27*(4), 99-110.

Baligh, M. M., & Azzouz, A. S. (1975). End effects on stability of cohesive slopes. *Journal of Geotechnical and Geoenvironmental Engineering*, *101*(ASCE# 11705 Proceeding).

Baligh, M. M., Azzouz, A. S., & Ladd, C. C. (1977). Line loads on cohesive slopes. In *Proceedings of the Ninth International Conference on Soil Mechanics and Foundation Engineering. Tokyo, Japan:[sn]* (pp. 13-17).

Bolton, H., Heymann, G., & Groenwold, A. (2003). Global search for critical failure surface in slope stability analysis. *Engineering Optimization*, *35*(1), 51-65.

Bromhead, E. N. (1992). The stability of slopes, blackie academic and professional. *Lond. UK*.

Bromhead, E. N., & Martin, P. L. (2004). Three-dimensional limit equilibrium analysis of the Taren landslide. In *Advances in geotechnical engineering: The Skempton conference: Proceedings of a three day conference on advances in geotechnical engineering, organised by the Institution of Civil Engineers and held at the Royal Geographical Society, London, UK, on 29–31* (pp. 789-802). Thomas Telford Publishing.

Cavounidis, S. (1987). On the ratio of factors of safety in slope stability analyses. *Geotechnique*, 37(2), 207-210.

Chen, R. H., & Chameau, J. L. (1983). Three-dimensional limit equilibrium analysis of slopes. *Geotechnique*, *33*(1), 31-40.

Cheng, Y. M., & Lau, C. K. (2014). *Slope stability analysis and stabilization: new methods and insight*. CRC Press

Cheng, Y. M., Lansivaara, T., & Siu, J. (2008). Impact of convergence on slope stability analysis and design. *Computers and Geotechnics*, *35*(1), 105–113.

Cheng, Y. M., Li, L., Chi, S. chun, & Wei, W. B. (2007). Particle swarm optimization algorithm for the location of the critical non-circular failure surface in two-dimensional slope stability analysis. *Computers and Geotechnics*, *34*(2), 92–103.

Cheng, Y. M. (2003). Location of critical failure surface and some further studies on slope stability analysis. *Computers and Geotechnics*, *30*(3), 255–267.

Cheng, Y. M., Li, L., Lansivaara, T., Chi, S. C., & Sun, Y. J. (2008). An improved harmony search minimization algorithm using different slip surface generation methods for slope stability analysis. *Engineering Optimization*, *40*(2), 95–115.

Chok, Y. H. (2009). *Modelling the effects of soil variability and vegetation on the stability of natural slopes,* The University of Adelaide School (Doctoral dissertation), Adelaide, Australia.

Cho, S. E., & Lee, S. R. (2002). Evaluation of surficial stability for homogeneous slopes considering rainfall characteristics. *Journal of Geotechnical and Geoenvironmental Engineering*, *128*(9), 756-763.

Cheng, Y. M., Lansivaara, T., & Siu, J. (2008). Impact of convergence on slope stability analysis and design. *Computers and Geotechnics*, *35*(1), 105–113.

Duncan, J. M., Wright, S. G., & Brandon, T. L. (2014). *Soil strength and slope stability*. Canada: John Wiley & Sons, Inc.

Duncan, J. M. (1996). State of the Art: Limit Equilibrium and Finite-Element Analysis of

Slopes. *Journal of Geotechnical Engineering*, *122*(7), 577–596.

Duncan, J. M. (1992). State-of-the-art: Static stability and deformation analysis. In *Proc. of Specialty Conf. Stability and Performance of Slopes and Embankments-II* (Vol. 1, pp. 222-266). ASCE.

EKSTRAND, D., & NYLANDER, P. Probabilistic Approach to Slope Stability, Department of Civil and Environmental Engineering, Master's Thesis, chalmers university of technology, Göteborg, Sweden.

Farah, K., Ltifi, M., & Hassis, H. (2011). Reliability analysis of slope stability using stochastic finite element method. *Procedia Engineering*, *10*, 1402–1407.

Feng, S. J., Chang, J. Y., Shi, H., Zheng, Q. T., Guo, X. Y., & Zhang, X. L. (2019). Failure of an unfilled landfill cell due to an adjacent steep slope and a high groundwater level: A case study. *Engineering Geology*, *262*, 105320.

Fredlund, D. G. (1987). Slope stability analysis incorporating the effect of soil suction. *Slope Stability*, 113-144.

Gens, A., Hutchinson, J. N., & Cavounidis, S. (1988). Three-dimensional analysis of slides in cohesive soils. *Geotechnique*, *38*(1), 1-23.

GEO-SLOPE International. (2015). Stability Modeling with SLOPE / W 2007 Version. In GEO-SLOPE International Ltd *Methods*.

Giger, M. W., & Krizek, R. J. (1976). Stability of vertical corner cut with concentrated surcharge load. *ASCE J Geotech Eng Div*, *102*(1), 31-40.

Griffiths, D. V., Huang, J., & Dewolfe, G. F. (2011). Numerical and analytical observations on long and infinite slopes. *International Journal for Numerical and Analytical Methods in Geomechanics*, *35*(5), 569-585.

Griffiths, D. V., & Lane, P. A. (1999). Slope stability analysis by finite elements. *Geotechnique*, *49*(3), 387-403.

Griffiths, D. V., & Marquez, R. M. (2007). Three-dimensional slope stability analysis by elasto-plastic finite elements. *Geotechnique*, *57*(6), 537-546.

Hammah, R., Yacoub, T., Corkum, B., & Curran, J. (2010). A comparison of finite element slope stability analysis with conventional limit-equilibrium investigation, University of Toronto, Toronto, Canada.

Hammouri, N. A., Malkawi, A. I. H., & Yamin, M. M. (2008). Stability analysis of slopes using the finite element method and limiting equilibrium approach. *Bulletin of Engineering Geology and the Environment*, *67*(4), 471.

Hovland, H. J. (1979). Three-dimensional slope stability analysis method. *Journal of Geotechnical and Geoenvironmental Engineering*, *105*(ASCE 14549 Proceeding).

Hungr, O. (1987). An extension of Bishop's simplified method of slope stability analysis to three dimensions. *Geotechnique*, *37*, 113-117.

Huvenne, V. A., Croker, P. F., & Henriet, J. P. (2002). A refreshing 3D view of an ancient sediment collapse and slope failure. *Terra Nova*, *14*(1), 33-40.

Itasca, U. D. E. C., & Code, U. D. E. (2011). Version 5.0, Itasca Consulting Group. *Inc., Minneapolis*.

Iverson, R. M. (1990). Groundwater flow fields in infinite slopes. *Geotechnique*, *40*(1), 139-143.

J Jiang, J. C., & Yamagami, T. (2006). Charts for estimating strength parameters from slips in homogeneous slopes. *Computers and Geotechnics*, *33*(6-7), 294-304.

Jiang, J. C., & Yamagami, T. (2008). A new back analysis of strength parameters from single slips. *Computers and Geotechnics*, *35*(2), 286-291.

Johari, A., Fazeli, A., & Javadi, A. A. (2013). An investigation into application of jointly distributed random variables method in reliability assessment of rock slope stability. *Computers and Geotechnics*, *47*, 42-47.

Kang, F., Han, S., Salgado, R., & Li, J. (2015). System probabilistic stability analysis of soil slopes using Gaussian process regression with Latin hypercube sampling. *Computers and Geotechnics*, *63*, 13-25.

Khabbaz, H., Fatahi, B., & Nucifora, C. (2012). Finite element methods against limit equilibrium approaches for slope stability analysis. In *Australia New Zealand Conference on Geomechanics*. Geomechanical Society and New Zealand Geotechnical Society.

Leshchinsky, D. O. V, Baker, R., & Silver, M. L. (1985). Three dimensional analysis of sslope stability. *International Journal for Numerical and Analytical Methods in Geomechanics*, *9*(3), 199-223.

Leshchinsky, D. O. V., & Baker, R. (1986). Three-dimensional slope stability: end effects. *Soils and Foundations*, *26*(4), 98-110.

Leshchinsky, D., & Huang, C. C. (1992). Generalized three-dimensional slope-stability analysis. *Journal of geotechnical engineering*, *118*(11), 1748-1764.

Lin, H., & Cao, P. (2012). Limit Equilibrium Analysis for the Relationships Among Slope c, Ø and Slip Surface. *Electronic Journal of Geotechnical Engineering*, *17*, 185-195.

Lin, H., & Cao, P. (2011). Potential slip surfaces of slope with strength parameters. In *Advanced Materials Research* (Vol. 243, pp. 3315-3318). Trans Tech Publications.

Li, B., Li, D., Zhang, Z., Yang, S., & Wang, F. (2015). Slope stability analysis based on quantum-behaved particle swarm optimization and least squares support vector machine. *Applied Mathematical Modelling*, *39*(17), 5253-5264.

Louis N.Y. Wong. (2014). Rock slope failure along non persistent joints insights from fracture mechanics approach. Nanyang Technological University, Singapore.

Malkawi, A. I. H., Hassan, W. F., & Sarma, S. K. (2001). Global search method for locating general slip surface using Monte Carlo techniques. *Journal of geotechnical and geoenvironmental engineering*, *127*(8), 688-698.

Matsui, T., & San, K. C. (1992). Finite element slope stability analysis by shear strength reduction technique. *Soils and foundations*, *32*(1), 59-70.

McCombie, P., & Wilkinson, P. (2002). The use of the simple genetic algorithm in finding the critical factor of safety in slope stability analysis. *Computers and Geotechnics, 29*(8), 699–714.

Mercier, D., Coquin, J., Feuillet, T., Decaulne, A., Cossart, E., Pall, H., & Sæmundsson, Þ. (2017). Geomorphology Are Icelandic rock-slope failures paraglacial ? Age evaluation of seventeen rock-slope failures in the Skagafjörður area , based on geomorphological stacking , radiocarbon dating and tephrochronology, *296*, 45–58.

Michalowski, R. L. (1989). Three-dimensional analysis of locally loaded slopes. *Geotechnique*, *39*(1), 27-38.

Mitchell, J. K., Chang, M., Seed, R. B., Mitchell, J. K. ;, Chang, M. ;, Cahill, E. G., & Cahill, J. R. (1993). The Kettleman Hills Landfill Failure: A Retrospective View of the Failure Investigations and Lessons Learned. In *International Conference on Case Histories in Geotechnical Engineering*, pp 1–15.

Naderi, M. A. (2013). *Determination of the critical slip surface in slope stability analysis* (Master dissertation), Eastern Mediterranean University (EMU) Doğu Akdeniz Üniversitesi (DAÜ), Famagusta, TRNC.

Namdar, A. (2011). Geometry in Slope Modeling and Design. *E-Journal of Science & Technology*, (C), 9–21.

NAVFAC, D. 7.01 (1986),“. *Soil Mechanics,” Design Manual*, *7*(01).

Nor, A. M. (2010). *Optimization of Cost Effectiveness for Slope Stability* (Doctoral dissertation), UMP.

Oghli, Z. (2011). *Analyzing slop stability by using shear strength reduction method*. (Master dissertation), Aleppo University, Aleppo, Syria.

Oh, S., & Lu, N. (2015). Slope stability analysis under unsaturated conditions: Case studies of rainfall-induced failure of cut slopes. *Engineering Geology*, *184*, 96–103.

Oh, S., & Lu, N. (2015). Slope stability analysis under unsaturated conditions: Case studies of rainfall-induced failure of cut slopes. *Engineering Geology*, *184*, 96–103.

Prajapati, G. 8, 2017). *Types of slope failure*. Retrieved from https://www.slideshare.net/GhanshyamPrajapati3/types-of-slope-failures.

Runesson, K., & Wiberg, N. E. (1984). *Stability analysis of natural slopes in clay by use of the finite element method*. Chalmers University of Technology.

Sengupta, A., & Upadhyay, A. (2009). Locating the critical failure surface in a slope stability analysis by genetic algorithm. *Applied Soft Computing Journal*, *9*(1), 387–392.

Serra.M (2013) Geotechnical stability analysis using student versions of FLAC, PLAXIS and SLOPE/W , Bachelor project . University of Southern Queensland. Australia .

Seed, R. B., Mitchell, J. K., & Seed, H. B. (1990). Kettleman hills waste landfill slope failure. II: stability analyses. *Journal of Geotechnical Engineering*, *116*(4), 669-690.

Sinai, C. (2012). Common Causes of Slope Failure. Retrieved from http://www.sinaiconstruction.net/LA-foundation-retrofit-blog/causes-of-slope-failure/

Spencer, E. (1967). A method of analysis of the stability of embankments assuming parallel inter-slice forces. *Geotechnique*, *17*(1), 11-26.

Stefano Utili, G. B. C. (2015). Landslide Hazards, Risks and Disasters,. Retrieved from https://www.sciencedirect.com/topics/earth-and-planetary-sciences/slope-stability

Suman, S. (2015). *Slope Stability Analysis Using Numerical Modelling* (Doctoral dissertation), National Institute of Technology, Rourkela, India.

Swan, C. C., & Seo, Y. K. (1999). Limit state analysis of earthen slopes using dual continuum/FEM approaches. *International Journal for Numerical and Analytical Methods in Geomechanics*, *23*(12), 1359-1371.

Tsai, T. L., & Yang, J. C. (2006). Modeling of rainfall-triggered shallow landslide. *Environmental Geology*, *50*(4), 525–534.

Ugai, K. (1985). Three-dimensional stability analysis of vertical cohesive slopes. *Soils and Foundations*, *25*(3), 41-48.

Ugai, K. (1988). Three-dimensional slope stability analysis by slice methods. In *Proc. 6th Inter. Conf. on Numer. Meth. in Geomech.,* Innsbruck, Austria.

Wiberg, N. E., Koponen, M., & Runesson, K. (1990). Finite element analysis of progressive failure in long slopes. *International Journal for Numerical and Analytical Methods in Geomechanics*, *14*(9), 599-612.

Whitman, R. V., & Bailey, W. A. (1967). Use of computers for slope stability analysis. *Journal of Soil Mechanics & Foundations Div*.

Widger, R. A. (1976). *Slope stability in unsaturated soils* (Doctoral dissertation, University of Saskatchewan), Canada.

Wright, S. G. (1969). *A study of slope stability and the undrained shear strength of clay shales* (Vol. 2). University of California, Berkeley.

Wright, S. G., Kulhawy, F. G., & Duncan, J. M. (1973). Accuracy of equilibrium slope stability analysis. *Journal of Soil Mechanics & Foundations Div*, *99*(Proc Paper 10097).

Xiao, S., Yan, L., & Cheng, Z. (2011). A method combining numerical analysis and limit equilibrium theory to determine potential slip surfaces in soil slopes. *Journal of Mountain Science*, *8*(5), 718–727.

Xing, Z. (1988). Three-dimensional stability analysis of concave slopes in plan view. *Journal of Geotechnical Engineering*, *114*(6), 658-671.

Zeroual Née Dadouche, F., Lazhar, B., & Zennir, A. (2011). Probabilistic analysis of slope stability towards the slip by the kinematic method. *Physics Procedia*, *21*, 93–100.

Zevgolis, I. E., Deliveris, A. V., & Koukouzas, N. C. (2019). Slope failure incidents and other stability concerns in surface lignite mines in Greece. *Journal of Sustainable Mining*, *18*(4), 182-197.

Zolfaghari, A. R., Heath, A. C., & Mccombie, P. F. (2005). Simple genetic algorithm search for critical non-circular failure surface in slope stability analysis, *32*, 139–152.

APPENDIECS

APPENDIX 1

A.1.1 Factor of safety of failed slopes

A.1.1.1 Samples of failed slopes by SLOPE/W software program

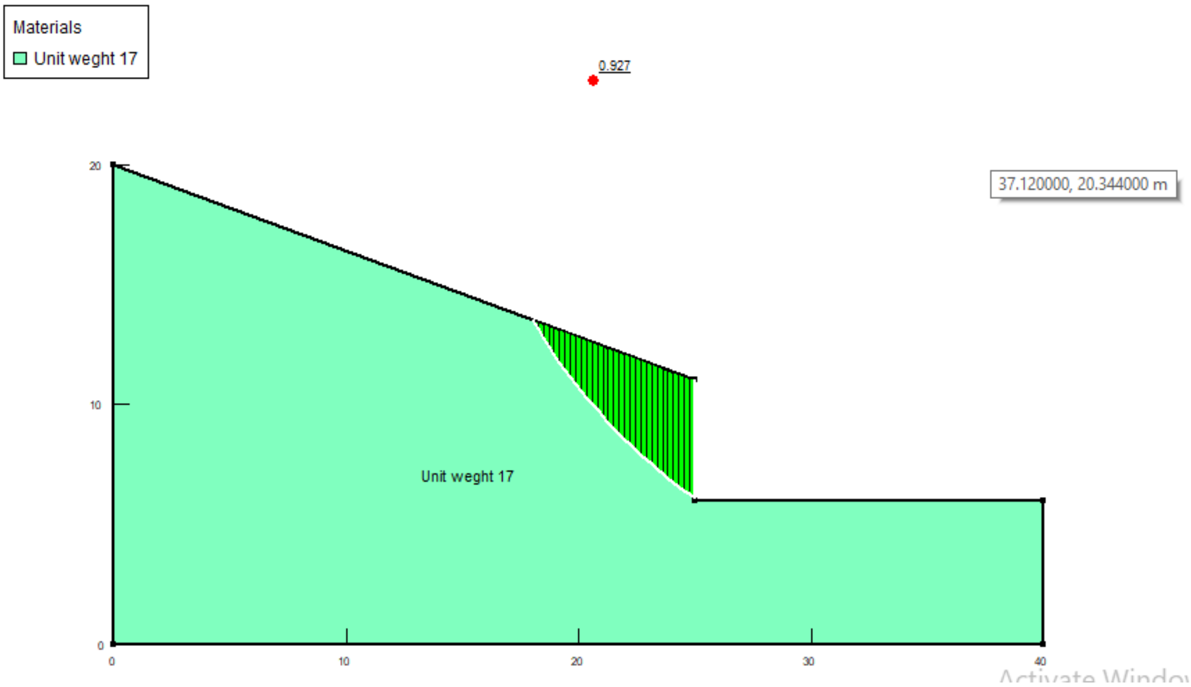

Figure A.1.1: Failed slope at value 17 kN/m^3 of unit weight.

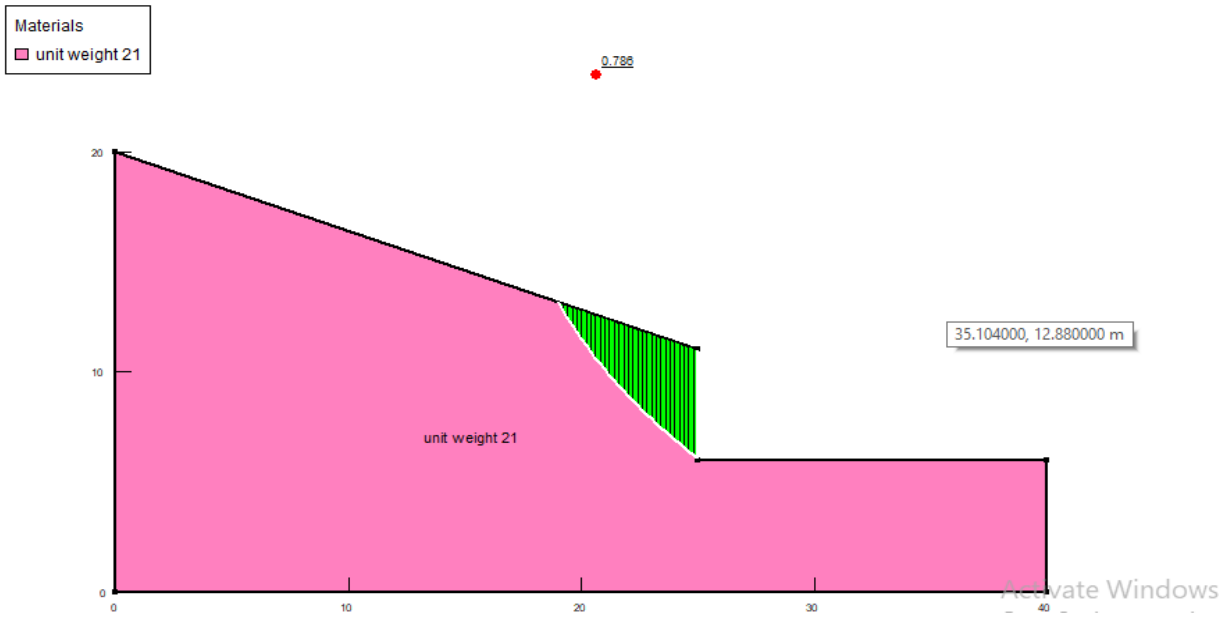

Figure A.1.2: Failed slope at value 21 kN/m^3 of unit weight by using SLOPE/W

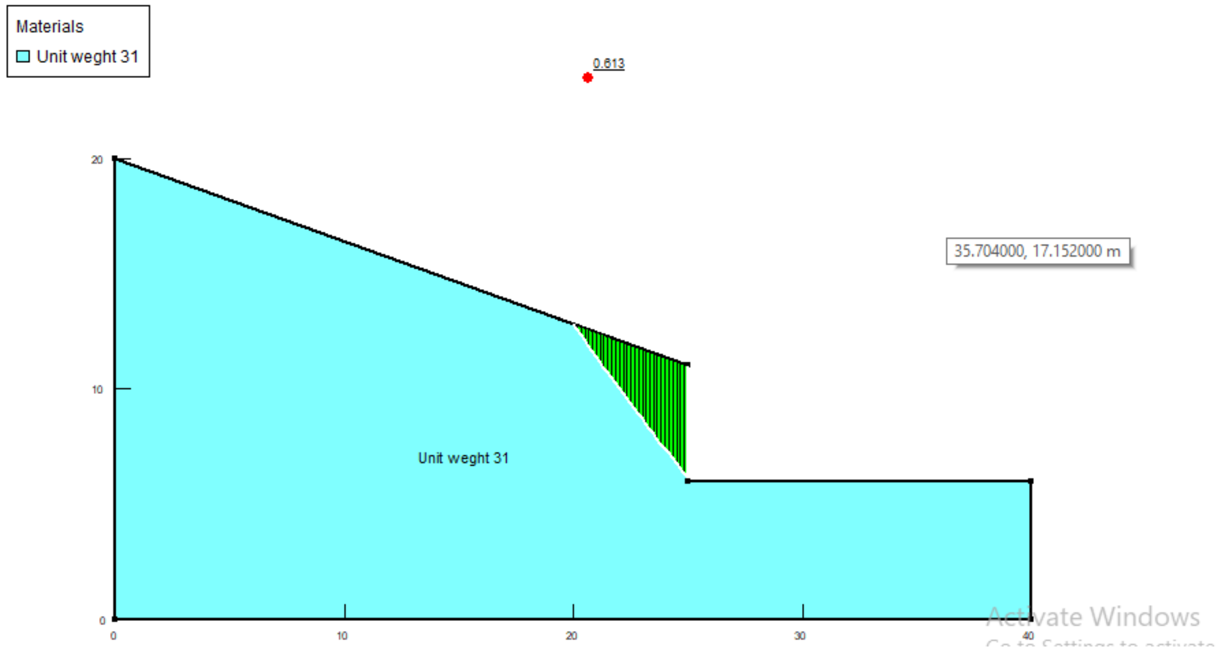

Figure A.1.3: Failed slope at value 31 kN/m^3 of unit weight by using SLOPE/W

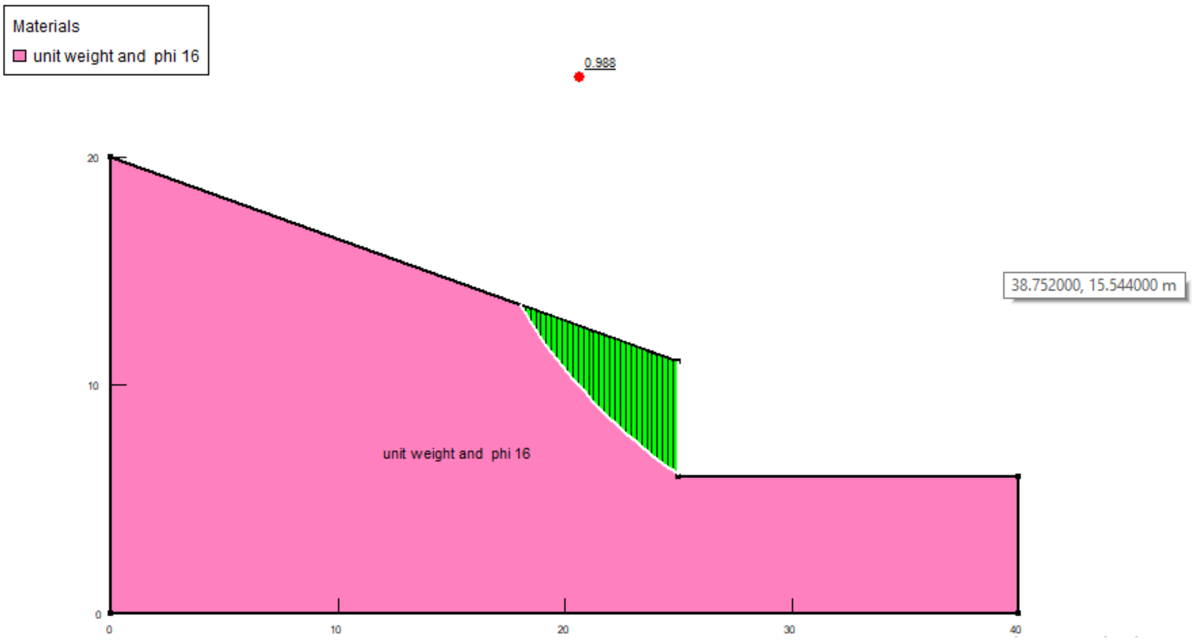

Figure A.1.4: Failed slope at value 16 of unit weight and internal friction angle by using SLOPE/W

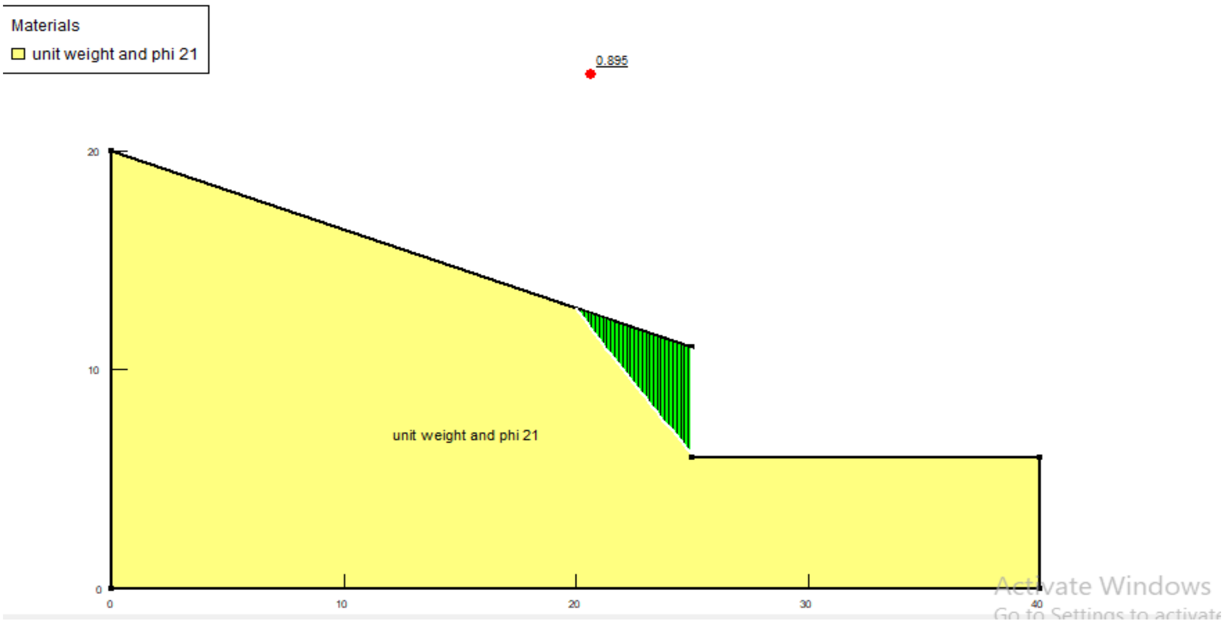

Figure A.1.5: Failed slope at value 21 of unit weight and internal friction angle by using SLOPE/W

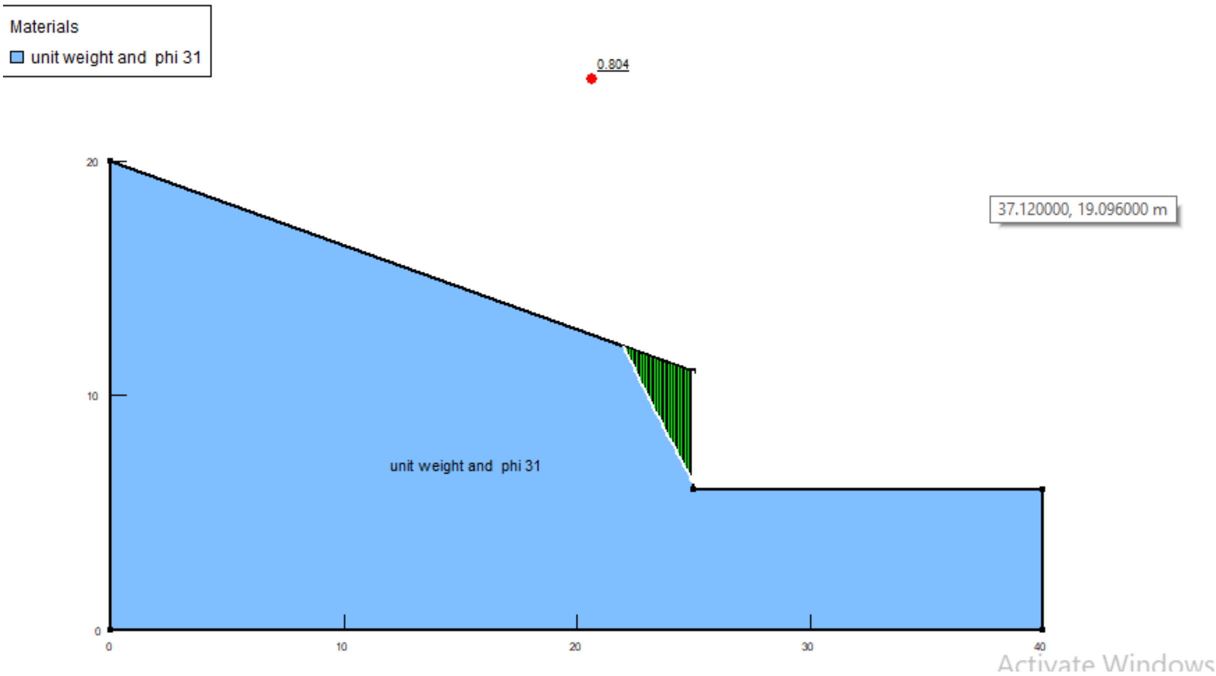

Figure A.1.6: Failed slope at value 31 of unit weight and internal friction angle by using SLOPE/W

A.1.1.2 Factor of safety values for failed slopes by FLAC/SLOPE software program

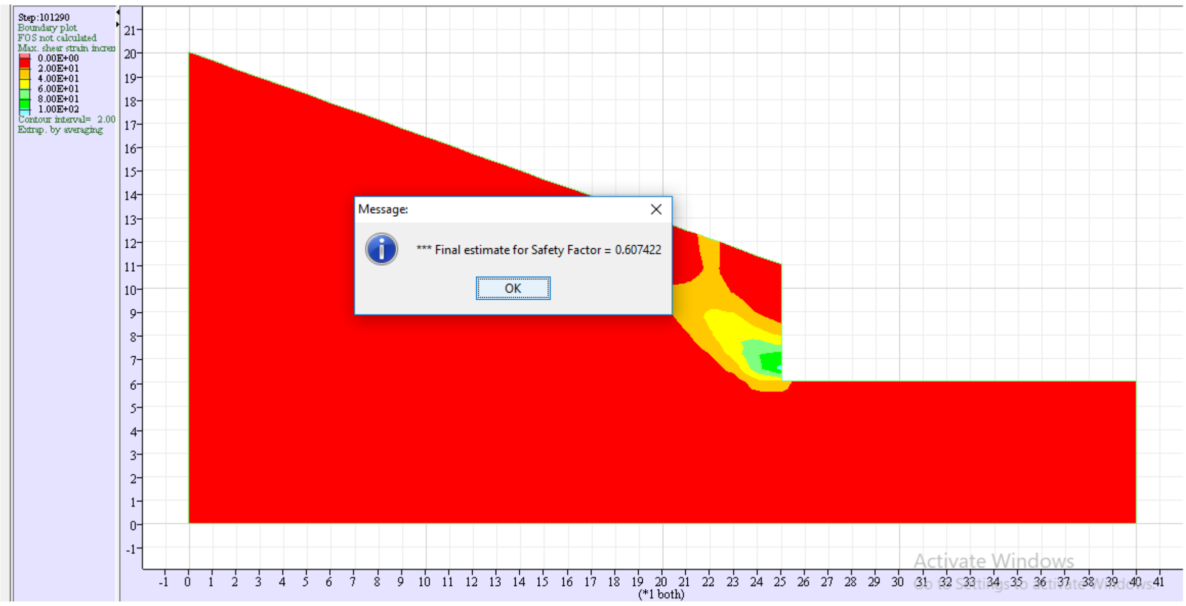

Figure A.1.7: Failed slope at value 25 kN/m^3 of unit weight by using FLAC/SLOPE

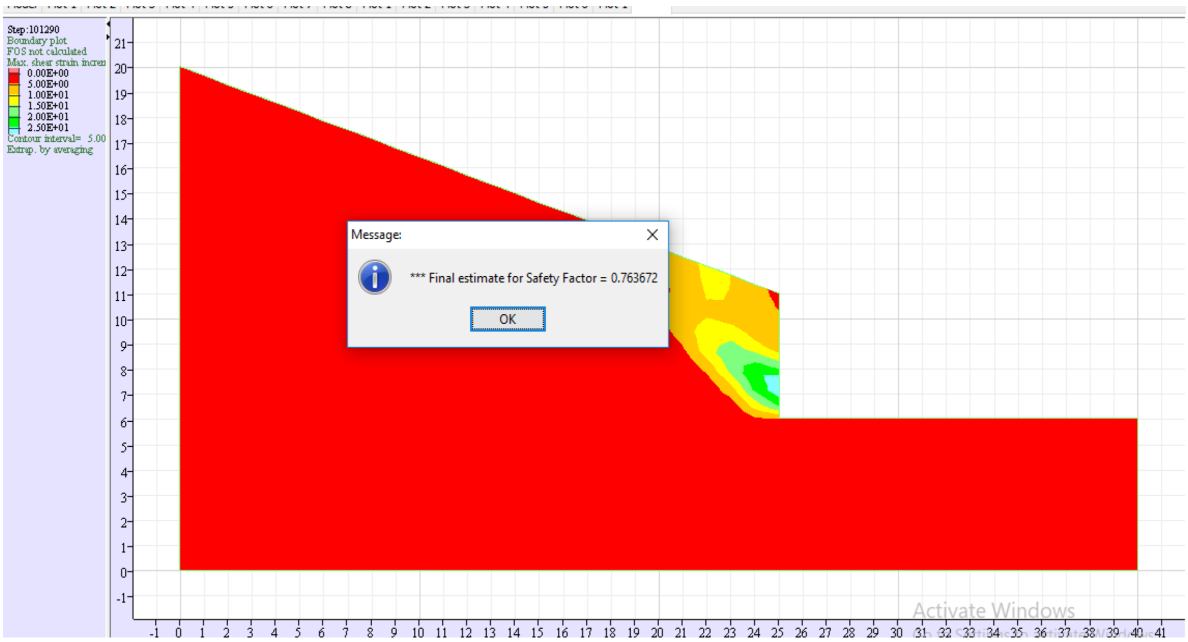

Figure A.1.8: Failed slope at value 25 of unit weight and internal friction angle by using FLAC/SLOPE

APPENDIX2

Failure arc possibilities of failed slope by SLOPE/W

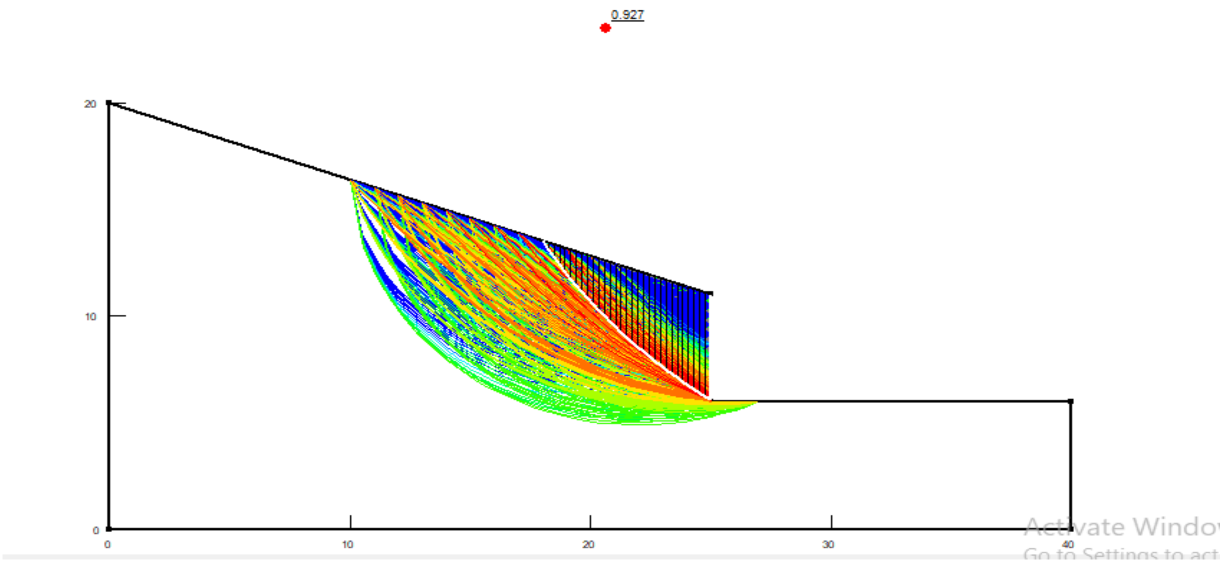

Figure A.2.1: Failure arc possibilities for the value 17 kN/m^3 of unit weight

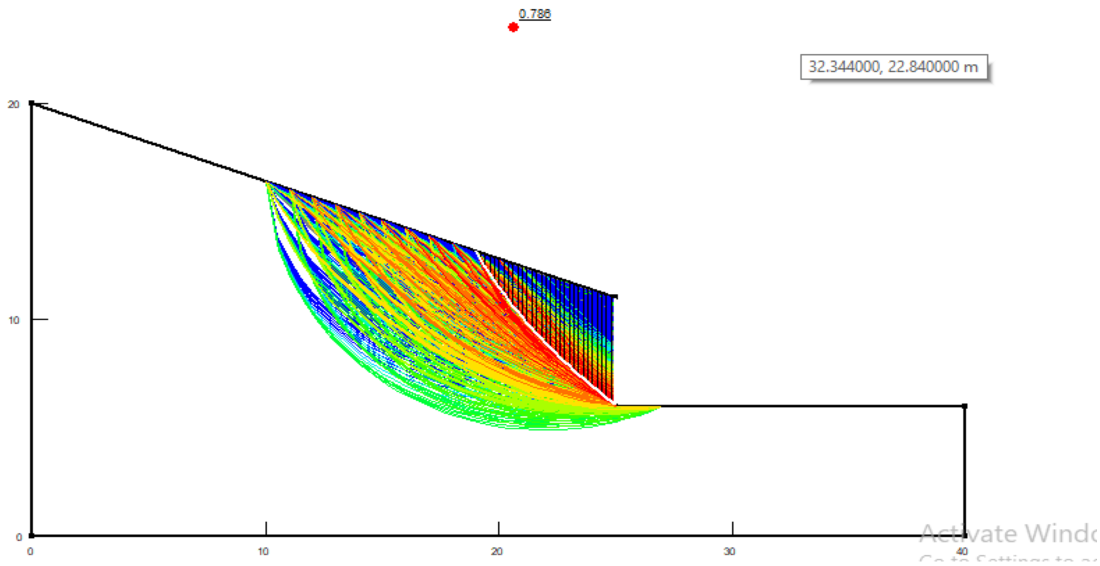

Figure A.2.2: Failure arc possibilities for the value 21 kN/m^3 of unit weight

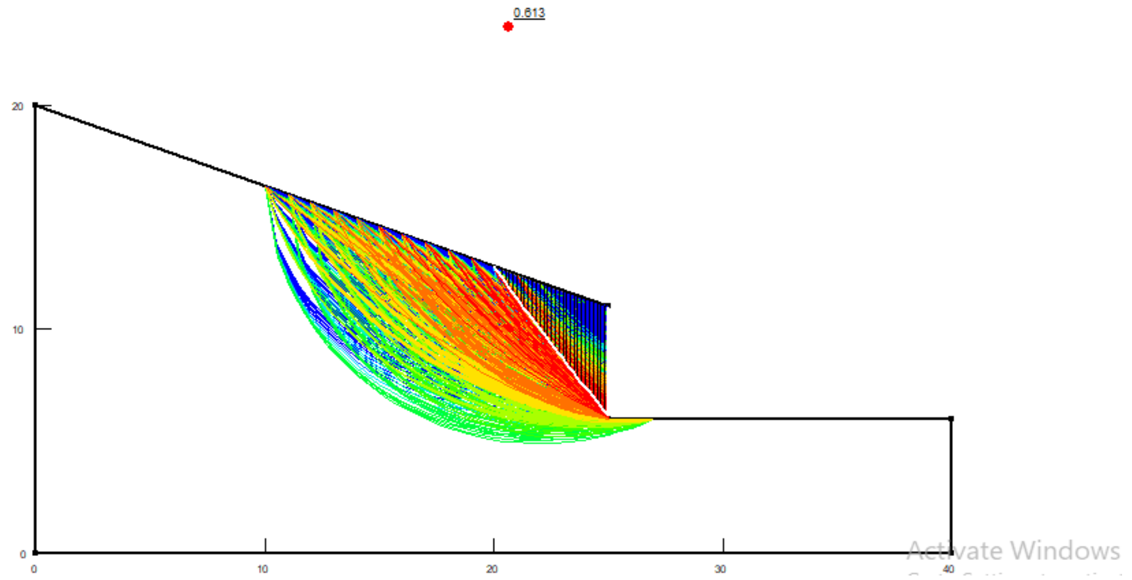

Figure A.2.3: Failure arc possibilities for the value 31 kN/m^3 of unit weight

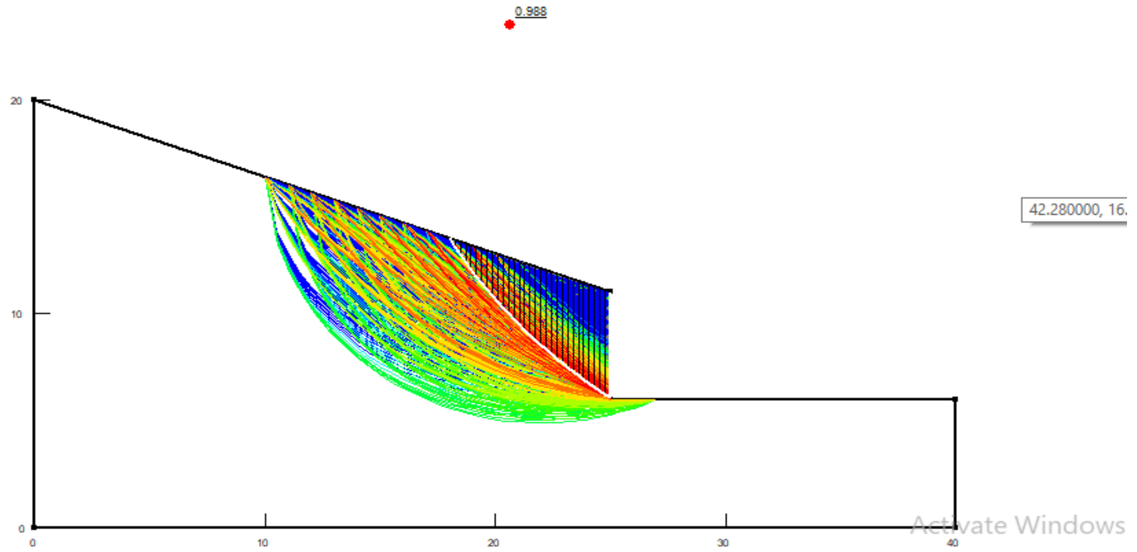

Figure A.2.4: Failure arc possibilities for the value 16 of unit weight and internal friction angle

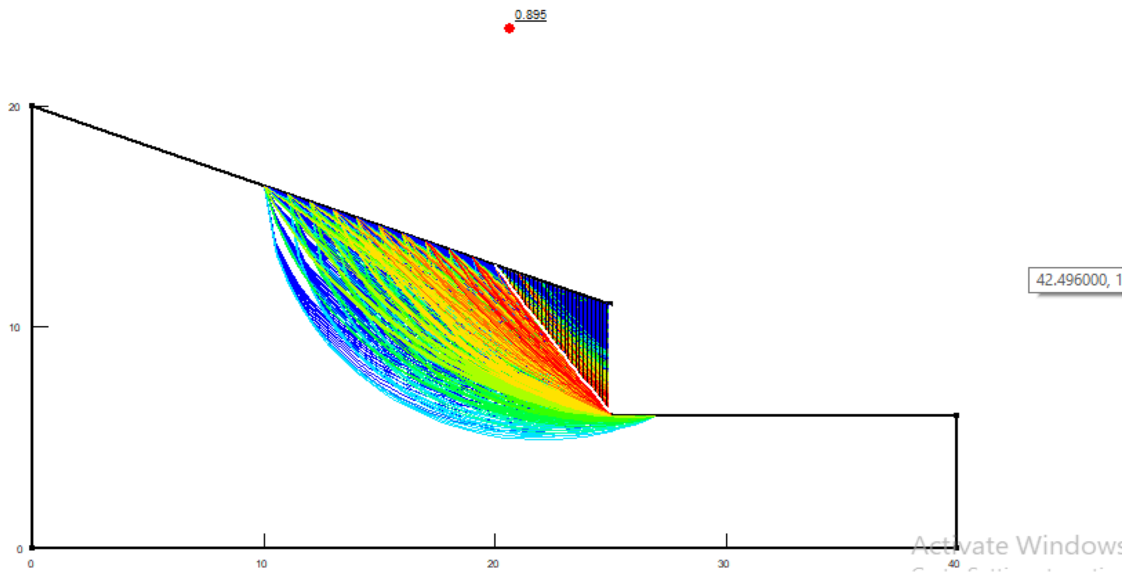

Figure A.2.5: Failure arc possibilities for the value 21 of unit weight and internal friction angle

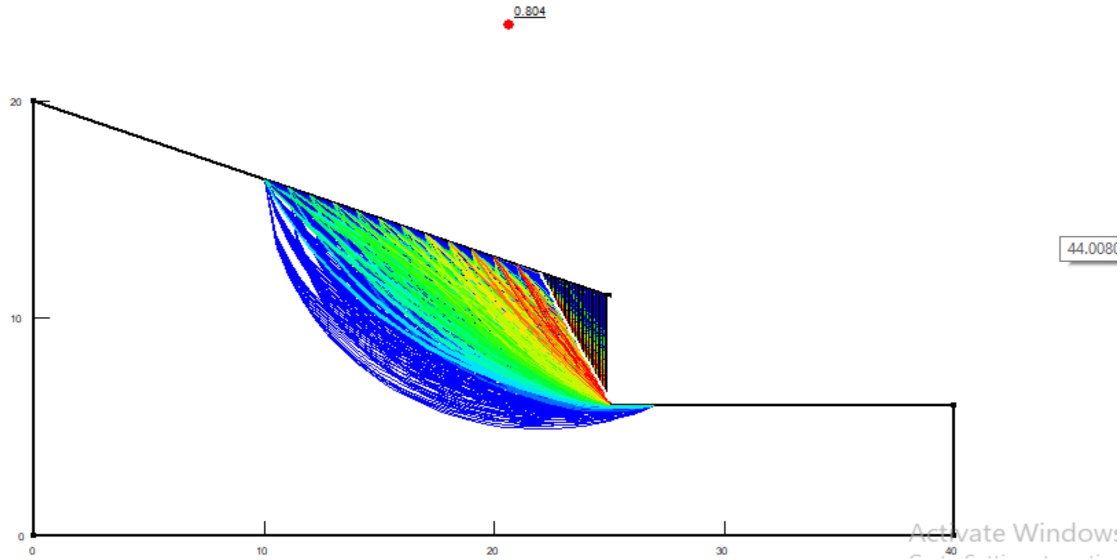

Figure A.2.6: Failure arc possibilities for the value 31 of unit weight and internal friction angle